[redacted]

E
S

ELECTRO-OPTICAL SYSTEMS, INC.
A Subsidiary of Xerox Corporation
300 N. Halstead Street, Pasadena, California

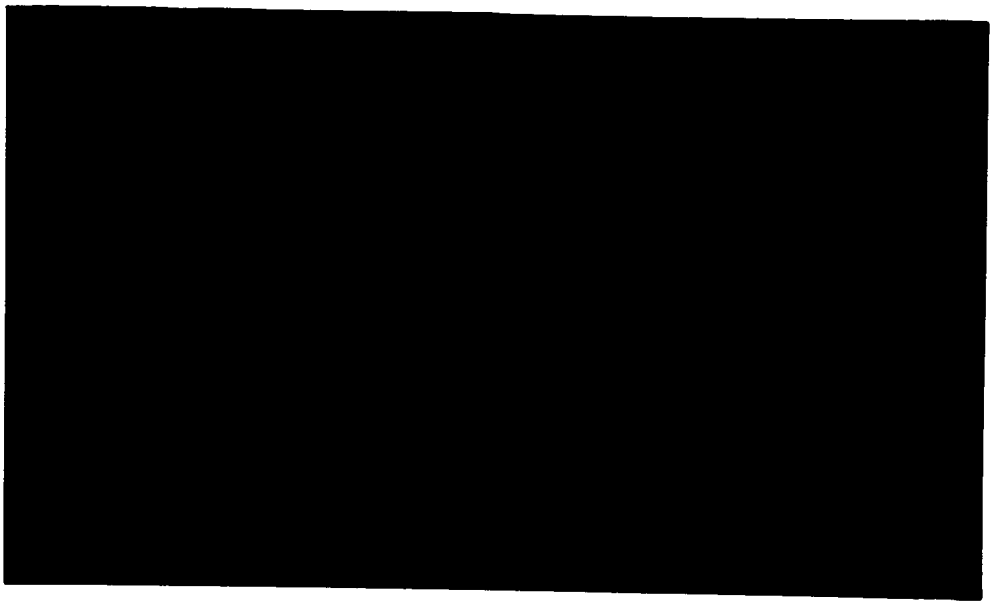

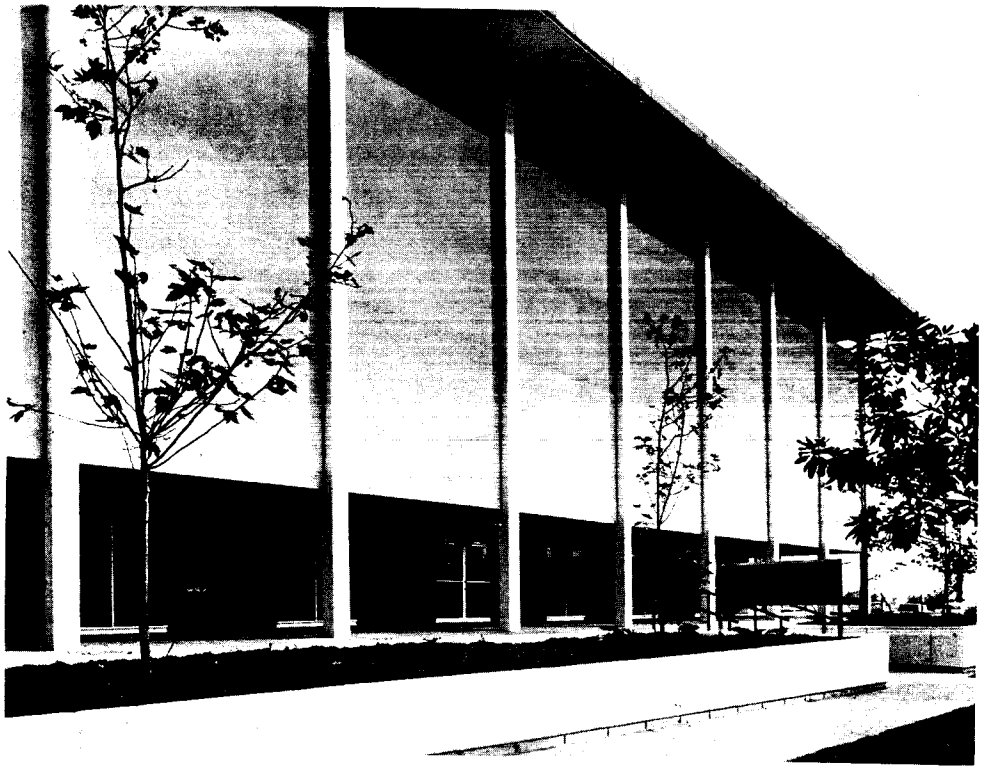

Phase I Report for

SOLAR REFLECTING BEACON

Prepared for
NASA Manned Spacecraft Center
Houston, Texas 77058

Contract NAS9-4790

EOS Report 6976-Phase I 3 December 1965

Prepared by
D. E. Stewart
B. E. Kalensher

Approved by

M. L. Pickel for EES

OPTICS DIVISION

ELECTRO-OPTICAL SYSTEMS, INC. — PASADENA, CALIFORNIA
A Subsidiary of Xerox Corporation

Solar Reflecting Beacon

Phase I Oral Presentation Schedule

9 December 1965

MSC, NASA, Houston

Time	Subject	Speaker
9:00-9:10 a.m.	Introduction	Donald E. Stewart
9:10-9:20	Terminology	Dr. Bernard Kalensher
9:20-9:40	Photometry	D. Stewart
9:40-10:00	Materials and Environmental Resistance	D. Stewart
10:00-11:00	Design Concepts	D. Stewart
11:00-11:40	Orientation	Dr. Kalensher
11:40-12:00	Recommendations and Summary	D. Stewart
1:15- p.m.	General Discussion	Dr. Kalensher and D. Stewart

ABSTRACT

This Phase I report covers the period 22 June through 22 November 1965 and is submitted in accordance with the requirements of Article VII - Reports of Work, Sections B and C of Contract NAS9-4790. Monthly reports M-1 through M-4 and the work performed during the 5th monthly reporting period are summarized along with specific recommendations and conclusions. The goal of this program has been to develop conceptual and engineering designs for two types of Lunar Solar Reflecting Beacons to be emplaced during the early Apollo Lunar Landing missions. One beacon will be visible from the earth. The other will be visible from both the Apollo Command Module (CM) and the Lunar Excursion Module (LEM) vehicles.

Phase I of this two-phase program encompasses static and dynamic beacon design concepts including tracking beacons, photometric analysis of beacon detection, reliability as affected by the lunar environment, materials analysis, beacon location requirements, and preliminary weight and packaging determinations. The second phase of the program will cover environmental and materials specifications definition and engineering designs of the specific beacon concepts chosen by MSC, NASA, Houston from the recommended concepts described in this Phase I report.

On the basis of this Phase I design study, a tracking flat specular earth reflector with an area of 33 sq ft and a field of view of 6.75×10^{-5} steradians is recommended. This beacon will easily meet the packaging requirements of 20 earth pounds, 1 cubic foot, 23 inches maximum dimension, and an assured 0.9 reliability as defined in the program design constraints for an earth-detected beacon.

For the cislunar beacon to be viewed at a maximum slant range of 400 nautical miles, an oscillating arch specular beacon having a total surface area of 19 sq ft and an effective reflective area of 4.44×10^{-2} sq ft is recommended. Such a beacon will meet the five-earth-pound weight, 0.25-cubic-foot volume, 23 inches maximum dimension, and 0.9 reliability design constraints. This beacon will transmit a flashing signal for 0.1 second once every 8.25 seconds using any one of various power sources and devices.

The detailed technical analyses of the above recommended concepts plus other beacon types that have been studied are included in the technical discussion of this report with actual data, analyses, tables, curves, diagrams, and sketches. This forms the background on which the matrix analysis of the beacon design concepts is based. The matrix in effect summarizes the technical discussion and all data presented in this and previous monthly reports. In addition, this report is organized to explain and expand the matrix analysis.

CONTENTS

1. CONCLUSIONS AND RECOMMENDATIONS

The primary purpose of this Phase I effort has been to provide NASA with parametric data, conclusions, and recommendations relative to two types of lunar emplaced beacons; an earth beacon and a cislunar beacon. This section will delineate specific conclusions and recommendations relative to these beacons.

1.1 Conclusions

1. Beacon Feasibility - Both the earth and cislunar beacons can be built within the design constraints using state-of-the-art hardware and technology to satisfy some, but not simultaneously all, of the desirable features of a cislunar or earth beacon. Therefore, beacon design compromises are necessary relative to orientation, field of view, flashing signal vs. continuous signal, motion, reliability, and signal viewing time to optimize the beacon performance within the weight and packaging constraints.
2. Diffuse or Specular Beacons - Specular spherical beacons are superior to diffuse spheres on an illuminance-to-weight ratio due to the higher reflectance, specific strength, and specific rigidity of a specular sphere relative to a diffuse sphere.
3. Beacon Areas - The recommended specular cislunar beacon area is 1.11×10^{-2} ft^2 and the equivalent diameter is 50.5 feet for a 400 nautical mile range, a 0^{o} phase angle, and average lunar maria reflectance of 0.065, and using the 1.58-inch, 28-power command module sextant as a sighting instrument. This spherical diameter is similar to the diameters proposed for the 175 nautical mile range Surveyor emplaced landing aid, when one considers that the relative beacon diameters under equivalent viewing conditions will vary as the range of the observation.

The recommended specular flat earth beacon area of 33 ft^2 falls midway between the earlier optimistic calculated areas reported in the literature and some more recent area calculations made prior to the initiation of this program. Cause of most of these variations is primarily due to the differences in assumptions relative to the magnification and resolution of telescopes under adverse earth atmosphere seeing conditions.

4. Beacon Uses - The earth beacon can be utilized as: 1) a selenographic reference for lunar mapping and motion studies; 2) a political beacon for the enhancement of both internal and external governmental programs and policies; (3) a heliograph for emergency communications in the event that all other communications fail; 4) another method of determining the surface degradation of reflectors due to the space environment.

   The cislunar beacon can serve as: 1) a lunar landing aid, 2) as a cartographic reference point for orbital and lunar surface mapping missions, 3) a navigational aid for updating the command module navigational system, 4) a bench point to measure the orbital precession of the Apollo command module due to the nonsphericity of the moon figure (this information can aid in refining the moment of inertia calculations for the moon); 5) as a heliograph for emergency communications to the command module.

5. Orientation - The computer programs formulated on the program have determined beacon orientation requirements and can predict the location and duration of the beacon signal at any point in space or on the earth surface. However, minor refinements are necessary before NASA can usefully employ the programs. These programs will be useful in orienting antennas and other directional devices utilized in communicating information from the moon to the earth or any other point in the solar system.

6. Power Systems and Drives - Presently photovoltaic power systems coupled with electric motors are proven state-of-the-art hardware

for imparting motion to dynamic beacons. However, it is also feasible to use thermal-mechanical devices, but these devices must be developed further.

7. Reliability - Beacon reliability will depend primarily on the beacon erectability, orientation, durability in the lunar environment (specifically in the areas of lunar temperatures, micrometeorite and dust impingement, ultraviolet and proton bombardment, and the load-bearing strength of the lunar surface) and LEM ascent dust protection.

1.2 Recommendations

Phase II of this program should proceed with the engineering designs and specifications for both the earth and cislunar beacons. Since the specific recommendations for the beacon designs are subject to interpretation, a first alternate is also included in the recommendations.

1.2.1 Earth Beacon Recommendations

The recommended earth beacon is a 33-foot-square, flat, tracking beacon mounted on a tripod and powered by a photovoltaic-motor system with four drive units to track the selenographic longitude and latitude of both the earth and sun. This beacon can be built within the weight and packaging constraints with the desired 0.90 reliability factor utilizing existing proven state-of-the-art space hardware. Due to its tracking abilities, which can be modified to track over a wider field of view than the earth surface to minimize effects of tracking errors, the beacon requires minimum orientation and permits viewing for a relatively high percentage of the time compared with static earth beacon concepts. These advantages more than outweigh the disadvantages of lower reliability due to the complexities of the photovoltaic-electrical system.

As a first alternate, three 33-square-foot-area static beacons can be employed which will meet the weight and packaging requirements. These will require careful orientation procedures and may be

subject to settling into the lunar surface. The primary advantage of this approach is its higher reliability due to a minimum number of parts, assuming that the beacons are aligned and stay aligned without difficulty.

1.2.2 Cislunar Beacon Recommendations

The recommended cislunar beacon is an oscillating faceted arch comprised of four cylindrical segments with a latitudinal angular width of $\pm 47^{\circ}$. This beacon will oscillate about an axis parallel to the north-south meridian passing through the beacon site, at the rate of 8.25 seconds per half cycle. The four cylindrical segments will cover an instantaneous field of view of over 2° in the longitudinal direction and $\pm 90^{\circ}$ in the latitudinal direction. This beacon can be built within the packaging and weight constraints with existing state-of-the-art hardware with a one-year operational reliability of 0.90 or greater.

The alternate beacon is a rotating beacon comprised of three 90-degree arcy cylindrical segments mounted symetrically and rotated about an axis parallel to the local vertical. This beacon flashed for 0.1 second once every 22.6 seconds to a minimum 2π steradian field of view, utilizing a photovoltaic-electric motor drive system. This concept meets the design weight and packaging requirements. Its major disadvantages are its short flash time and its slight inefficiency in reflecting some rays into the lunar surface, i.e., greater than 2π steradian field of view under all but the least optimum sun angle positions.

These two beacon recommendations have assumed that the beacon is more useful as landing and navigational aid than as a lunar mapping photographic bench mark. If this latter use proves to be the most important, either the cap or the oscillating cap should be considered.

1.2.3 Design Specification

Consideration should be given to the following alternative beacon design changes to improve the probability and frequency of beacon detection.

1. Increase allowable weight and packaging volume.
2. Decrease detection range.
3. Decrease area factors of safety.
4. Use larger aperture cislunar camera systems.
5. Increase the number of photographs, i.e., increase the percentage overlap between photographic frames, over the beacon site.
6. Tailor the beacon field of view to the probable range of orbit heights, descent approach angles, and solar coordinates for the specific missions which will utilize the beacon.

1.2.4 Orientation Program

Maximum value can be derived from the beacon orientation computer programs by the revision of several subroutines and the incorporation of JPL's ephemeris tape data within the present programs. This additional work would require 200 hours of Dr. Kalensher's time, 200 hours for a programmer, and $1,000 of computer time. For this, NASA would receive the revised computer program card decks, illustrative examples to check the programs, sample calculations and printouts, and a brief explanation of the card decks. This effort can be completed within two months after initiation.

2. SUMMARY

This report covers the first of two phases of lunar beacon instrument development. This first phase completes the conceptual and engineering feasibility design of two types of solar reflecting beacons emplaced by early Apollo lunar landing missions. Phase II will encompass the preparation of detailed design specifications and engineering drawings.

The beacon, to be viewed from earth, has 20-pound weight and one-cubic-foot volume design limitations. Another, the cislunar beacon, will be visible to an astronaut in the command module orbiting the moon at a 200-nautical-mile maximum altitude at a maximum slant range of 400 nautical miles or to astronauts in the descending LEM. This beacon has 5-pound weight and 0.25-cubic-foot volume design limitations. Common design specifications include a one-year operating life, 0.90 reliability, and 23-inch maximum packaging dimension.

The beacons will be detected both visually and photographically. Visual recognition can be readily achieved by a continuous signal or by short or long duration flashes. Visual navigational sightings and photographic detection are best accomplished with long flashes or a continuous signal. Any type of signal is appropriate for visual detection, though flashes may be more readily detected.

2.1 Specular or Diffuse Beacons

Oriented specular flat beacons are 4.65×10^4 times more efficient on an area basis than a diffuse flat. Diffuse spheres are 2.67 times as efficient as a specular sphere, on an illuminance-to-area ratio, under optimum reflecting and incident angles. However, a specular sphere is more efficient than a diffuse sphere on an illuminance-to-weight ratio under all incident and reflected angle conditions. For these reasons, plus the extensive studies by and for NASA on similar

diffuse beacons, only specular beacons were studied in detail in this program.

2.2 Beacon Concepts

All the beacon concepts relate to a spherical beacon shape--either as complete or segmented sections of a sphere, faceted or cylindrical segmented approximations to these sections, or miscellaneous approximations in both static and dynamic modes. A classification system is defined and illustrated for each general section type.

2.3 Beacon Area, Viewing Time, Field of View, and Flash Frequency

Beacon areas were calculated using accepted photometric telescopic and photographic calculation methods plus assumptions which were more realistic than used in earlier beacon area calculations. The resultant beacon flat areas and equivalent spherical diameters were 1.1×10^{-2} ft^2 and 50.5 ft for cislunar and 33 ft^2 and 2790 ft for earth beacons. These represent photographic and visual detection factors of safety of 2 and 7.2 for the cislunar and 11 and 10 for earth beacons respectively based on the various assumptions made.

It is impractical to fabricate spherical sections within the weight and packaging specifications which will cover the fields of view required to produce a continuous beacon signal to either the earth or cislunar space. Therefore, if a wide field of view is required, the continuous beacon signal must be sacrificed and a flashing signal tolerated. The length and frequency of the flash will depend upon the beacon field of view, the motion of the beacon, and the position of the observer. Generally, the beacon field of view depends on the reflective area which, in turn, is proportional to the total package weight assigned to reflective area. The choice of a particular beacon design will depend heavily on the type of detection which has the highest mission priority.

2.4 Materials

The proposed beacons will utilize space-qualified metals, plastics, and plastic metal composites with high structural reliability,

specific strength, specific rigidity, and environmental resistance. The proposed concepts rely heavily on aluminum and Kapton plastic.

2.5 Orientation

Orientation requirements have been defined and basic programs computed relative to beacon orientation accuracy, orientation angle calculations, and signal viewing time.

2.6 Drive Mechanisms, Power Systems, and Bearing Seals

Various drive mechanisms including electric and clock motors, bi-metallics, and solar wind are summarized together with the power systems which might be considered for dynamic beacons. Space-proven photovoltaic systems are the most promising. However, thermal-mechanical concepts also appear attractive.

2.7 Reliability

Reliability, herein defined as the probability of the beacon meeting its design specifications after a one-year lunar operating life, is primarily dependent on the erectability, orientation, durability in the lunar environment, and the dust problem during LEM ascent. The prelaunch, launch, and translunar environmental phases should not affect the reliability of any of the beacon concepts.

2.8 Beacon Concepts

Several beacon concepts are described for both the earth and cislunar beacons. The recommended flat tracking earth beacon was chosen primarily for its high percentage of viewing time, ease of erectability, lack of orientation requirements, and ease in dust protection. The high rated cislunar segmented arch and cylindrical segment dynamic beacons were chosen on the basis of a wide field of view, high flashing frequency, minimum orientation, high durability of metal panels or foils, and ease in dust protection. If photographic detection receives major emphasis, the flash frequency and duration requirements would change along with the cislunar beacon concept ratings. Rough estimated costs are included for the various beacon concepts.

3. TECHNICAL DISCUSSION

This Phase I report provides NASA with parametric data relative to the tradeoff considerations used in establishing percentage of time beacon signal will be visible, estimated lifetime of beacon reflector in the lunar environment, cost, weight, volume, and overall feasibility.

The following design constraints have been placed on the beacon study:

Constraint	Earth Beacon	Lunar Beacon
Weight	20 earth pounds	5 earth pounds
Package volume	1 cubic foot	0.25 cubic foot
Maximum packaging dimension	23 inches	23 inches
External power source	Only solar energy	Only solar energy
Minimum operating lifetime	One year (self-contained)	One year (self-contained)
Reliability*	0.90	0.90
Environmental criteria	Environment specifications for Apollo scientific equipment	Environment specifications for Apollo scientific equipment

The beacons will be emplaced within a corridor ±5 degrees latitude by ±45 longitude and will be considered to be viewed under full moon background brightness.

This section discusses the various details associated with conceptual designs and the engineering feasibility of both types of solar beacons including:

1. Comparison between specular and diffuse beacons
2. General concepts for static, rotating, and oscillating reflector rays

---

*Reliability refers to the probability of receiving a detectable signal from the beacon within the design field of view after one year of operation.

3. Beacon size, viewing time, observation, frequency, and field of view
4. Materials
5. Orientation
6. Drive mechanisms and power systems
7. Reliability
8. Conceptual design including cost, weight, volume, and feasibility analysis

Various detector-instrument combinations for the earth and lunar beacons are listed in Table 3-I. Photographic detection presents a much more difficult beacon design problem than visual detection especially in the case of the cislunar beacon. The proposed lunar cartographic cameras will take a square format picture representing a field of view of 74 degrees across the flats and approximately 94 degrees across the diagonals. This means that the maximum field of view of the beacon for photographic purposes should be ±47 degrees about the local vertical to encompass all probable camera positions that could detect the beacon. On the other hand, visual landing recognition from the LEM requires only that the beacon reflect into the π steradian solid angle pointed in the positive increasing longitudinal direction as shown in Fig. 3-1. Visual navigational updating requires that the beacon signal reflect into the entire 2_{π} steradian field of view surrounding the beacon.

Optimum beacon flash times will also vary with each of these three cases. In photographic detection, the flash time must be long with respect to the shutter speed to insure that sufficient photons from the beacon strike the photographic emulsion. A short flash signal may not be detected. For example, if the camera shutter speed is 1/50 second, if the flash duration is 0.1 second; if a minimum of 1/50 second is required for detection; and if the camera views the flash when the photograph is taken, then the probability of detection is 0.6 for a picture taken within the 0 to 0.1 second flash time period. If the flash duration is increased to 1.0 second then the probability increases to 0.96.

TABLE 3-I

VARIOUS DETECTOR-INSTRUMENT COMBINATIONS

EARTH BEACON

Combination	Detector	Instrument	Comments
1	Photograph	Camera with 10 to 60-inch aperture telescope	Long flash time desirable over specific field of view on earth.
2	Eye	10 to 60-inch aperture telescope	Either long or short flash time acceptable over specific field of view.

CISLUNAR

1	Eye	1.58-inch aperture 28X sextant	High- or low-frequency flashing over wide field of view desirable;
2	Photograph	Camera	Long flash time over field of view within $\pm 47^{\circ}$ of local vertical to improve probability of photographic detection.
3	Eye	Eye	High- or low-frequency flashing over wide field of view desirable; short flash time acceptable.
4	Eye	Sighting telescope	High- or low-frequency flashing over wide field of view desirable; short flash time acceptable.

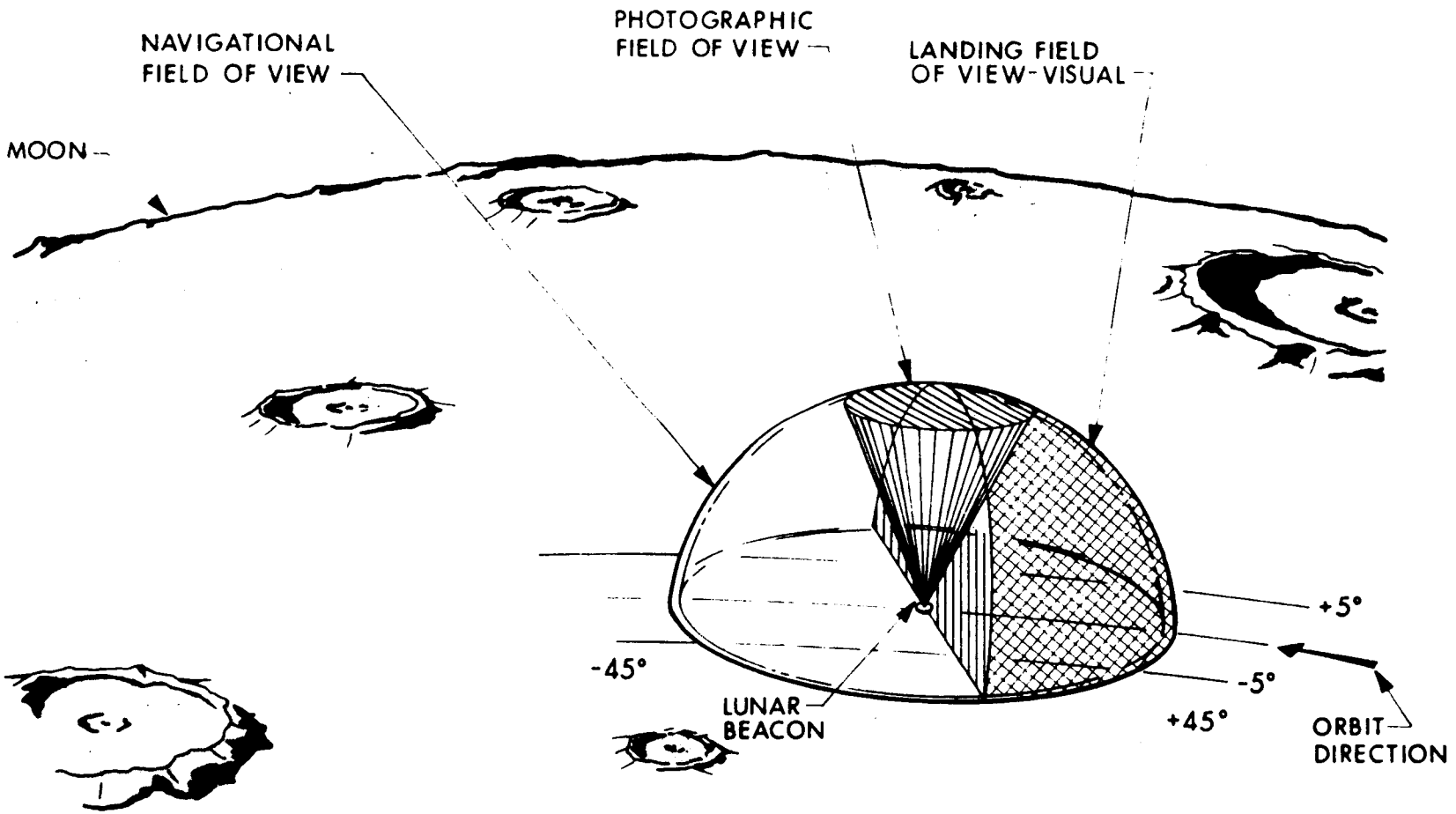

FIG. 3-1 CISLUNAR BEACON FIELDS OF VIEW FOR NAVIGATIONAL, PHOTOGRAPHIC, AND LANDING MISSIONS

The percentage of flash time within the maximum ±47 degree field of view should be high in order to increase the probability of photographic detection. The percentage of flash time within the maximum ±47 degree field of view can be increased by any of the following methods:

1. Increase the beacon instantaneous field of view by either:
    a. Decreasing the area factor of safety.
    b. Increasing the weight limitations and therefore the total area.
    c. Decreasing the range.
    d. Designing the beacon for use at less than maximum background illumination.
2. Increase the percentage of beacon flash dwell time within the ±47 degree field of view by programming the angular oscillation velocity so that a major portion of the cycle time is within the ±47 degree field of view.
3. Decrease the total beacon field of view thereby increasing the percentage of time within the ±47 degree field of view.

For visual landing recognition from the LEM vehicle, the beacon flashes can be short in duration (0.1 second or less) as long as the photon intensity from the flash is above the minimum detectable illuminance. The flashes should be frequent enough, however, to permit multiple beacon sightings within the landing time span and thereby improve the detection probability.

The use of the beacon as a visual navigational updating marker may require large enough flash times so that the Command Module sextant can be carefully aligned with the beacon flash. This alignment may require several seconds of flash time to permit accurate navigation. This requirement may dictate a relatively slow oscillating or rotating beacon if beacon motion is employed.

The factors which affect the beacon field of view and beacon flash times will be discussed in more depth in Subsection 3.2.

3.1 Comparison Between Specular and Diffuse Reflectors

Reflectors are characterized by two different surface characteristics specular and diffuse reflectance. The photometric analysis of lunar-emplaced solar specular or diffuse reflecting beacons is discussed in Appendices A and B respectively. Table 3-II summarizes the comparison of various optical and physical characteristics for specular and diffuse reflectors.

The illuminance from a flat specular reflector is 4.65×10^4 times more intense than a diffuse flat of equivalent area and reflectance when the phase, incident and reflected angles are all zero degrees. However, for spherical reflectors the diffuse reflector has a reflectance advantage for phase angles less than or equal to $|83|$ degrees of arc. The attractiveness of the diffuse sphere over this range of phase angles has been a major factor in the design considerations for a Lunar Landing Aid to be emplaced by the Surveyor Vehicle. However, the attractiveness of a diffuse reflector decreases rapidly when one considers the strength, weight, and environmental resistance penalties which must be applied to diffuse surfaces. The weight of the diffuse layers is almost equal to the substrate weight for balloon (or balloon-erected) designs. Also, diffuse surfaces have a specific strength almost an order of magnitude less than specular reflecting layers. In addition, diffuse surfaces made with organic binders probably will exhibit much greater losses in reflectance than specular metallic surfaces.

Since a cislunar spherical diffuse beacon would weigh almost 10 times the cislunar design weight limit; since diffuse beacons have been studied in depth by NASA as a lunar landing aid to be emplaced by the Surveyor, and since the illuminance from a small diffuse spherical cap is much less than from a specular cap, only specular beacons have been studied in detail during this program.

TABLE 3-II

COMPARISON OF SPECULAR AND DIFFUSE REFLECTORS

Comparison Characteristic	Units	Specular Reflector	Diffuse Reflector	Comments
1. Basic Physical Law		angle of incidence ψ = angle of reflection ϕ	$E = E_o \cos\phi$ Lamberts Law	1. Diffuse elemental area omnidirectional; specular elemental area unidirectional
2. Illuminance from Flat Reflector, F		$E = \frac{a_s r_b E_s}{\Omega_s R^2} \cos\psi$	$E_d = \frac{a_d a_b E_s}{R^2} \cos\psi \cos\phi$	2. $E_s/E_d = \frac{a\ r_b}{a_d a_b} \frac{\cos\frac{\theta}{2}}{\Omega_s \cos\psi \cos\phi}$ $= 4.65 \times 10^4$ at $a = a_d$; $r = a_b$; θ, ψ, and ϕ = 0
3. Intensity of signal from spherical reflector (collimated incident radiation)		$I_{bs} = r_b \left(\frac{d_b^2}{16}\right) E_s$	$I_{bd} = a_b \left(\frac{d_b^2}{6\pi}\right) [\sin\theta + (\pi-\theta)\cos\theta] E_s$	3. $I_{bd} = 2.67\ I_{bs}$ at $\theta = 0^o$ $I_{bd} = I_{bs}$ at $\theta = \pm 83^o$
4. Reflectance		r_b; 0.80-0.93	a_b; 0.70-0.90	4. Specular reflectance generally greater than diffuse reflectance
5. Reflectance Layer				
5.1 Thickness	inches	$2\text{-}4 \times 10^{-6}$ to 0.18×10^{-3}	$0.5\text{-}2 \times 10^{-3}$	5.1 Specular thickness much less than diffuse
5.2 Roughness	inches, rms	$\sim 1\text{-}2 \times 10^{-6}$	$8\text{-}32 \times 10^{-6}$	5.2 Specular surface much smoother
5.3 Strength	psi	$2\text{-}4 \times 10^5$ to	$0.5\text{-}10 \times 10^3$	5.3 Specular layer strength

			4×10^{4}		higher than diffuse
5.4	Weight	lb/in.^{2}	$\sim 1 \times 10^{-6}$ to 2.52×10^{-2}	$\sim 1 \times 10^{-4}$	5.4 Diffuse layer much heavier than specular and almost equal to substrate weight in many cases
5.5	Application		vacuum coated — foil	spray-coated, fired, or embossed foil	5.5 Specular application easier to control
5.6	Reflectance Material		homogeneous layers of metals or inorganic dielectrics	Heterogeneous or homogeneous nonmetallic pigments; organic carriers or carriers	
5.7	Environmental Resistance		not susceptible to low energy uv, high energy uv, or protons	organic carriers darken under vacuum uv	5.7 Organic diffuse reflectors highly susceptible to uv

Nomenclature

- a = area, albedo
- d = diameter
- E = illuminance
- I = intensity
- r = reflance
- R = range
- = phase angle
- = angle of reflection
- = angle of incidence
- = solid angle

Subscripts

- b = beacon
- d = diffuse
- s = specular, sun

3.2 Basic Beacon Concept Classifications

Before considering the detailed analysis of beacon size, viewing time, observation frequency, field of view, and conceptional design concepts, the basic beacon geometry classifications will be discussed. Beacon designs can be classified into static and dynamic categories with spherical, faceted spherical approximations, and miscellaneous subcategories. Figure 3-2 gives classification numbers for various beacon geometry types. These will be of value in comparing different types of beacon designs.

The various spherical segment alternates show different ways to reduce the total spherical area while maintaining a large field of view (or field of reflection).

The faceted approximations use multiple flat or cylindrical segments to project the reflected beacon signal to a large field of view. If each facet is inclined ≤ 0.00464 radians with respect to each other, the reflected signal will appear to be reflected continuously from a spherical surface. Therefore, these faceted approximations can be used in the same manner as the spherical shapes. Faceted approximations are usually easier to package. The miscellaneous static category includes such concepts as an umbrella-type reflector, etc.

The dynamic spherical beacon concepts use either spherical or cylindrical segments plus rotation, oscillation, or solar tracking modes of motion to approximate a spherical or spherical segment surface.

3.3 Beacon Area, Viewing Time, Observation Frequency, and Field of View

The variables affecting beacon area, viewing time, observation frequency, and field of view factors are listed in Table 3-III. These factors will be discussed in the subsections below.

3.3.1 Beacon Area Analysis

Beacon area analyses for specular and diffuse reflectors are listed in Appendices A and B respectively. Due to the weight and area penalties for diffuse beacons, as discussed above, the Phase I effort has concentrated entirely on specular beacon design concepts.

1. STATIC
1.1 SPHERICAL

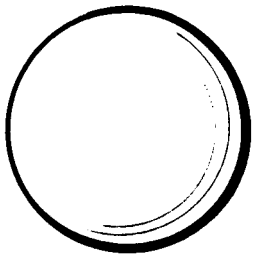

1.1.1. SPHERE

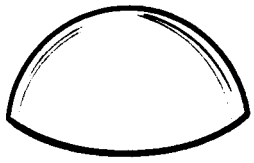

1.1.2. HEMISPHERE

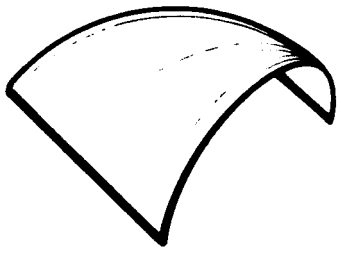

1.1.3 LUNE

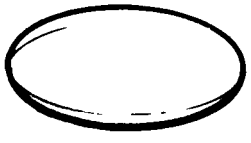

1.1.4 CAP

1.1.5 ARCH

1.2 FACETED APPROXIMA

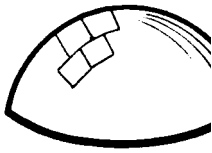

1.2.1 HEMISPH

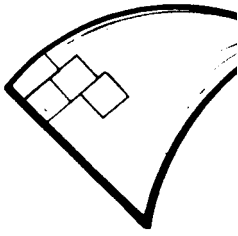

1.2.2. LUNE

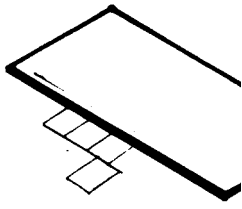

1.2.3 CAP-

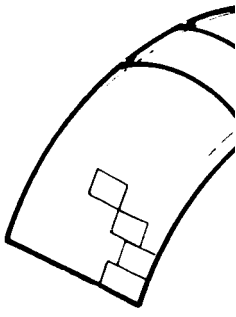

1.2.4 ARCH

TIONS

ERE

1.3 MISCELLANEOUS

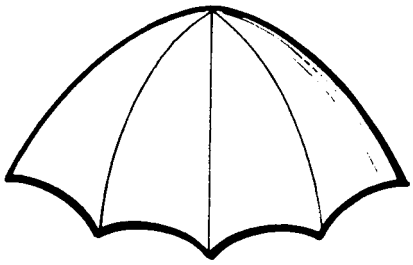

1.3.1 UMBRELLA

2.1.4 OSCILLATING

2.0 DYNAMIC

2.1 SPHERICAL

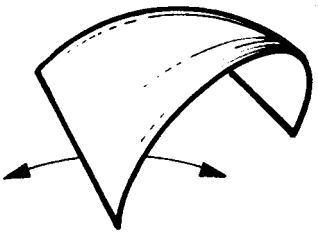

2.1.1. OSCILLATING, TRACKING LUNE

2.2 FACETED APPRO

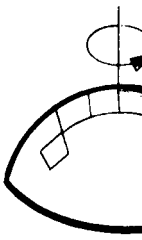

2.2.1 ROTATING HEMISP

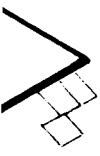

►FLAT

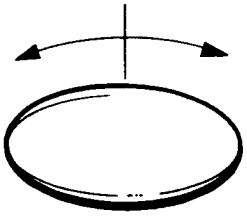

2.1.2 OSCILLATING TRACKING CAP

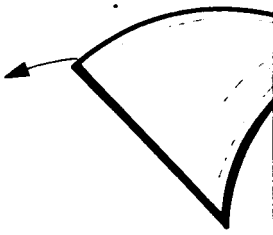

2.2.2 OSCILLAT LUN

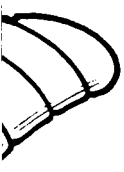

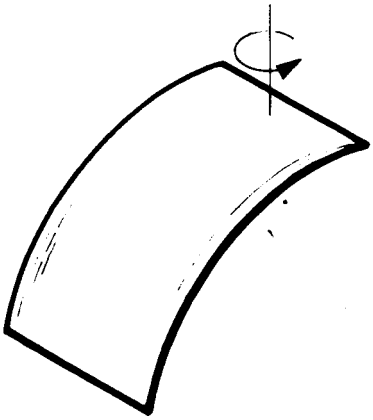

2.1.3 ROTATING OSCILLATING CYLINDRICAL SEGMENT

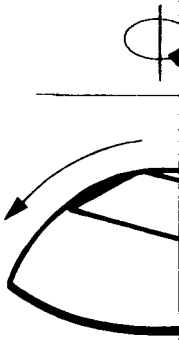

2.2.3 CAP►FLAT ROTATING, TR

FIG. 3-2 BEACON

92

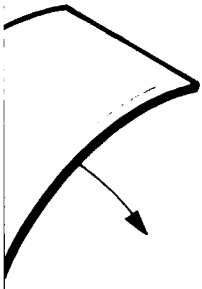

, TRACKING ARCH

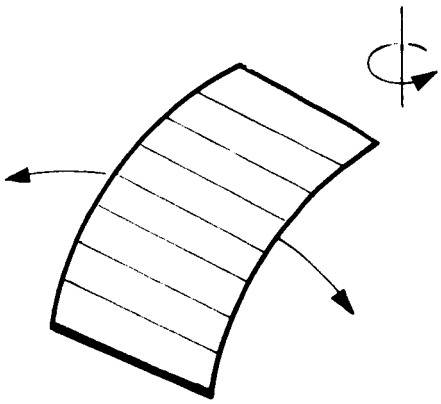

2.2.4. ROTATING, OSCILLATING FACETED CYLINDER

)XIMATIONS

, OSCILLATING
HERE

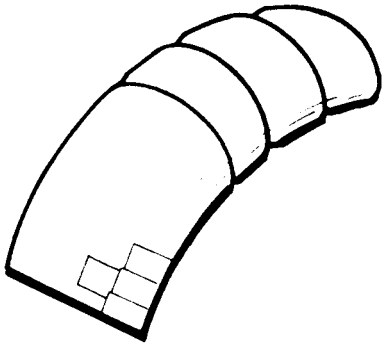

2.2.5 OSCILLATING, TRACKING ARCH

2.3 MISCELLANEOUS

ING, TRACKING
E

2.3.1 ROTATING TRACKING UMBRELLA

OSCILLATING
RACKING

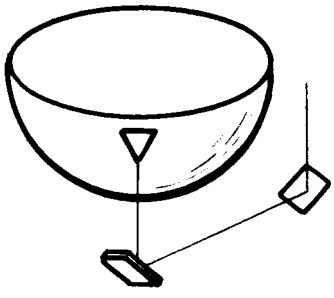

2.3.2 SUN PUMPED LASER

TABLE 3-III

VARIABLES AFFECTING BEACON AREA, VIEWING TIME, OBSERVATION FREQUENCY, AND FIELD OF VIEW

	Variable	Area	Viewing Time	Observation Frequency	Field of View
1.	Background brightness, B_f	X			
2.	Beacon reflectance, r_b, a_b	X			
3.	Sun-moon-instrument phase angle, θ	X			
4.	Instrument beacon range, R	X			
5.	Integrated instrument optical transmittance, T_t	X			
6.	Integrated instrument angular resolution as a function of aperture, instrument errors, atmospheric seeing (and for photographic records of the detector errors), β	X			
7.	Atmospheric transmittance, T_e	X			
8.	Contrasts required for a given detector and probability of detection, C_v — visual, C_p — photographic	X			
9.	Lunar beacon location	X			
10.	Beacon surface geometry	X	X		X
11.	Beacon alignment to the sun, static or tracking		X	X	
12.	Beacon motion, static, rotary, oscillatory		X	X	X
13.	Beacon earth-sun orientation, static or tracking		X	X	

Table 3-IV summarizes the minimum beacon areas calculated for photographic and visual observations from earth and cislunar orbit. The minimum design areas were calculated using a 3.18 multiplication factor for the Tiffany data which represents contrasts for 50-percent probability of detection. Low multiplication factors have been questioned. Therefore, the areas calculated when this factor is 10 X and 100 X Tiffany data (a_{10} and a_{100}) have been tabulated also for comparison. The factors of safety, FS, based on the calculated, design, and minimum design area (a, a_d, and a_{md} respectively) are also shown where:

$$FS = \frac{a_d}{a} \text{ or } \frac{a_{md}}{a}$$

Recommended design areas for the beacons, a_d, for zero degree phase angle detection are also presented based on arbitrary safety factors of 2 for the earth-photographed beacon, 7.2 for the earth-visually-detected beacon (using 10 to 60-inch telescopes) and 11 and 10 for the cislunar photograph and visual beacons. These factors of safety will increase by almost a factor of 10 as the phase angles approach $\pm 90^{\circ}$. Correspondingly, telescopic seeing conditions may grow poorer by a factor of $\sqrt{10}$ if the phase angles approach $\pm 90^{\circ}$ or the beacon design areas could be decreased by a factor of 10.

The photographic factors of safety are different from the visual factors of safety, FS, because the factors of safety were assigned so that the beacon size is the same for both photographic and visual detection. The FS for the earth-photographed beacon is relatively low compared to the cislunar-photographed beacon FS because low photographic area was chosen to permit a design solution within the packaging limitations. Multiexposure and electronic image enhancement techniques are available to improve the detection probabilities of photographic techniques whereas visual observations, being less objective, require a greater FS.

Even if the Tiffany 50-percent detection factor multiplier should be 100, the design areas for visual detection have a factor

TABLE 3-IV

BEACON AREA CALCULATIONS

Beacon Area Analysis for Various Viewing Cases and Assumptions

Case	Contrast 1/ C_p or C_{50}	Minimum Design Area a_{md} ft^2	Calculated Area a ft^2	Factor of Safety a	2/ a_{10} ft^2	Factor of Safety a_{10}	3/ a_{100} ft^2	Factor of Safety a_{100}	Recommended Design Area a_d ft^2
1. Earth-photograph	0.08	16.5	16.5	1	---	---	---	---	33
2. Earth-visual	0.016	16.5	4.56	3.6	6.07	2.5	14.9	1.11	33
3. Cislunar-photograph	0.08	1.11×10^{-3}	0.98×10^{-3}	1.13	---	---	---	---	1.08×10^{-2}
4. Cislunar-visual	0.0495	1.11×10^{-3}	1.11×10^{-3}	1	1.43×10^{-3}	0.77	5.42×10^{-4}	0.205	1.08×10^{-2}

Case	Factor of Safety d	Factor of Safety d/a_{100} 4/	Range Resolution R nm	Range Resolution β sec	Transmittance Telescope T_t	Transmittance Atmosphere T_e	Phase Angle Reflectance Factor K_θ	Beacon Reflectance r_b	Diametrical Magnification Factor M/D_o X/inch	Instrument Aperture Diameter D_o inches
1. Earth-photograph	2	---	207,000	0.5	0.7	0.7	1.0	0.80	---	11-60
2. Earth-visual	7.2	2.2	207,000	1.0	0.7	0.7	1.0	0.80	25.4	10-60
3. Cislunar-photograph	11	---	400	2.0	0.7	1.0	1.0	0.80	---	>2.8
4. Cislunar-visual	10	2	400	5.0	0.27	1.0	1.0	0.80	17.8	1.58

See text and Appendix A for nomenclature.

1/ C_p = Photographic contrast

C_{50} = Tiffany 50 percent detection contrast

2/ a_{10} = area based on $10C_{50}$ visual contrast figure

3/ a_{100} = area based on $100C_{50}$ visual contrast figure

4/ FS d/a_{100} = design FS relative to a_{100} (instead of a)

of safety of 2 (i.e., twice the area required). The photographic beacon areas, assigned the same design values as the visual beacons, have a FS of 2 and 11, respectively, for earth and cislunar detection.

The effect of good seeing requirements, particularly for terrestrial photography, is discussed in Appendix A.

Based on these large cislunar safety factors, omnidirectional spherical caps or lunes would require a spherical diameter of 50.5 feet. This is impractical, considering the tight weight tolerances. Therefore, since the beacon diameter varies as the square root of the beacon area, $\sqrt{a}$, or as the detection range, R, consideration should be given to the reduction of the factor of safety or the range over which the beacon is visually sighted or to increasing the weight constraints.

A greater factor of safety seems to be essential for visual sightings, as opposed to photographic, since there are more uncertainties about the visual contrasts used. The tradeoffs between diameter, weight, and factors of safety will be discussed in conjunction with the beacon concepts.

The beacon design areas cited above and in Table 3-IV are much larger than earlier area calculations found in the literature. Depending on the FS and contrast values used, the areas are equal to or less than some related current beacon calculations. The variations in the values cited herein and other past and current computed sizes are due to such factors as:

1. Lunar background assumptions
2. Limitations of seeing conditions on resolution angle and the choice of resolution angle for computational purposes
3. Telescope magnification factor and its interrelationship with seeing conditions.
4. Range
5. Telescope transmission
6. Atmospheric transmission
7. Choice of beacon reflectance

The effect of these is explained in Appendix A.

Of the above seven variables, all but the range and telescope transmission vary with time. The lunar background varies cyclicly; the beacon reflectance is a decaying function, and the resolution angle, telescope magnification, and atmospheric transmission are interrelated factors which vary statistically from hour to hour and night to night in a general yearly cycle basis. Instead of arbitrarily choosing a given value for each of these time-dependent variables, a time function could be applied to the cyclical and decaying functions and a probability function to the other variables. These could all then be integrated to yield a time-dependent probability of detection. Such an expression would be complex and expensive to develop. However, the resultant calculations would give a more realistic concept of beacon detectability than when using arbitrarily chosen values such as have been listed in this report. Despite the arbitrary choice of values for many of these values, the beacon areas calculated appear conservative.

3.3.2 Beacon Area, Viewing Time, Observation Frequency and Field of View

The variables affecting beacon area, observation frequency, and field of view are shown in Table 3-V. It is desirable to obtain a maximum field of view for a given beacon area. Either a sphere or hemisphere will give the desired large field of view. However, each of the structures is inefficient in its use of reflective area. If one is willing to increase the orientation specifications for a given beacon, the beacon field of view can be maintained while decreasing beacon area up to a certain point. The concepts of spherical arches and caps efficiently provide a large field of view with minimum area. Figures 3-3 and 3-4 list the beacon areas for the arch and cap-type beacon concepts as a function of the fields of view that are attainable.

The cap can be closely approximated by a series of flat facets to simulate the continous reflected signal which is attainable from a spherical surface. The half angle of the field of view attainable from a flat reflector, having the required design area, is equivalent to

TABLE 3-

VIEWING TIME, FIELD OF VIEW AN
FOR VARIOUS BASIC B

Beacon Type			Viewing Time Fraction of Calend Beacon Visible fr	
Name	Classification Number (see Fig. 3-2)	Field of View FOV = Field of Reflection	Earth Observation (single point)	Cislu from
Sphere	1.1.1	4π steradians	1.0	
Hemisphere	1.1.2	2π steradians	1.0	
Lune	1.1.3	$2\theta^{*}$ steradians max	1.0 if $\theta \geq 8^{\circ}$	
Cap	1.1.4	$\frac{8\theta^2}{\pi}$ steradians max	1.0 if $\upsilon \geq \frac{\pi}{2}$	
Arch $\pm 4^{\circ}$ latitude	1.1.5	$\pm 8^{\circ}$ selenographic latitude	1.0	
$\pm 45^{\circ}$ longitude		$\pm 90^{\circ}$ selenographic longitude		
$\pm 47^{\circ}$ latitude $\pm 90^{\circ}$ longitude		2π steradians	-	
$\pm 47^{\circ}$ latitude $\pm\theta^{\circ}$ longitude		4θ steradians	-	
N facets	1.2.3	$Nx7.13x10^{5}$ steradians	$Nx1.1x10^{-4} \sim$ Nx29 min/yr max	Nx
Rotating 90° cylindrical segment	2.1.3	2π steradians	$\frac{a_b}{a_{\text{earth hemisphere}}}$	$\frac{a}{a_c}$
Oscillating $\pm 47^{\circ}$ cylindrical segment $\pm\theta$ oscillation		4θ steradians	$\frac{a_b}{a_{\text{earth arch}}}$	
N-flats rotating about 2 axes	2.2.3	4π steradians	$\frac{a_b}{a_{\text{earth sphere}}}$	

* θ = angular measurement; lune width; cone half angle, arch length from arch

** rps or cps = rota[illegible] cycles per second = 0.1 x 360° ; instantaneous f

V

D OBSERVATION FREQUENCY
EACON CONCEPTS

- lar Year om Random inar Observation 2π steradian FOV	Observation Frequency within FOV	Orientation Requirements
1.0	continuous	none
1.0	continuous	Axis of symmetry in line with local vertical
$\frac{\theta}{94^{o}}$	continuous	Longitudinal axis of lune parallel with lunar latitude; axis of symmetry of lune oriented to mean solar selenographic latitude
$\frac{2\theta}{\pi}$ max	continuous	Attain maximum field of view by pointing axis of symmetry at the bisector of the angle defined by local vertical and moon-sun axes
-	continuous	a. Longitudinal axis of arch parallel with lunar latitude axis of symmetry pointed to mean solar selenographic latitude
1.0	continuous	b. Same as above
$\frac{2\theta}{\pi}$ max	continuous	c. Same as above
$..135x10^{-5}$ max		Accurate orientation required for specific earth detection point
$\frac{a_b}{\text{islunar hemisphere}}$	1 ≤ 0.1 sec flash in 1/* rps seconds	90^{o} cylindrical segment rotated to form an hemispherical approximation; axis of rotation parallel with the local vertical
$\frac{a_b}{a_{\text{cislunar arch}}}$	2 ≤ 0.1 sec flashes in ** 1/cps sec	Axis of oscillation is perpendicular to the axis of symmetry and parallel to local latitude for earth detection; parallel to local meridian for cislunar case
$\frac{a_b}{a_{\text{cislunar sphere}}}$	N ≤ 0.1 sec flashes in $1/(rpm_1 \times_{**} rps_2)$ sec	

:enterline; oscillation angle

ield of view

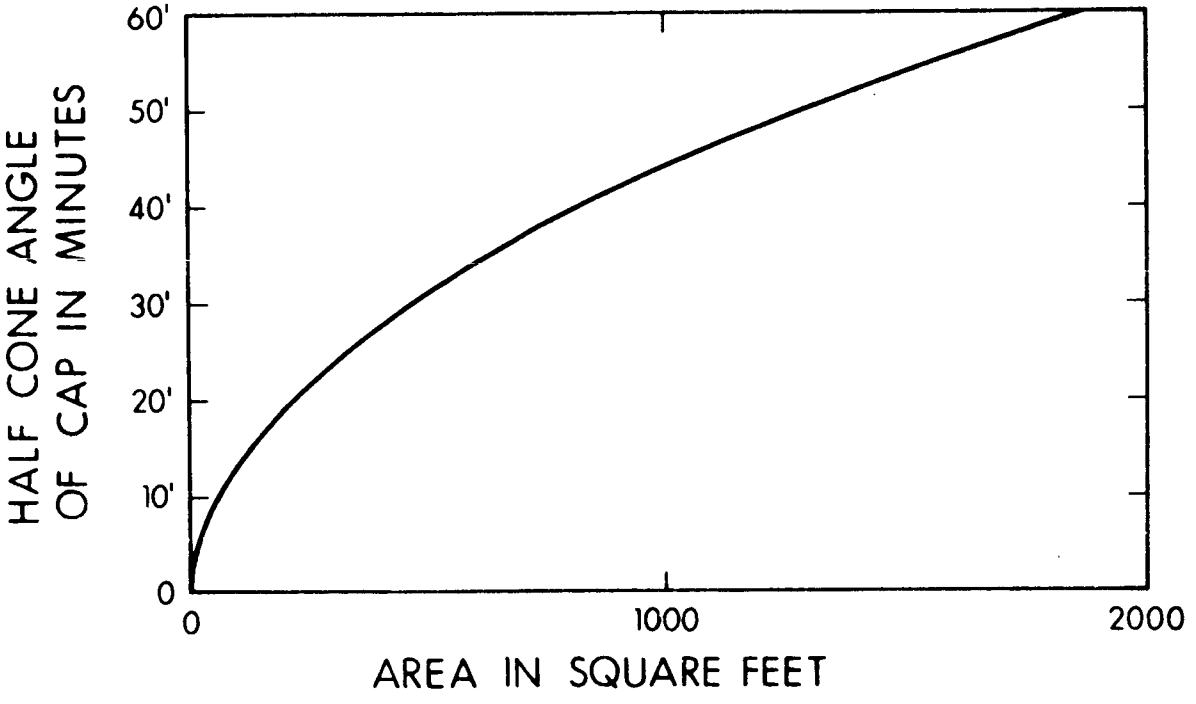

FIG. 3-3 AREA OF EARTH CAP BEACON VS CONE HALF ANGLE BASED ON A 2790 FT SPHERICAL DIAMETER

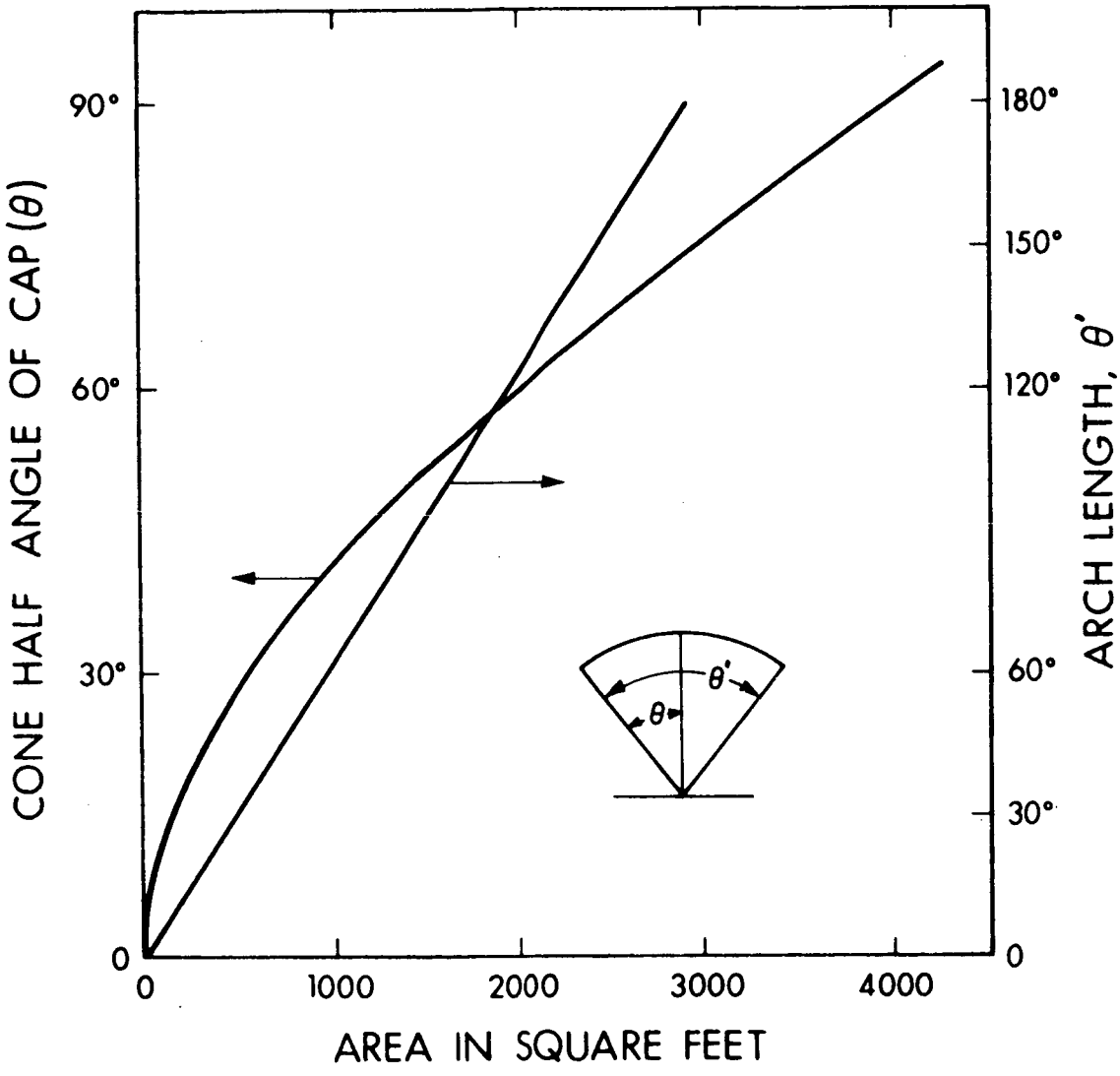

FIG. 3-4 AREA OF CISLUNAR CAP AND ARCH BEACONS, BASED ON A 50.5 FT SPHERICAL RADIUS, VS CAP HALF CONE ANGLE AND $\pm 47^{o}$ ARCH ANGULAR LENGTH

the half angle of the solar disc or 0.00464 radians. To attain a continuous signal over a greater field of view, additional facets must be located with respect to the first facet such that the separation angle between facets is equal to half the solar angular subtend at the moon, 0.00464 radians; therefore, two flats can be seen twice as long as a single flat. Similarly, additional flats can be combined such that the series of facets approximates a spherical surface. Alternatively, the facets can be approximated by a spherical cap having a diameter, d_s, which can be calculated from the solar angular subtend, α, and the required flat surface area, a, such that $d_s = \frac{8}{\alpha}\sqrt{\frac{a}{\pi}}$. The field of view and, therefore, the total time which such a spherical beacon can be seen will depend upon the angular dimensions of the spherical cap.

Since it is impractical to make either the spherical or the hemispherical beacons within either the earth or cislunar weight constraints, the maximum field of view cannot be achieved within the weight limitations without either increasing the complexity of beacon orientation problems or reducing the beacon signal viewing time. Reducing the beacon signal viewing time means that a flashing signal must replace a continuous beacon signal. The minimum required area for the earth beacon is a spherical arch $\pm 4^{\circ}$ wide and $\pm 45^{\circ}$ long and 2790 ft in diameter. Such an arch will continuously reflect solar rays to the earth throughout each lunar month over the maximum variation of the librations of the moon with respect to the earth, if aligned with its longitudinal axis parallel to the lunar latitude.

Since the selenographic latitude of the sun varies by less than $\pm 2^{\circ}$, a cislunar beacon arch $\pm 47^{\circ}$ wide and $\pm 90^{\circ}$ long, located with its longitudinal axis parallel to the lunar landing site latitude and its axis of symmetry pointed to the median solar selenographic latitude, will continuously reflect to the hemisphere defined by the local horizon. Similarly, if the mission time is known, then only a spherical cap $\pm 45^{\circ}$ in every direction, with its optical axis pointed at the bisector of the angle defined by the local vertical and the moon-sun axes at the mission time will be sufficient to cover the entire hemispherical field of view bounded by the local horizon at the beacon.

It is shown by the above examples that by increasing the complexity of beacon orientation, that the maximum field of view can be maintained, even with beacons of decreasing area. Similarly rotating beacons can retain the same field of view at a sacrifice in viewing time. The smaller the beacon size for a specific concept, the less frequent will be the beacon flashes to a given portion of the field of view.

Figure 3-5 shows the viewing time which an orbiting vehicle sees the beacon site for 100 and 200 nautical mile orbits for various fields of view which are symmetrical about the local vertical. The maximum viewing time is 16 minutes; therefore, the flash frequency of flashing beacons should be as short as possible. This would result in a large number of flashes per unit time which would increase the chances and, therefore, the probability of detection. Note that the maximum time per orbit for viewing the beacon site, about 16 minutes, is similar for both the 100 and 200 nautical mile orbits for the 400 nautical mile slant range limitation. This similarity arises because the field of view for the 200 nautical mile orbit is much less than that of the 100 nautical mile orbit because of the 400 nautical mile slant range limitation. The resultant arc lengths divided by the respective orbit velocities of 5000 ft/sec and 5220 ft/sec, for the 200 and 100 nautical mile orbits, gives the similar viewing times.

For equivalent longitudinal fields of view which are symmetrical about the local vertical, the total view time for the 100 nautical mile orbit is 0.5 that of the 200 nautical mile orbit. As an approximation, the view times for any other orbit heights for a given longitudinal field of view, $t_{h,\theta}$, can be approximated by the relationship $t_{h,\theta} = t_{200,\theta} \times \frac{h}{200}$ where $t_{200,\theta}$ is the 200 nautical mile orbit and h is the orbit height in nautical miles. The number of flashes visible during the one-orbit pass, N, are related to the time, $t_{h,\theta}$, and the flash frequency, f, by the relationship $N = t_{h,\theta} f$. Therefore, the flashes visible in any orbit can be increased by either varying

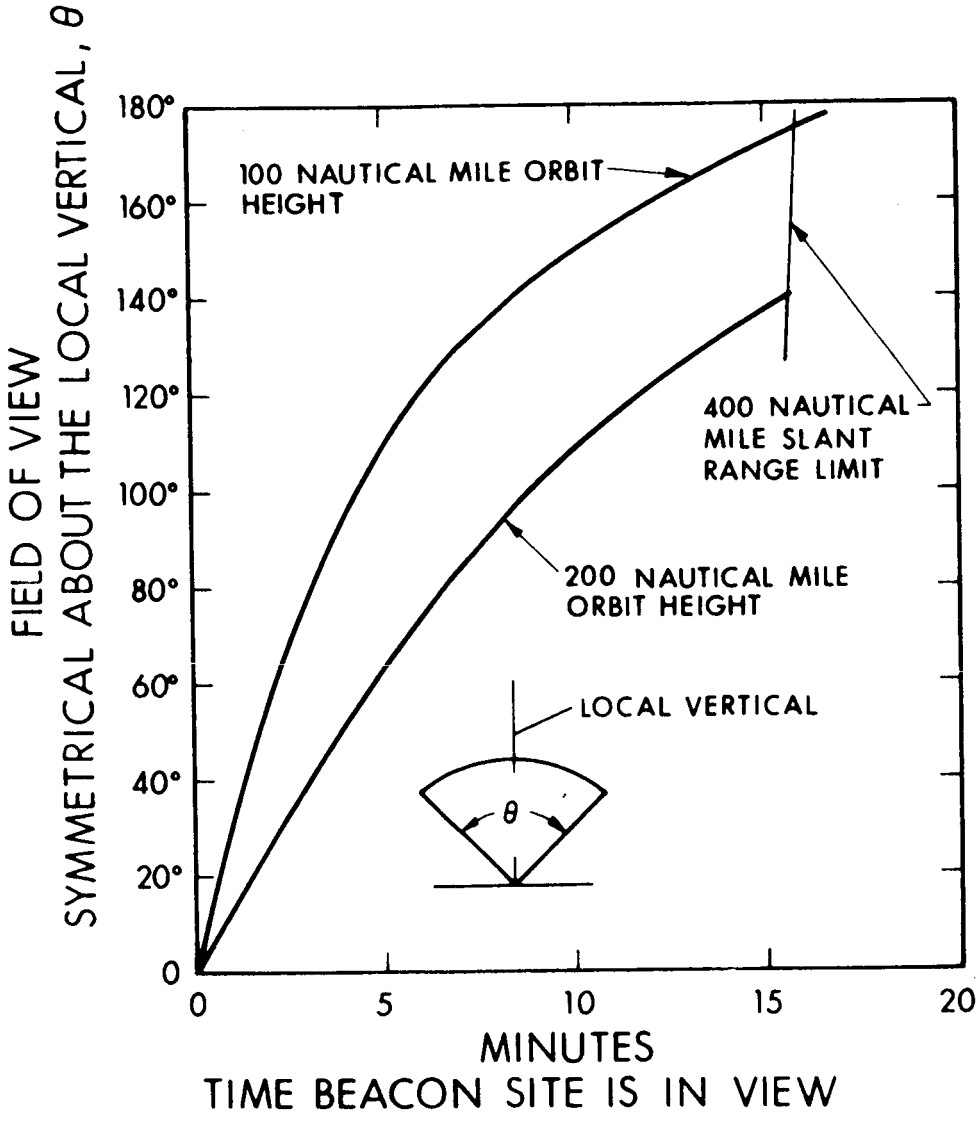

FIG. 3-5 FIELD OF VIEW VERSUS BEACON SITE VIEWING TIME

the orbit height, beacon field of view, flash frequency or the orbit velocity as in the deceleration prior to the LEM descent.

The relationships between area and beacon flash will be discussed in greater breadth under the discussion of specific beacon concepts.

The accuracy of the beacon surface will affect both the beacon field of view and the required area to produce a given signal intensity. In many types of flat designs it may be more advantageous, from a weight standpoint, to accept the optical sag due to gravitational effects than to provide the rigidity necessary to minimize distortion. Using a paraboloidal sag approximation where the sag, $S = \frac{r^2}{2R}$, where r is the mirror radius and R the mirror radius of curvature; the edge slope correspondingly is $\frac{dS}{dr} = \frac{r}{R}$; therefore, the allowable mirror sag is $\frac{S}{r} = \frac{1}{2}\left(\frac{dS}{dr}\right)$. Assume that the maximum error in mirror flatness is ±1 minute of arc, then the flatness tolerance would be ±0.000147 inches/radial inch.

A rim error of ±1 min. in flatness would require an area increase of 17.5 percent to insure the required beacon intensity. Correspondingly, the area increase for any other rim angular error would be

$$\left(1 + \frac{2.67\,|\theta|}{0.00928}\right)^2 - 1$$

where θ is the edge error in radians.

Since a torus rigidized flat is attractive from a weight standpoint, the tension, T, the film thickness, t, and lunar density, ρ, are plotted for various square areas, A, as a function of the maximum angular error on the flat in Fig. 3-6. From this, the maximum tension required to keep a 33-plus square foot earth beacon optical flat accurate to within ±1 minute of arc would be 68 pounds, which can easily be attained with an inflatable torus.

The angular positions of the LEM or CM vehicles as a function of altitude at the $\pm 5^{\circ}$ latitude mission corridor walls with

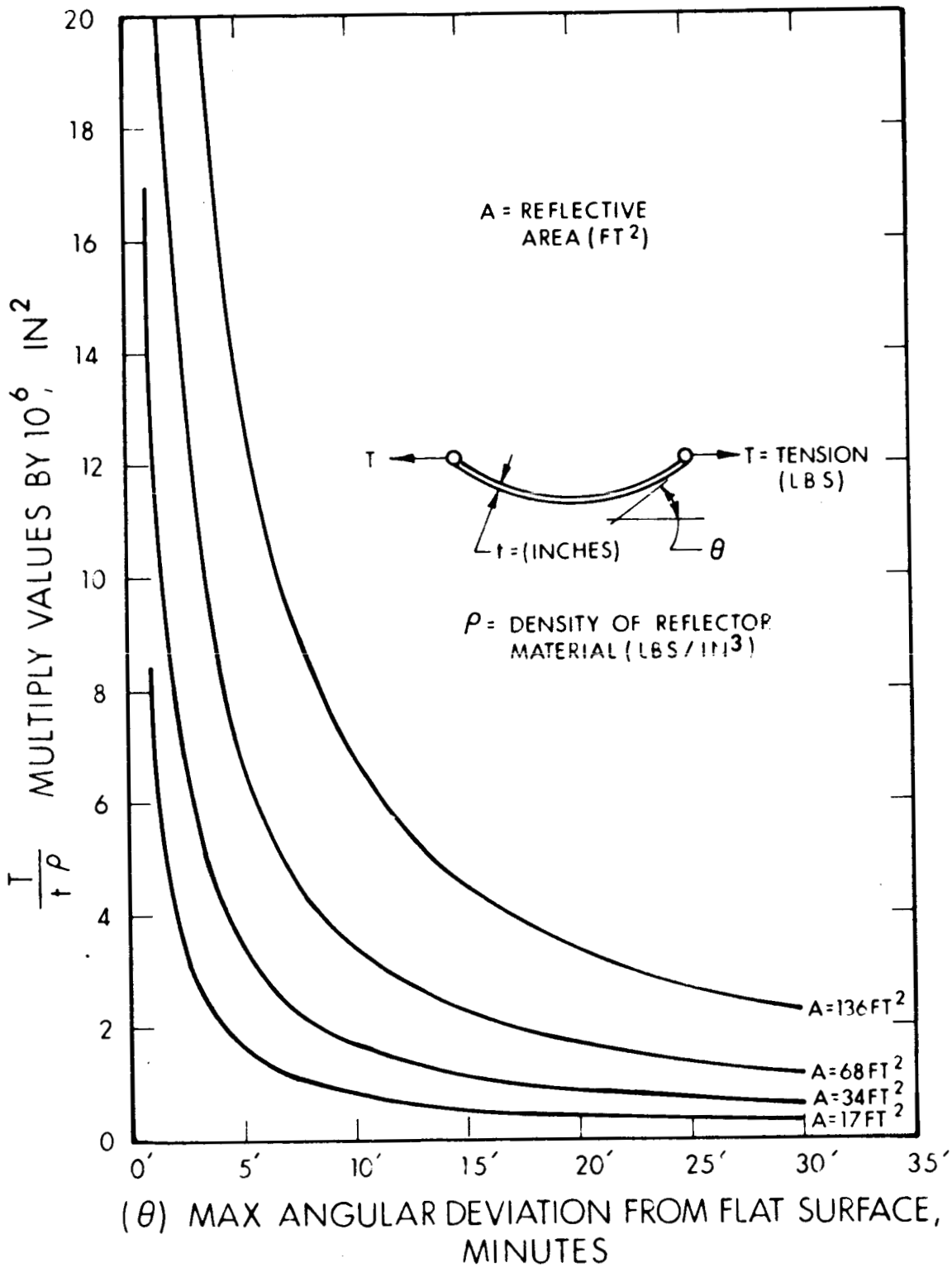

FIG. 3-6 TENSION FACTOR VERSUS ANGULAR ERROR FOR VARIOUS REFLECTOR AREAS

respect to a beacon located on the lunar equator are shown in Fig. 3-7. This indicates that, as the lunar orbit altitude increases, the required angular subtend of the arch required to reflect to the vehicles, decreases and will be equal to $\pm\frac{(94-\Phi)}{2}$ degrees. For a 50-nautical-mile orbit, this means that the arch need only be $\pm 33^{o}$ wide as compared with a basic design of $\pm 47^{o}$.

Figure 3-8 shows the effect of increasing orbit altitude on the viewing angle for a fixed slant range as measured in the same latitudinal plane as the beacon reflector. If the mission altitude were 200 nautical miles, then a minimum of α, or 20^{o}, could be cut from the 180^{o} length of the reflecting arch and the reflector would still maintain the desired field of view. By limiting the phase of the moon at which the beacon is observed, the beacon dimensions can be reduced still further.

3.4 Materials

Beacon materials can be chosen from a wide range of ceramics, metals and plastics. However, the environmental and design constraints limit the logical material choices to plastics, metals, and metal-plastic composite structures. Due to the severe design weight constraints, and therefore the necessity for lightweight beacon designs, the materials chosen should have high specific strength and specific rigidity in the thin foil thicknesses and lightweight sections. Table 3-VI summarizes many of the materials which can be chosen for beacon construction.

Of the plastic materials, DuPont's "Kapton" type H film has superior temperature and structural properties. Of the metal foils, aluminum is the most desirable. However, electroformed nickel can achieve slightly higher specularity and will resist micrometeoroid attack better than aluminum.

Micrometeoroid mirror attack has been correlated with the density of the mirror material, the specific heat of the mirror material, the temperature difference between the mirror melting point and ambient

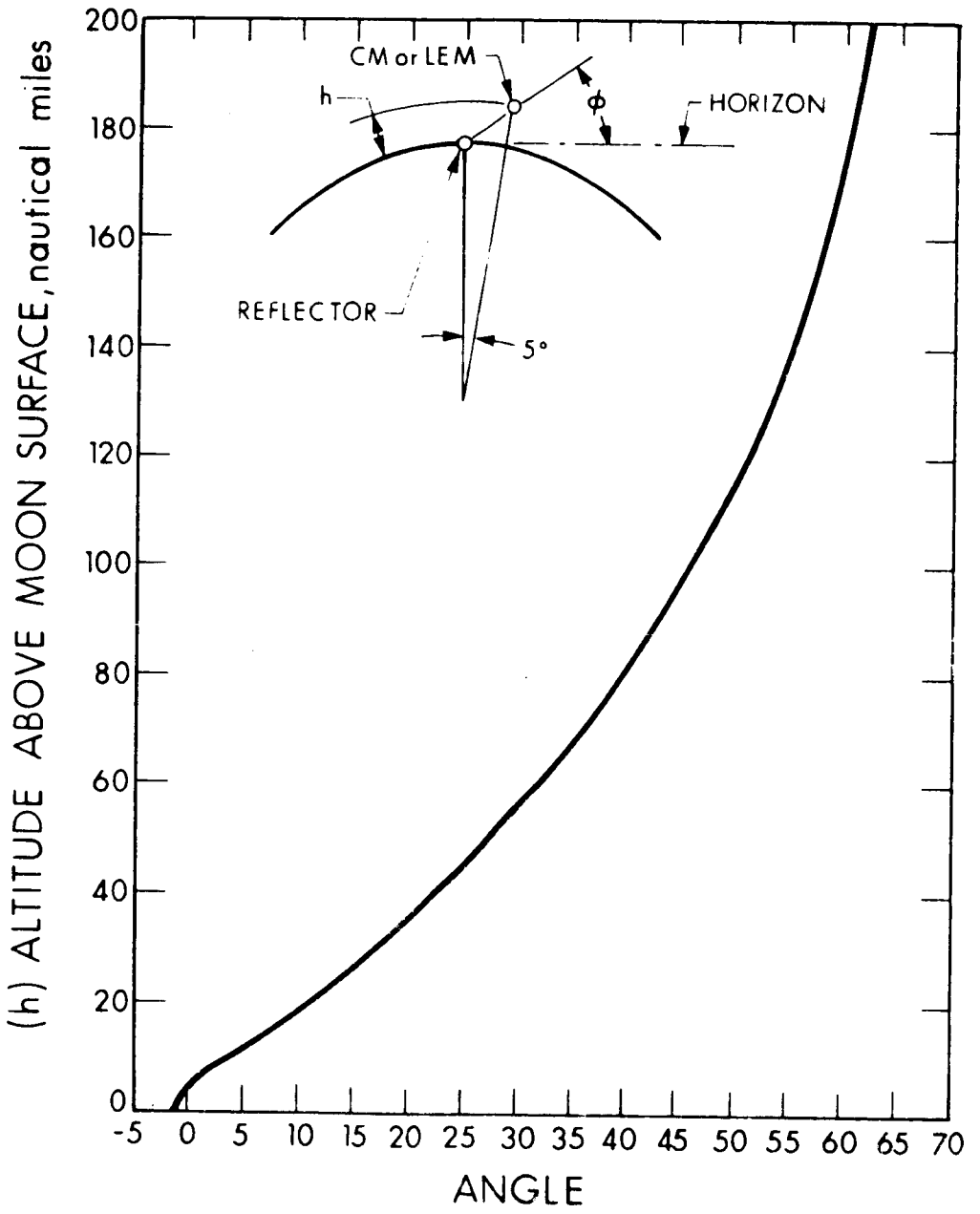

FIG. 3-7 ORBIT HEIGHT VERSUS ELEVATION ANGLE FOR A $\pm 5^{\circ}$ LATITUDE ORBIT IN THE PLANE DEFINED BY THE NORTH/SOUTH MERIDIAN THROUGH THE BEACON

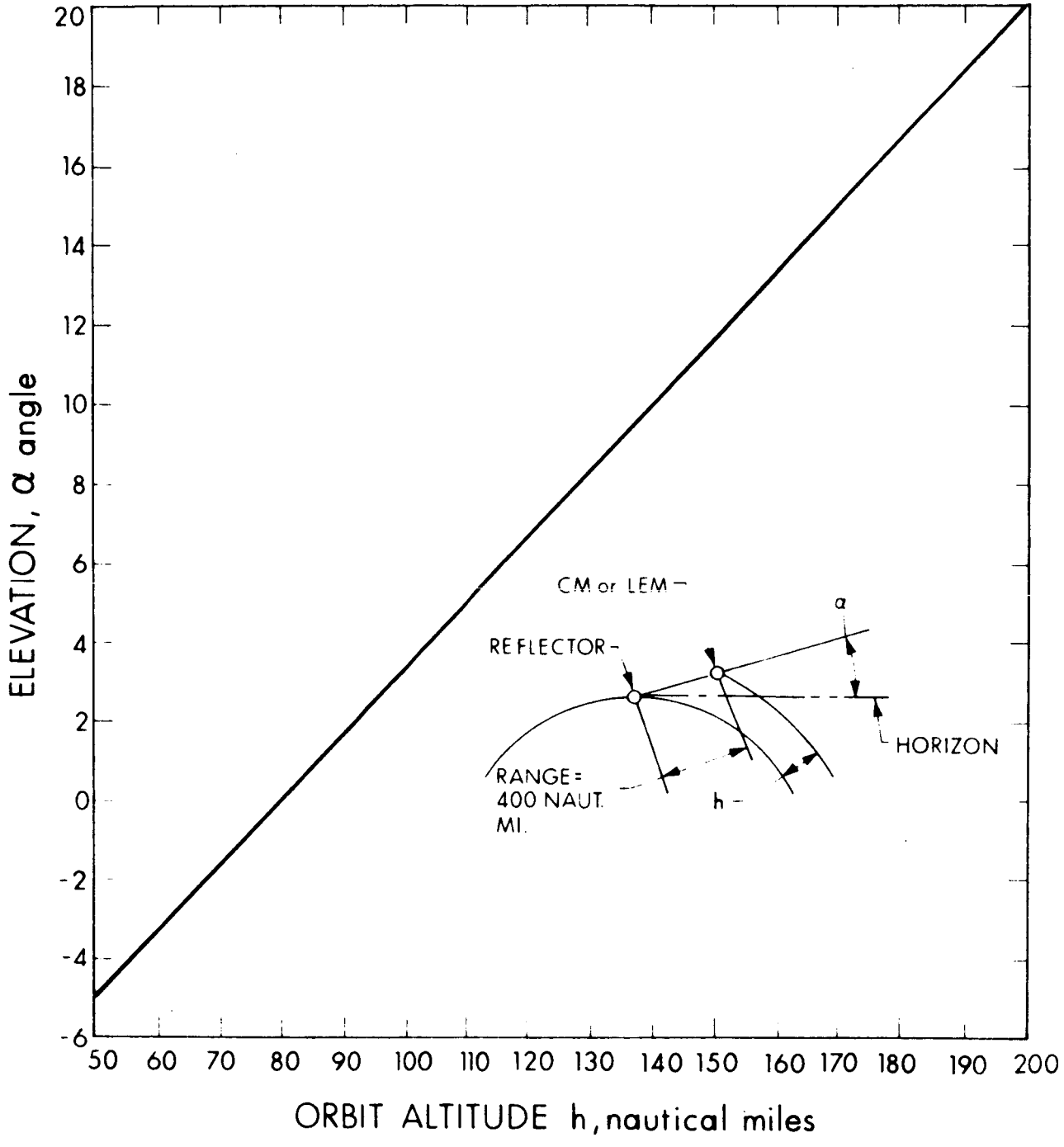

FIG. 3-8 ELEVATION ANGLE VERSUS ORBIT ALTITUDE FOR A 400-NAUTICAL-MILE SLANT RANGE IN THE PLANE THROUGH THE LATITUDE OF THE BEACON

TABLE 3-VI BEACON MATERIAL COMPARISON

CODE	MATERIAL	DENSITY (LBS/IN³)	WT/1000 FT² AT 1-MIL THICK (LBS)	ROOM TEMP. ULT. TENSILE STRENGTH (PSI)	TENSILE MOD. OF ELASTICITY (PSI)	SOLAR RADIATION RESISTANCE	MAX. CONTINUOUS TEMP. (°F)	MIN. CONTINUOUS TEMP. (°F)			COMMENTS
1	TITANIUM (6AL-4V)	.164		130,000	$\frac{15.5}{16.0} \times 10^6$	EXCELLENT	[A]	[A]			
1	MAGNESIUM	.064		30,-40,000	6.5×10^6	EXCELLENT	[A]	[A]			
1	ALUMINUM ALLOY	.098		18,-80,000	$\frac{10.0}{10.6} \times 10^6$	EXCELLENT	[A]	[A]			
1	STAINLESS STEEL	.286		75,-185,000	$\frac{28.0}{29.0} \times 10^6$	EXCELLENT	[A]	[A]			
1	BERYLLIUM COPPER	.297		60,-195,000	$\frac{17.0}{19.0} \times 10^6$	EXCELLENT	[A]	[A]			
1	BERYLLIUM	.066		30,000	40×10^6	EXCELLENT	[A]	[A]			
1	TEFLON	.08		2,-4,300	$.058 \times 10^6$	GOOD	550	-425			DYNAMIC & STATIC COEF. OF FRICTION = .04
2	ALUMINUM FOIL	.10	14.4	13,000	10.0×10^6	EXCELLENT	[A]	[A]			
2	ETCHED ALUMINUM FOIL		4.3	13,000	10.0×10^6	EXCELLENT	[A]	[A]			USED FOR INNER SURFACE OF EXPANDABLE REFLECTORS. 70% OF ALUMINUM IS REMOVED BY CHEMICAL ETCHING.
2	NICKEL FOIL	.32	46.0	45,000	30.0×10^6	EXCELLENT	[A]	[A]			VALUES GIVEN ARE FOR ELECTROLYTIC NICKEL
3	"KAPTON" TYPE H	.051	7.4	25,000	$.43 \times 10^6$	GOOD	752	-452			
3	TEDLAR (PVF)	.050	7.17	19,000	$.28 \times 10^6$	GOOD	225	-100			
3	POLYPROPYLENE	.033	4.7	26,000	$.32 \times 10^6$	POOR	330	-80			VALUES GIVEN ARE FOR UNION CARBIDES' ORIENTED FILM
3	TEFLON FEP	.077	11.4	3,000	$.07 \times 10^6$	GOOD	400	-425			TYPE "C" CAN BE BONDED WITH CONVENTIONAL ADHESIVES.
3	MYLAR	.050	7.25	25,000	$.55 \times 10^6$	POOR	300	-75			
4	THERMAL COATING (WHITE PAINT)	.087	12.5	——	——	GOOD	[B]	[B]			APPLIED .001" THICK. COATING # S-13 DEVELOPED BY ILLINOIS INSTITUTE OF TECHNOLOGY RESEARCH INSTITUTE
4	PRIMER-THERMAL COATING	.056	8.0	——	——	GOOD	[B]	[B]			APPLIED .0005" THICK
4	ADHESIVE-FILM & FOIL LAMINATES	.069	10.0	——	——	GOOD	300	-328			APPLIED .00003" THICK. VALUES GIVEN ARE APPROX. MFG. BY SCHUELDAHL - # GT-301

CODE:
1 = STRUCTURAL & BEARING MAT'L
2 = METAL FOILS
3 = PLASTIC FILMS
4 = THERMAL COATINGS & ADHESIVES
5 = SELF RIGIDIZING LAMINATES

NOTES:
* .18 MIL AL FOIL ON BOTH SIDES
** .18 MIL AL FOIL ON OUTSIDE & .18 MIL ETCHED AL FOIL ON INSIDE

[A] WILL WITHSTAND LUNAR TEMP. RANGE INDEFINITELY
[B] MAT'L WAS NOT AFFECTED AFTER BEING TESTED IN SIMULATED SPACE ENVIRONMENT FOR 6 MONTHS.

CODE	LAMINATE	FILM THICKNESS (MILS)	METAL FOIL THICKNESS (MILS)	ADHESIVE THICKNESS (MILS)	TOTAL THICKNESS (MILS)	WT/1000FT² * (LBS)	WT/1000FT² ** (LBS)			COMMENTS
5	AL-KAPTON-AL	.5	2x.18	2x.03	.92	9.5	7.7			
5	AL-TEDLAR-AL	.5	2x.18	2x.03	.92	9.4	7.6			
5	AL-POLYPROPYLENE-AL	.5	2x.18	2x.03	.92	8.1	6.3			
5	AL-FEP-AL	.5	2x.18	2x.03	.92	11.5	9.7			
5	AL-MYLAR-AL	.5	2x.18	2x.03	.92	9.4	7.6			

mirror temperature and the latent heat of fusion of the mirror material. These physio-thermal properties favor a nickel reflector surface for minimum micrometeorite damage. However, aluminum reflector surfaces will yield greater net reflective area per unit weight even after micrometeorite damage.

3.5 Reflector Orientation Studies

3.5.1 Purpose of Study

The purpose of the reflector orientation study is sevenfold:

1. Determine the orientation angles (γ_o, σ_o) of the reflector, relative to the moon's surface, which enable the reflected light to strike a given point on the earth's surface at a specified time.
2. Determine the path [$\Theta(t')$, $\Phi(t')$] of the reflected light across the earth's surface, for a given orientation of the mirror.
3. Determine if the reflected light from the fixed mirror intercepts the earth in succeeding months.
4. Determine the times (t_{mi}) that an observer on earth enters and leaves the cone of reflected light, or merely enters or leaves the light.
5. Develop a method (i.e., mechanical device) for orienting the reflector on the moon's surface.
6. Determine the perturbed path of the reflected light on the earth's surface due to errors in the orientation of the reflector by the astronaut.
7. Determine the orientation of the mirror which allows the reflected light to intercept the Apollo vehicle orbiting the moon.

3.5.2 Completed Tasks

Item 1

The computation of the reflector orientation angles γ_o, σ_o requires the use of Programs I and II (refer to "Schematic of Computer Program", Fig. 3-9) plus the values of i(t), $\Lambda(t)$, $\Omega'(t)$ (orientation angles of moon relative to earth), and X_{em}, Y_{em}, Z_{em};

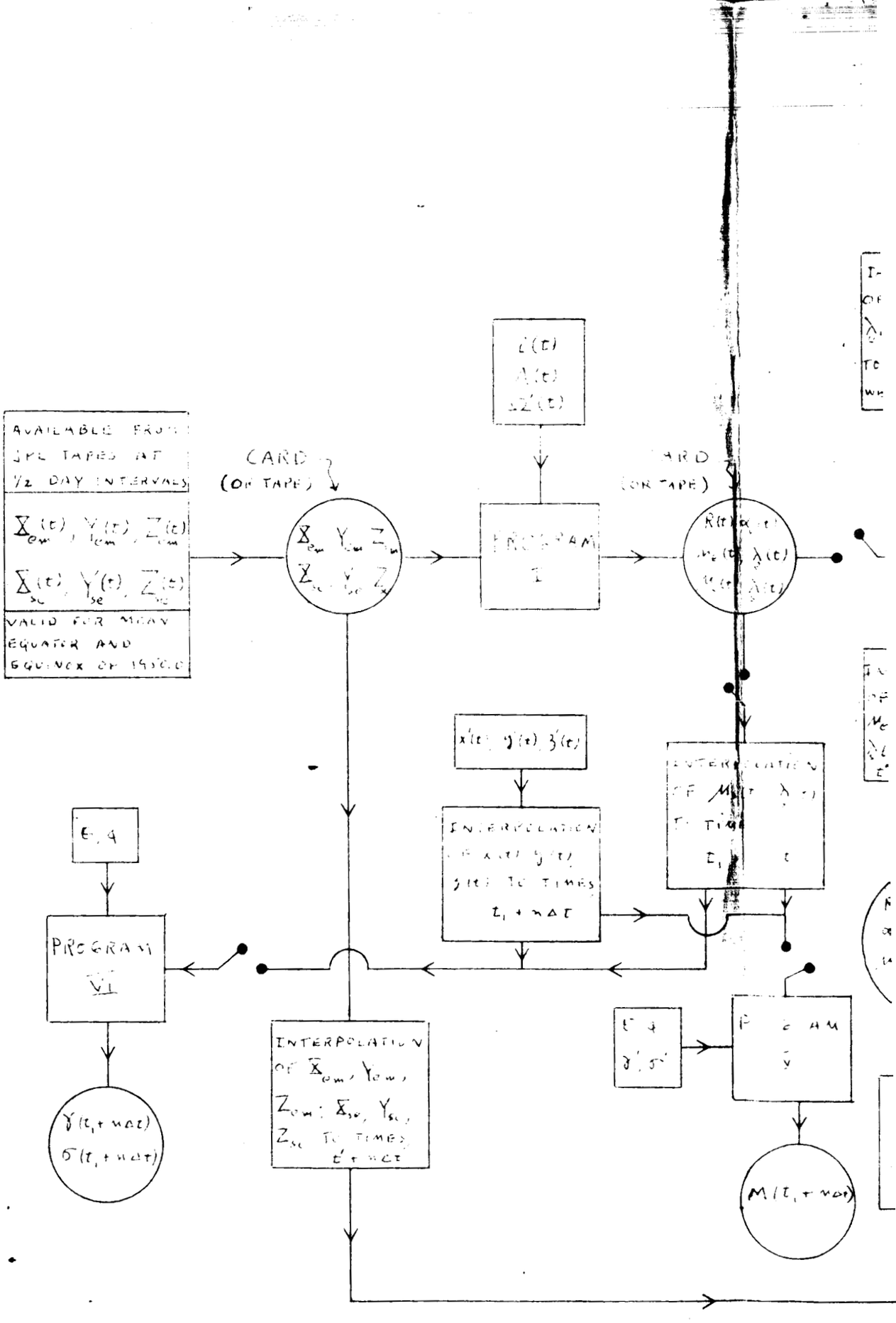

FIG. 3-9 SCHEMATIC OF COMPUTER PROGRAM

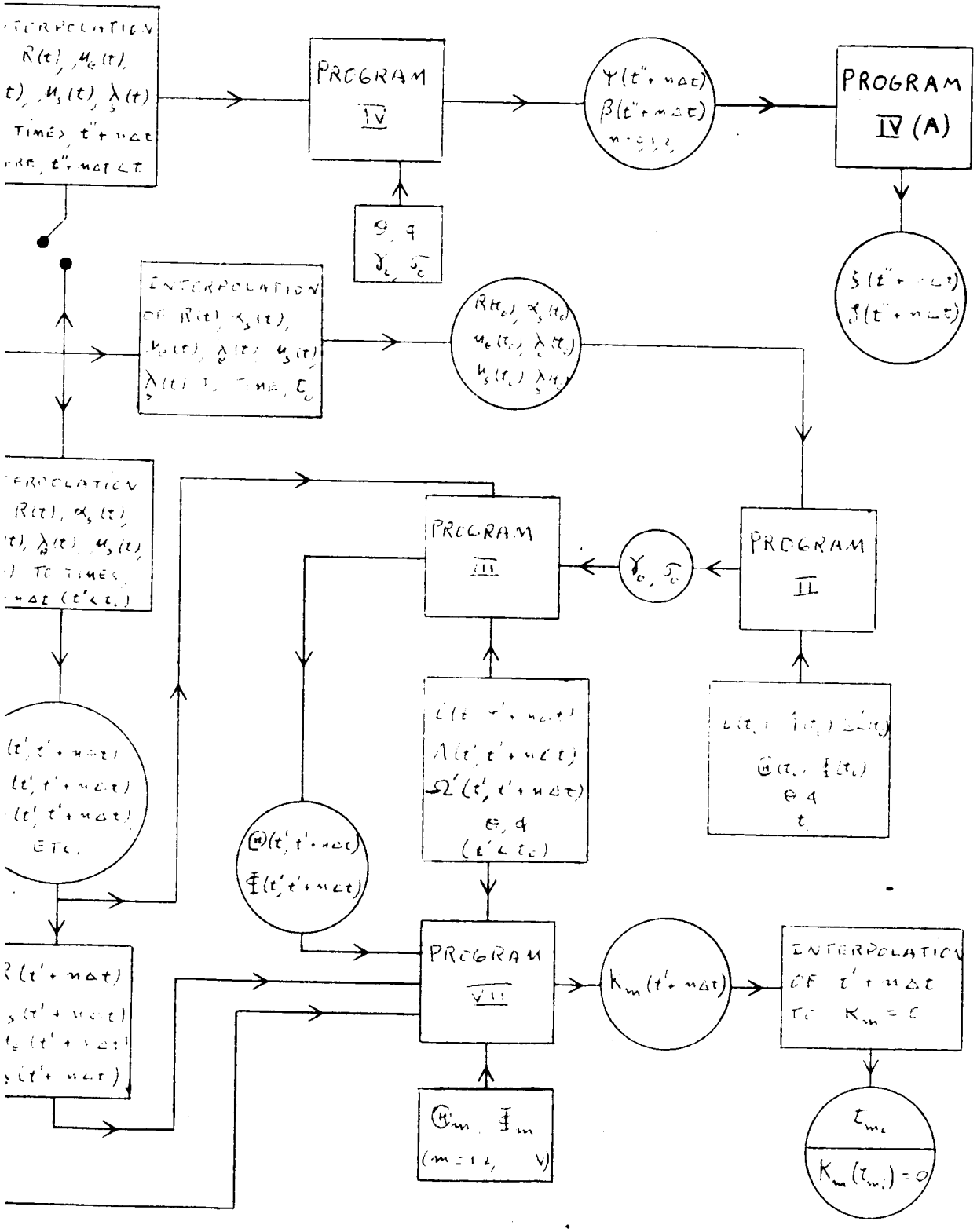
PROGRAM IV
PROGRAM IV (A)
PROGRAM III
PROGRAM II
PROGRAM VII

X_{se}, Y_{se}, Z_{se} (position coordinates of moon relative to earth, and earth relative to sun) at one or one-half day intervals. The latter six coordinates will eventually be obtained from the JPL ephemeris tapes. For the purpose of early machine computation, these six coordinates have been obtained (at one-day intervals) from the 1962 edition of the American Ephemeris and Nautical Almanac. Programs I and II, along with $i(t)$, $\Lambda(t)$, $\Omega'(t)$, have been programmed on the EOS IBM 1620 digital computer (refer to appendix) and values of γ_o σ_o have been obtained. The results of a sample calculation are shown on pages 15 and 17 of the September monthly report.

JPL has promised to provide EOS with the earth's and sun's selenographic coordinates (μ_e, λ_e and μ_s, λ_s, respectively) at one-day intervals for the years 1965-1980. If we make use of their results, then that part of Program I which calculates these coordinates can be eliminated.

Item 2

The computation of the path $\Theta(t')$, $\Phi(t')$ (= longitude and latitude, respectively, of the axis of the reflected light cone) of the reflected light across the earth's surface requires the use of Programs I and III, and the values γ_o, σ_o. Program III (refer to appendix) has been put on the digital computer and values of $\Theta(t')$, $\Phi(t')$ have been obtained. The results of a sample calculation are shown on page 17 of the September monthly report.

Item 3

In order to learn if the reflected light from the fixed (i.e., γ_o, σ_o are fixed) mirror intercepts the earth in succeeding months, the computation of Θ, Φ would have to be initiated each month, at a time when the relative positions of the earth, moon, and sun would seem favorable for such an interception. The computation would continue until the reflected light no longer shone on the earth, or until it was clear that this light would not intercept the earth. This computation has not been done.

Item 4

The computation of the entrance and exit times t_{mi} (m identifies the observation station; i = 1 signifies entrance, i = 2 signifies exit) of an earth-bound observation station into and out of the reflected light cone, requires the use of Programs I and VII, the values of $\Theta(t')$, $\Phi(t')$, and the coordinates of the station(s) Θ_m, Φ_m. Program VII was put on the digital computer and an initial attempt to generate the t_{mi} was unsuccessful, due to the use of $\cos H_1$, instead of $\sin H_1$ (refer to appendix). The desired Program VII is given in the appendix, but it has not yet been programmed on the digital computer.

Item 5

According to the scheme devised by B. E. Kalensher for orienting the reflector on the moon's surface (refer to pages 14-15 and pages 20-23 of the September and October monthly reports, respectively), a knowledge of the four angles ψ, β, ζ, ξ is required. The computation of ψ, β requires the use of Programs I and IV and the values of γ_o, σ_o, θ, φ (θ, φ = longitude and latitude, respectively, of reflector on moon), and the computation of ζ, ξ requires Program IV(A) and the values of ψ, β. Program IV (refer to appendix) has been put on the digital computer and values of ψ, β have been obtained. The results of a sample calculation are given on page 15 of the September monthly report. Program IV(A) is given in the appendix, but it is not yet programmed on the digital computer.

Item 6

The perturbed path, $\Theta(t') + \Delta\Theta$, $\Phi(t') + \Delta\Phi$, of the reflected light on the earth's surface can easily be determined by introducing perturbed values $\gamma_o + \Delta\gamma_o$, $\sigma_o + \Delta\sigma_o$ into Program III. Since the reflected light will move a distance of approximately 7200 n.mi. across the earth's disc per degree change in γ_o or σ_o, we see that $\Delta\gamma_o$ and $\Delta\sigma_o$ must be less than 3440/7200 deg. = 0.48 degrees. A calculation of the perturbed path has not yet been made.

Item 7

The computation of the mirror orientation angles γ, σ which enable the reflected light to intercept the module orbiting the moon, requires the use of Programs I and VI and the position coordinates of the module, $x'(t)$, $y'(t)$, $z'(t)$, measured in the orthogonal coordinate system x', y', z' fixed in the moon. The computation of the angle, M, between the reflected ray and the radius vector from the reflector to the module requires the use of Programs I and V and the instantaneous orientation angles, γ', σ'. Programs V and VI (refer to appendix) have been programmed on the digital computer, but values of γ, σ, M have not yet been computed.

3.5.3 Conclusions and Recommendations

The computer program shown in Fig. 3-9 should be able to solve all of the geometrical problems associated with the proper orientation of the moon-based reflector. Although it was originally intended for the reflector to have a fixed orientation γ_o, σ_o, the computer program is quite able to determine the time-dependent angles $\gamma(t)$, $\sigma(t)$ which would enable the reflected light to continuously strike a specified point on the earth's surface, or continuously intercept the Apollo vehicle orbiting the moon.

If future studies reveal that the reflected light does not intercept the earth in succeeding months, then it may become desirable to drive the mirror with an elementary servomechanism. The use of a servomechanism seems particularly appropriate for the reflector whose light must intercept the module orbiting the moon.

In the near future, it may become desirable to establish communications between a space probe going to Mars or Venus and a point on the moon's surface. Communicating by means of a laser beam would be especially appropriate over these long distances. The correct pointing direction of the laser beam could readily be determined from the present computer program.

3.6 Power Systems, Drives, and Seals

Any motion imparted to the beacon will have to be initiated by energy, either external or internal to the beacon system. Various sources of power are given in Table 3-VII along with ratings for each system. Despite the complexities of a photovoltaic system, the successes of photovoltaic power systems in space still rate this as the leading space power system today. Though photovoltaic systems have been described for many dynamic beacon concepts, thermal-mechanical drives can be readily substituted for the photovoltaic system in some design concepts.

Table 3-VIII describes various drives that can be used with dynamic beacons. Though the ac motor drive is listed with the highest rating, recent developments with brushless sealed dc motors indicate that a dc drive is almost as reliable as an ac drive. Figure 3-10 depicts a typical thermal expansion drive with a clock motor. Figures 3-11, 3-12, 3-13, and 3-14 show various proven methods for sealing bearings from the high-vacuum environment including the harmonic drive, labyrinth seal, and hermetically-sealed bellows approaches. Sealing bearings by any of these methods should present no design or reliability problems.

3.7 Reliability

The reliability of the lunar-emplaced solar reflecting beacon will depend upon the following factors:

1. Erectability
2. Orientation
3. Durability in the lunar environment
4. LEM ascent dust protection

3.7.1 Erectability

Beacon erectability is primarily dependent upon the mobility of the space-suited astronaut. Stooping and bending movements will be difficult because these operations reduce the volume of

TABLE 3-VII

COMPARISON OF POWER GENERATING SYSTEMS

Generating Source	Power Generation System	Power Output	Advantages	Disadvantages	*Relative Rating
SOLAR RADIATION	Solar Cells	Electrical	Lightweight, compact, no moving parts. Prior experience with solar cells.	Solar cells are degraded due to solar radiation, meteorites, dust, etc. Power output is not constant, depends on sun-cell orientation and temperature of cells. Solar cell efficiency reduced about 60% on the moon	1
SOLAR RADIATION	Thermionic Converter	Electrical	Capable of large power output, high power-to weight ratio.	State of the art not sufficiently developed yet. Requires continuous, accurate alignment of solar concentrator with respect to converter.	5
SOLAR RADIATION	Thermal Expansion Drive	Mechanical	Simple construction, lightweight, large forces can be produced but output movement is small. Not degraded by environment.	Limited motion, must radiate heat away before output cycle can be repeated, long cycle time.	3
SOLAR RADIATION	Bimetallic Drive	Mechanical	Simple construction, lightweight, can be used for limited motion, low force applications. Prior experience with bimetals. Not degraded by environment.	Limited motion, low force output, must radiate heat away before output cycle can be repeated.	4

SOLAR RADIATION	Solar Pressure	Mechanical	Utilizes environment	Forces produced are too small (solar pressure = 1.3×10^{-9} psi), necessitating extremely large reaction areas to obtain usable output force.	9
CHEMICAL REACTION	Battery	Electrical	Self-contained power source. Space experience.	Limited operational life. May need further development to meet temperature and vacuum environment. Excessive weight for required life.	8
CHEMICAL REACTION	Hydrogen-Oxygen Fuel Cell	Electrical	Self-contained unit, three or four times the output per pound as compared to a battery.	Requires fuel supply, plumbing, etc. Excessive weight for required life.	7
NUCLEAR RADIATION	Radioisotope Thermoelectric Generator	Electrical	Self-contained, extremely long life (many years). Output independent of environment. Fairly compact (approx. size = 4" x 4" x 4"). Larger units have been successfully tested in space.	Cost of plutonium fuel element is high. Weight is about 2 to 4 pounds.	2
ASTRONAUT	Spring or Weight System	Mechanical	Astronaut can either wind a spring or use lunar objects to drive pendulum system.	Decaying force output; limited storage life; storable energy limited by spring weight or structural strength to bear pendulum weight.	6

*1 = Highest Rating

TABLE VIII

COMPARISON OF DRIVES

Power Input Required	Drive	Power Output	Advantages	Disadvantages	*Relative Rating
Electrical	Brushless dc Motor	Continuous Rotation	Long operating life, direct utilization of dc power, no inverter required.	Relatively new development.	2
Electrical	Ac Motor	Continuous Rotation	Long operating life, conventional motor construction.	Requires an inverter to convert dc to ac.	1
Electrical	Dc Motor	Continuous Rotation	Conventional motor construction, direct utilization of dc power, no inverter required.	Short operating life due to excessive brush wear in vacuum environment.	3
Mechanical	Clock-Motor	Continuous Rotation	No electronics involved.	Requires a "self-winding" mechanism such as a thermal or bimetallic expansion drive.	4
Thermal	Thermal Expansion Drive	Limited Motion	Simple, lightweight, not degraded by environment.	Limited motion, long cycle time.	5
Thermal	Bimetallic Drive	Limited Motion	Simple, lightweight, not degraded by environment.	Limited motion, long cycle time.	6

*1 = Highest Rating

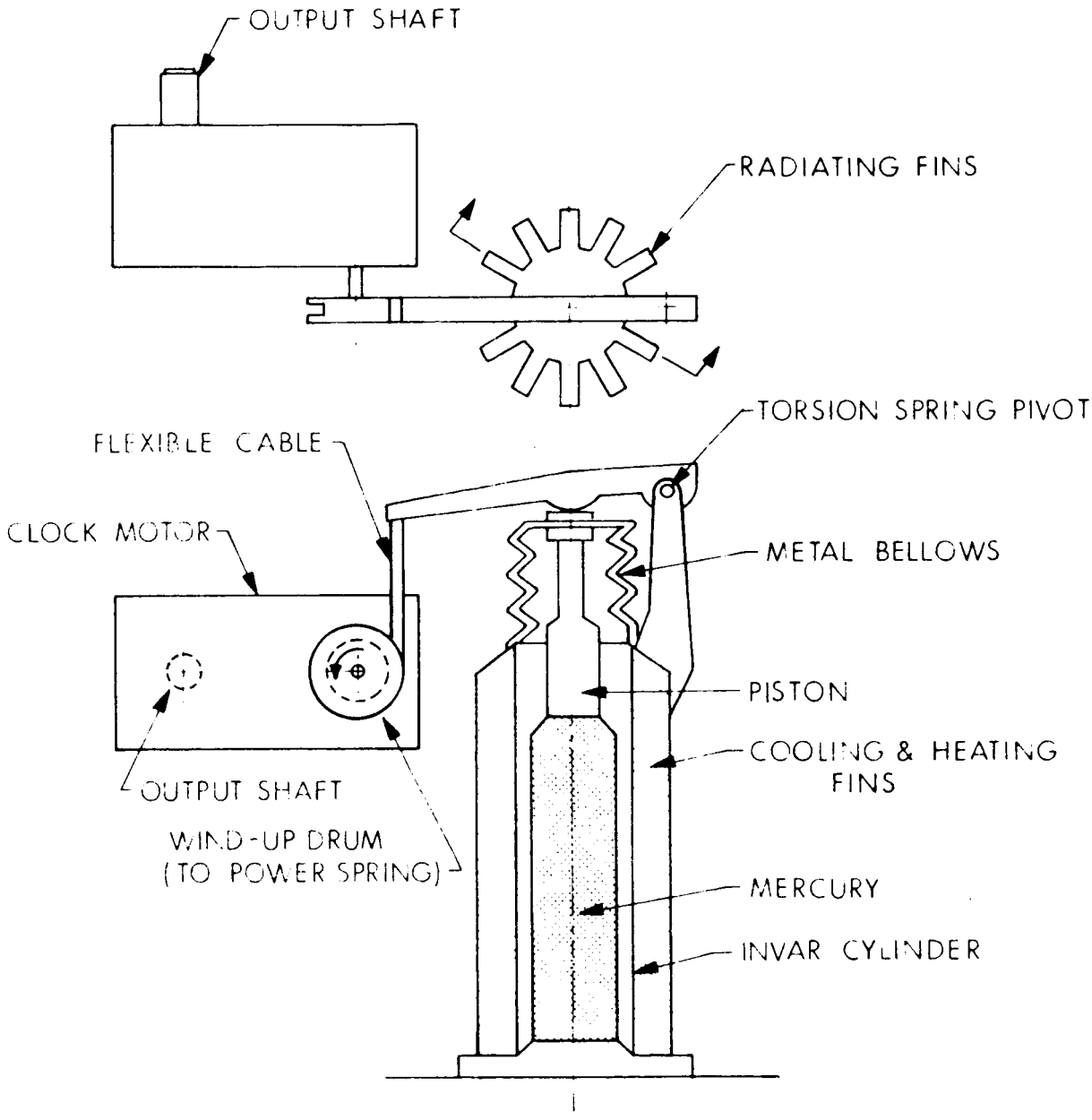

FIG. 3-10 THERMAL EXPANSION DRIVE - CLOCK-MOTOR WIND-UP DEVICE
(Thermally actuated shade regulates thermal cycle)

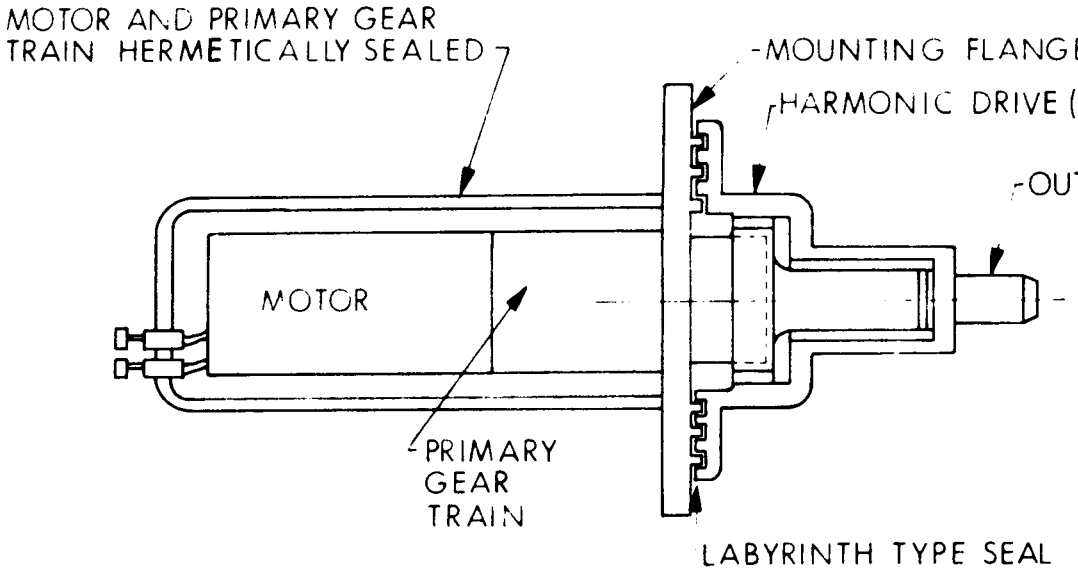

NOTE: THE MOTOR AND PRIMARY GEAR TRAIN COULD BE PRESSURIZED AND A D.C. MOTOR USED WITHOUT EXCESSIVE BRUSH WEAR, THUS ELIMINATING THE NEED FOR THE INVERTER AND A.C. MOTOR COMBINATION OR THE RELATIVELY NEW BRUSHLESS D.C. MOTOR

FIG. 3-11 HARMONIC DRIVE (primary stage hermetically sealed)

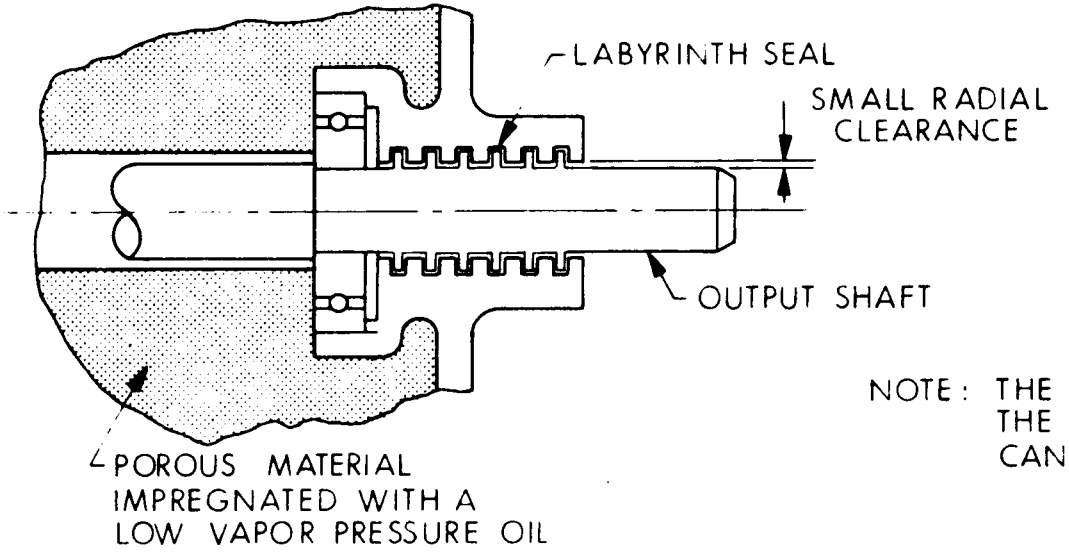

NOTE: THE LOSS OF LUBRICANT AND THEREFORE THE REQUIRED RESERVOIR OF LUBRICANT CAN BE DETERMINED

FIG. 3-12 LABYRINTH SEAL

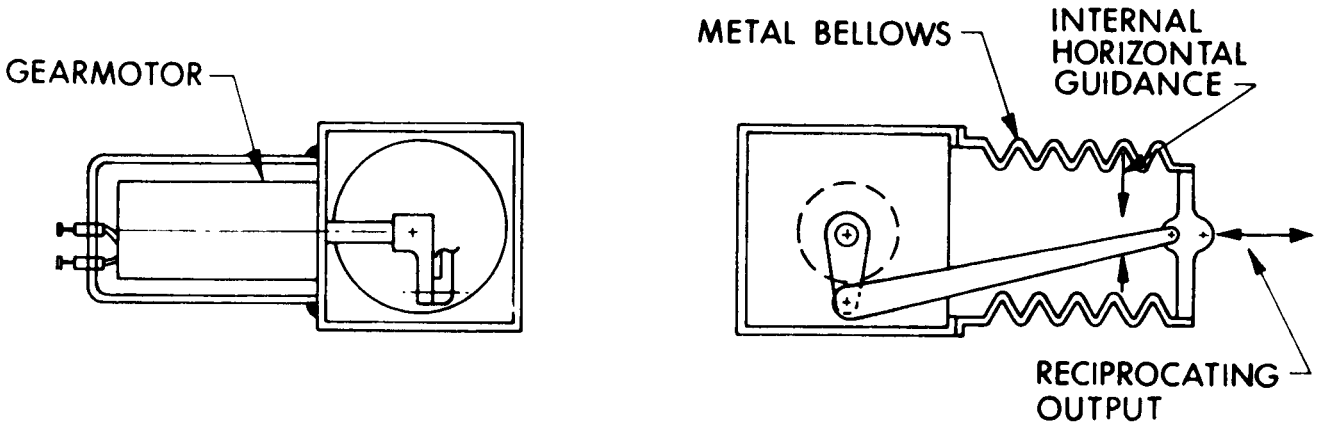

FIG. 3-13 HERMETICALLY SEALED RECIPROCATING UNIT

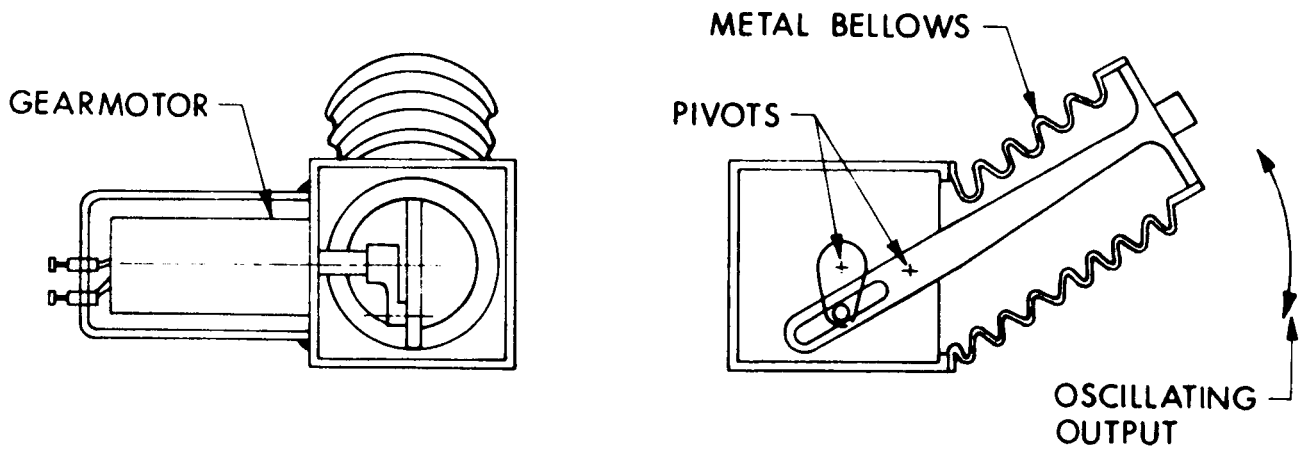

FIG. 3-14 HERMETICALLY SEALED OSCILLATING UNIT

the pressure suit. These movements will require a definite exertion to counteract the changes in the pressure suit, particularly since the low lunar gravity reduces the effective weight of the astronaut in the bending process. The manual dexterity of the suited astronaut will be equivalent to when one wears heavy mittens over rubber gloves. Though the space suit gloves are designed to curve naturally, gripping small-diameter objects for extended periods will require effort, since the pressure within the suit tends to restore the fingers to the normal position. The reduced sensitivity of the gloved fingers will present problems in handling fragile thin foils or beacon sections. It will be difficult to lift the arms higher than the head or to hold any object in front of the helmet face plate.

Erectability is also dependent upon the number of component assemblies required for the final beacon assembly. Each assembly operation will require additional time which will vary with the movements and forces required. High assembly forces may tax the astronaut and increase the total assembly time. Orientation requirements to maximize beacon effectiveness also affect erectability.

Erectability relates to reliability in that a beacon which can be readily assembled within the schedule without difficulty will have a high probability of success, and therefore reliability. Those beacons which are difficult to erect may be left unassembled if the astronaut encounters difficulties, thus reducing the reliability of the beacon concept.

3.7.2 Orientation

Primary consideration in the orientation of the solar beacons is the accuracy of the alignment sighting and adjustments. The sighting accuracy depends upon the instrument accuracy, the astronaut's precision, and the coupling between the alignment instrument and the beacon structure. The alignment instrument accuracy is dependent upon its optical and mechanical design. The precision with which

the astronaut takes the alignment sightings will depend upon the astronaut's training, the relationship between the helmet face plate and the alignment instrument, the dexterity required for instrument alignment and manipulation, and the coupling of the alignment instrument upon the beacon. If the beacon does not have sufficient rigidity to withstand the vibration and shocks attendant with the attachment and detachment of the alignment instrument from the beacon, the alignment and adjustment of the beacon orientation may be adversely affected. Beacon orientation will also be dependent upon the number and accuracy of the beacon adjustments.

The load-bearing strength of the lunar surface may be insufficient to hold the aligned beacon within the orientation accuracy tolerances even after using large pads to reduce the penetration within the lunar surface. The present penetration predictions should be verified as soon as possible to increase the reliability of the beacon design and orientation.

If the orientation problem is difficult, time consuming, and inaccurate, the reliability of the beacon will be adversely affected.

3.7.3 Durability in the Lunar Environment

Table 3-IX summarizes characteristics of the lunar environment. The major potential problem areas in the lunar environment are the lunar and beacon surface temperatures, the meteoroid and micrometeoroid impact, ultraviolet and x-ray radiation, the nozzle dust from the LEM ascent, and the lunar surface bearing strength, as discussed above.

The lunar temperature range will not adversely affect the structural materials proposed for the various beacon concepts. However, the temperature extremes will affect electronic components and storage batteries. High lunar temperatures will reduce the efficiency of photovoltaic cells as much as 60 percent and may affect

TABLE 3-IX

LUNAR ENVIRONMENT SUMMARY

Characteristic	Subheading	Quantity	Remarks
Temperature	Maximum lunar	400 ±25°K	Kapton plastic film solves plastics durability problems. High temperatures reduce solar cell efficiency and accuracy of electronic components
	Minimum lunar	120 ± 5°K	
	Maximum reflector	470°K	
	Minimum reflector	100°K	
Atmosphere	Pressure	10^{-10} mm Hg	Presents no design difficulties
	Composition	50-70% CO_2 45-27% H_2O 4-2% H_2	No chemical corrosion problems
Meteoroids		1/2 earth impact rate indicated	NASA, Lewis FY'64 ground experimental tests indicate up to 50% reflectance loss, more data required; 1/2% reflectance loss/year estimated on basis of analytical data
Gravitational Field		0.16 g ≈ 162.2 cm/sec^2	Presents no design difficulties
Electromagnetic Radiation	Solar Constant > 3000Å	2.0 ±0.04 cal/cm^2/min 15.2 ±0.6 lumens/cm^2	Can accentuate thermal control problem of power system, plastics; depends on absorptivity and emissivity NASA, Langley FY'66 ground experimental program; plastic and dielectric overcoatings may be affected significantly; helps rigidize some plastics.
	Solar UV x-rays < 3000Å	0.0028 cal/cm^2/min	
	Planetary albedo radiation Planetary thermal emission Moon albedo radiation	0.073 average	Effect on beacon varies with phase angle, local terrain and composition and beacon altitude
Charged Particles	Galactic Cosmic Rays Solar Cosmic Rays	2 x 10^8/cm/sec 0.5 to 5 keV higher flux and energies in periods of high solar flare activity	~ 1Å/year erosion ≤ 1% reflectance loss/year. NASA, Langley FY'66 ground experimental program; 10-23%/year reflectance rates possible during high solar activity

TABLE 3-IX (contd)

LUNAR ENVIRONMENT SUMMARY

Characteristic	Subheading	Quantity	Remarks
Surface Dust and Crust Thickness	Charged Particle Levitation Meteoroid Ricochet LEM Nozzle Dust Sprays Bearing Strength	10 cm penetration/ 1 psi static load 30 cm penetration/ 12 psi dynamic load	Thickness of dust layer and bearing strength determine beacon supports design beacon; surface charges should be minimized, shielding desirable where optically practical; low bearing strength may accentuate orientation problem
Magnetic Field		10^{-3} Gauss	No design problems

electronic components such as photomultiplier tubes. Specific regulation of the thermal characteristics of the components or component packaging will be necessary to maintain operating temperatures within desired limits.

Micrometeoroid impact is still being studied in space probes and ground experiments. Such a wide variation in empirical and analytical reflectance degradation tests exists, that the estimation of degradation characteristics of any reflective surfaces is difficult to predict. Prediction of the durability of inflated balloons and toruses and thin-shell, self-rigidized structures is also difficult. Based on earlier analytical and empirical investigations at EOS, it appears that a reflectance loss of as much as 50 percent per year should be a conservative figure. The uncertainty in this figure accounts for the large beacon area factor of safety.

High-energy ultraviolet and proton radiation will also reduce the surface reflectance. A present ground experiment funded by NASA/Langley is investigating this phenomena for electroformed nickel and vacuum overcoated plastic-coated aluminum panels.

3.7.4 LEM Ascent Dust Protection

Methods of protecting the beacon reflective surfaces from the dust created by the LEM ascent include:

1. Reflector Orientation. If the reflector is oriented such that the reflective surface does not see the LEM vehicle, then the reflective surface will not receive direct impingement of dust particles other than those whose trajectory lobs the particle onto the reflective surface. If the beacon is oriented upside down during the LEM ascent, then no particles will directly strike the reflective surface. However, this upside-down orientation is not practical for all beacon concepts.

2. Coated Reflector. The reflector surface can be overcoated with a subliming material which will boil off or evaporate under the effects of ultraviolet and solar radiation. This coating will reduce the degradation caused by direct dust impact and can serve as a gas bearing for the removal of dust particles on surfaces which oscillate or are steeply inclined. Such a coating may have little or no value in the removal of dust from surfaces which are horizontal.

3. Shields. Smaller beacons can utilize a plastic or foil shield placed on the blast-off side of the reflector which can be swung out of the way after the LEM vehicle has departed. Such a shield could consist of a lean-to foil or plastic sheet which utilizes a camphor plug, mousetrap-type mechanism as a timing and removal device. The camphor plug will eventually evaporate. When evaporated, it will activate the release mechanism.

4. Physical Location. Depending on the mobility of the astronaut, it may be possible to carry the beacon package to a site away from the immediate vicinity of the LEM vehicle. This preferred site would also improve beacon reliability.

3.8 Beacon Concepts

The beacon concept analysis matrix, Table 3-X, summarizes various earth and cislunar beacon concepts. Note that some very impractical beacon concepts are included for illustrative and comparative purposes. Sketches of the concepts, a discussion of advantages and disadvantages, and a material and weight analysis are included as backup material.

Estimated rough costs for the various beacon concepts are shown in Table 3-XI. Probability of photographic detection analyses for selected beacon concepts are given in Appendix C.

Beacon Classification Type	Reference Figure	Beacon Weight (earth pounds)	Beacon Volume (cubic feet)	Beacon Area (square feet) total/effective	Beacon Factor of Visual	Phot
EARTH BEACONS						
1.1.1 Sphere	3-15	~400,000	~10,000	$24.5 \times 10^6/33$	7.2	
1.1.4 Cap	3-16	20	1.0	$1.1 \times 10^3/33$	7.2	
1.2.3a Flat (frame & panel)	3-17	20	1.0	(3)* 33	7.2	
1.2.3 Flat (torus - stretched)	3-18	19.5	1.0	(12)* [illegible]	7.2	
1.2.3 Flat (stretched film)	3-19	20	1.0	(9)* [illegible]	7.2	
2.2.3 Tracking Flat	3-20	18.1	1.0	33	7.2	
2.3.2 Sun Pumped Laser	See App D	~20 - 30	1.0-2.0	?	?	
CISLUNAR BEACONS						
1.1.1 Sphere	3-15	52.8	1.0	$8 \times 10^3 / 1.1 \times 10^2$	10	
1.1.4 Cap	3-16	5.0	0.25	$570/1.1 \times 10^{-2}$	10	
1.2.4 Faceted Arch	3-21	5.0	0.25	$323/1.1 \times 10^{-2}$	10	
2.1.2 Oscillating Cap	3-22	5.0	0.25	$113/1.1 \times 10^{-2}$	10	
2.1.3 Rotating or Oscillating Cylindrical Segment	3-23	4.8	0.25	$4.75/1.1 \times 10^{-2}$	10	
2.2.5 Oscillating Faceted Arch	3-24	4.9	0.25	$19/1.1 \times 10^{-2}$	10	

* = number of duplicate units

TABLE 3-X

BEACON CONCEPT ANALYSIS MATRIX

Area Safety / ographic	Beacon Signals per unit time lunar day - d minute - min	Length of Signal	Beacon Field of View	Reflector Materials	Beacon Orientation	Bea
2	Continuous	Continuous	2π steradians	Al-Kapton-Al composite	None	Non
2	1/yd; once or twice/year	90 min max	±90 min cone	Al-Kapton-Al composite	Yes	Non
2	3 times/year	29 min max	±16 min cone	Al honeycomb or foil	Yes - (3)	Non
2	12 times/year	29 min max	±16 min cone	Al-Kapton-Al composite	Yes - (12)	Non
2	9 times/year	29 min max	±16 min cone	Al-Kapton-Al composite	Yes - (9)	Non
2	Continuous	~Continuous	±16 min cone	Al honeycomb or foil	Self-orienting	Tra ear
?	Continuous	Continuous	±1 min cone	Al panels - collector	Self-orienting	Tr ear
11	Continuous	Continuous	2π steradians	Al-Kapton-Al composite	None	Non
11	Continuous	7.0 min @ 200 nm	±40° cone	Al-Kapton-Al composite	Yes	Non
11	Continuous	3 min @ 200 nm	±18.5° longitude x ±90° latitude	Al	Yes	Non
11	Flashing ~ 1/sec	~ 0.1 sec	±23° cone x 90° longitudinal oscillations	Al-Kapton-Al composite	Yes	Os
11	Flashing ~ 1/22.5 sec	0.1 sec	2π steradians	Al sheet	No	Rot Osc
11	Flashing; 1/8.25 sec	0.1 sec	2π steradians	Al sheet	Yes	Osc

:on Motion	Power Requirements	Erection and Orientation Time (minutes)	Reliability	Rating
e	None	15-30	0.40	6
e	None	10	0.90	3
e	None	15	0.96	2
e	None	30	0.92	4
e	None	30	0.90	5
:king th & sun	Photovoltaic	10	0.90	1
:king of th & sun	Photovoltaic	10	0.50-0.9	Unrated
e	None	5	0.95	5
e	None	5	0.95	3
e	None	20	0.90	4
illatory	Photovoltaic or thermomechanical	15	0.85	6
ıry or illatory	Photovoltaic or thermomechanical	10	0.90	2
illatory	Photovoltaic or thermomechanical	10	0.91	1

TABLE 3-XI

ROUGH ESTIMATED BEACON CONCEPT COSTS*
(in Thousands)

Beacon Classification Type	First Prototype	Type Testing	Flight Units (ea)
EARTH BEACONS			
1.1.1 Sphere	(Impractical)	(Impractical)	(Impractical)
1.1.4 Cap	$ 50	$25	$30
1.2.3a Flat (frame and panel)	40	15	20
1.2.3 Flat (torus stretched)	15	5	5
1.2.3 Flat (stretched film)	10	5	2
2.2.3 Tracking Flat	60	20	40
2.3.2 Sun Pumped Laser	200	35	100
CISLUNAR BEACONS			
1.1.1 Sphere	60	40	25
1.1.4 Cap	30	10	20
1.2.4 Faceted Arch	40	10	30
2.1.2 Oscillating Cap	60	20	30
2.1.3 Rotating or Oscillating Cylindrical Segment	50	20	30
2.2.5 Oscillating Faceted Arch	60	20	40

*Costs may vary by $^{+100\%}_{-\ 50\%}$; detailed specifications for prototype type testing and flight units required before valid costs can be determined.

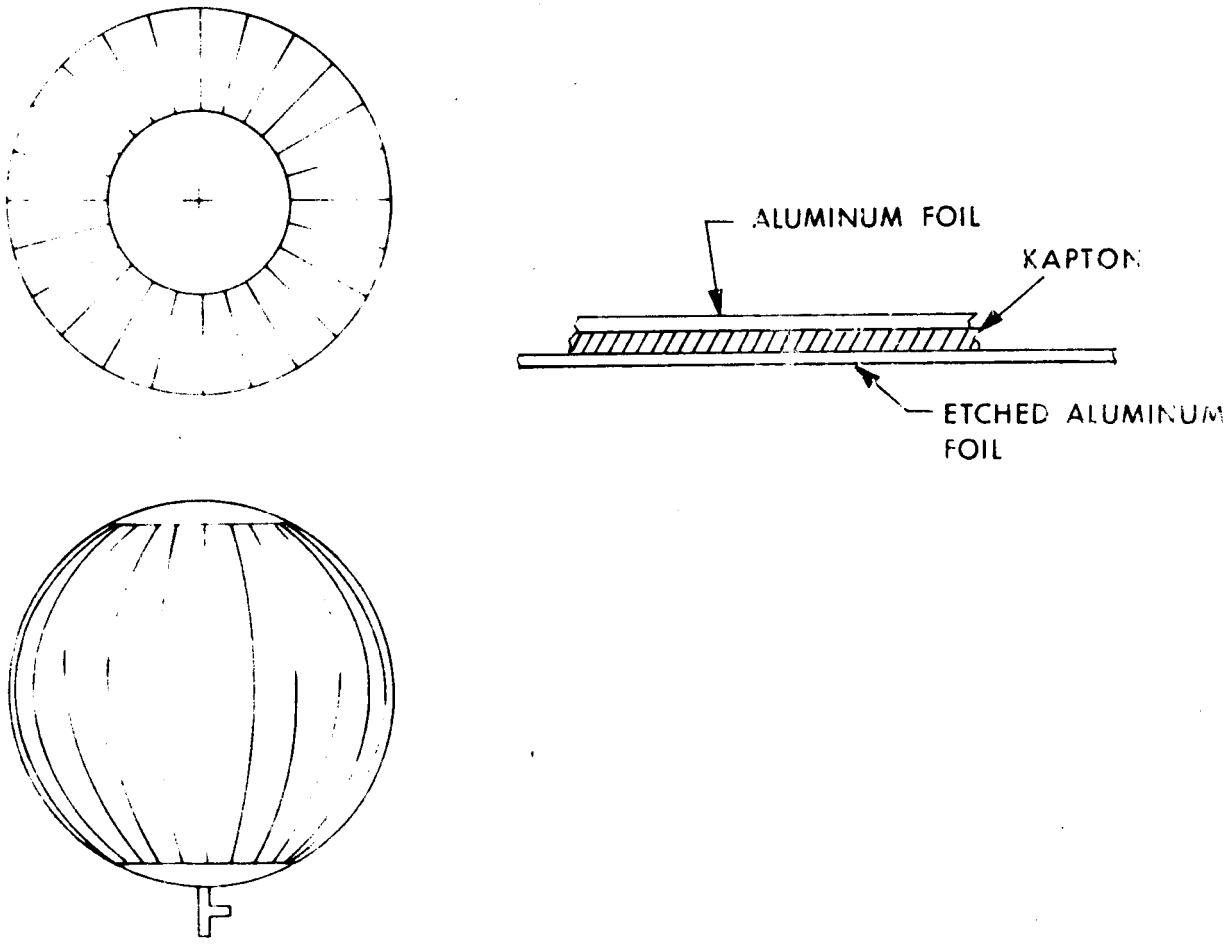

FIG. 3-15 SPHERICAL INFLATABLE REFLECTOR (1.1.1)

1.1.1 Sphere

Advantages

Omnidirectional, 2π steradian field of view

Continuous Signal

Smaller diameter structures of similar design are space-qualified.

Disadvantages

Weight and volume exceed design constraints by over 4 orders of magnitude, using a structural design applicable to much smaller beacons.

Sphere of this diameter (2790 ft) probably impractical to make.

Possibility of failure due to micrometeorite damage is extremely high.

2π steradian field of view is not necessary for an earth beacon.

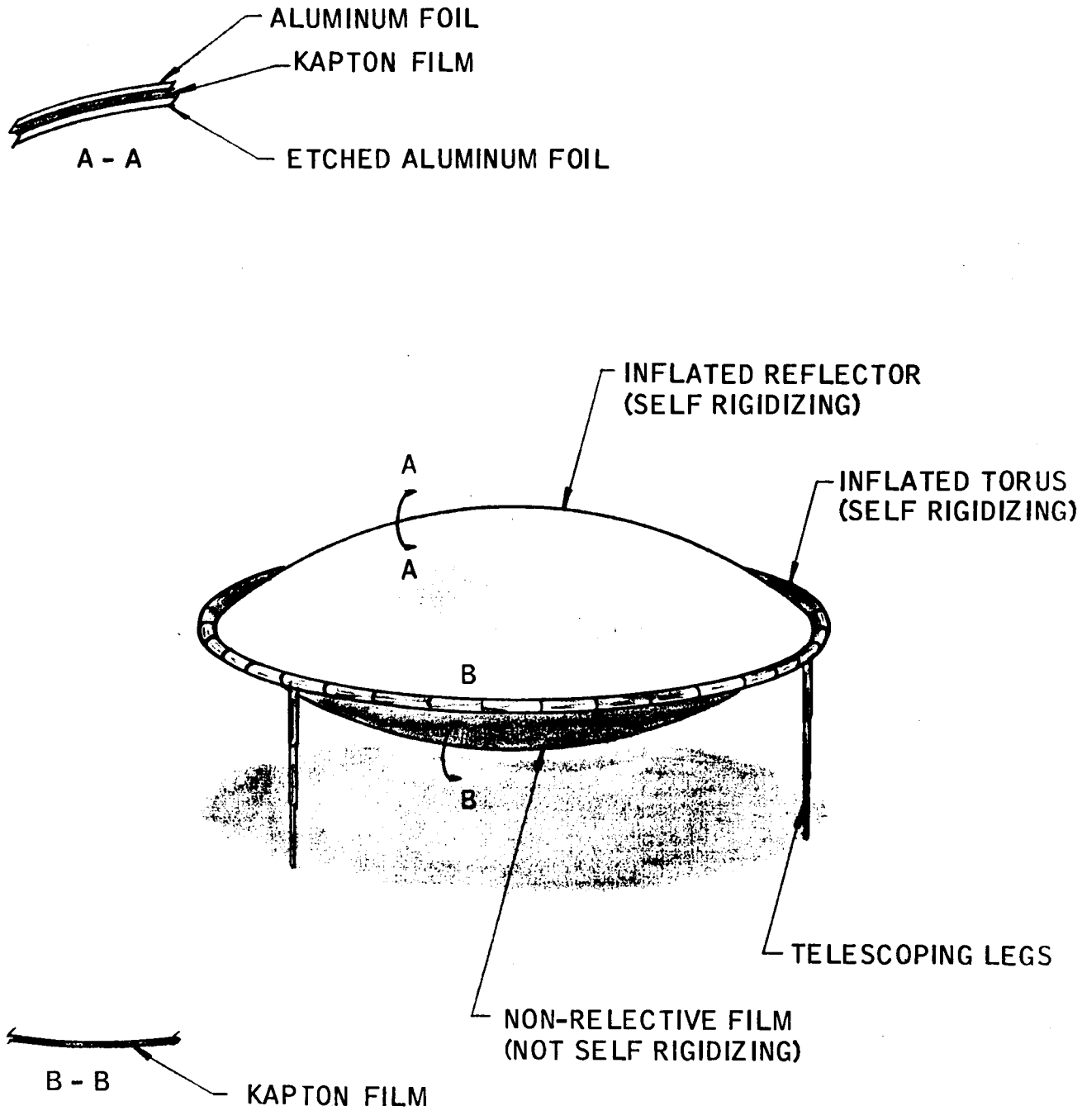

FIG. 3-16 SELF-RIGIDIZING INFLATABLE CAP BEACON (1.1.4)

1.1.4 CAP

MATERIAL AND WEIGHT ANALYSIS

Component	Material	Size	Weight (lbs)	Comments
Reflective Surface	Al-Kapton-Al	±45 minute cap of 2790' sphere 1.1 x 10^3 ft^2 + 10%	9.3	0.18 mil x 0.5 mil x 0.18 mil etched
Lower Cap	Kapton	±45 minute cap of 2790' sphere, 1.1 x 10^3 ft^2 + 10%	4.5	0.5 mil
Inflatable Torus	Al-Kapton-Al	37 ft diam. x 4" diam.	1.4	0.18 mil x 1 mil x 0.18 mil
Subliming Material			0.3	
Legs	Aluminum	Telescoping	1.0	
Alignment Instrument	Aluminum-glass		2.0	
Shipping Container	Aluminum/ fiberglass	1 ft^3	1.5	
			20.0 lbs	

Advantages

Wider field of view than flat.

Orientation not as critical as a flat.

Easily erected.

Similar structures have been space-qualified.

Meets weight and volume constraints.

Disadvantages

Difficult to protect against dust during LEM ascent.

Micrometeorite resistance low.

Reliability as a self-supporting - i.e., no inflation, structure in the lunar gravitational field may be low.

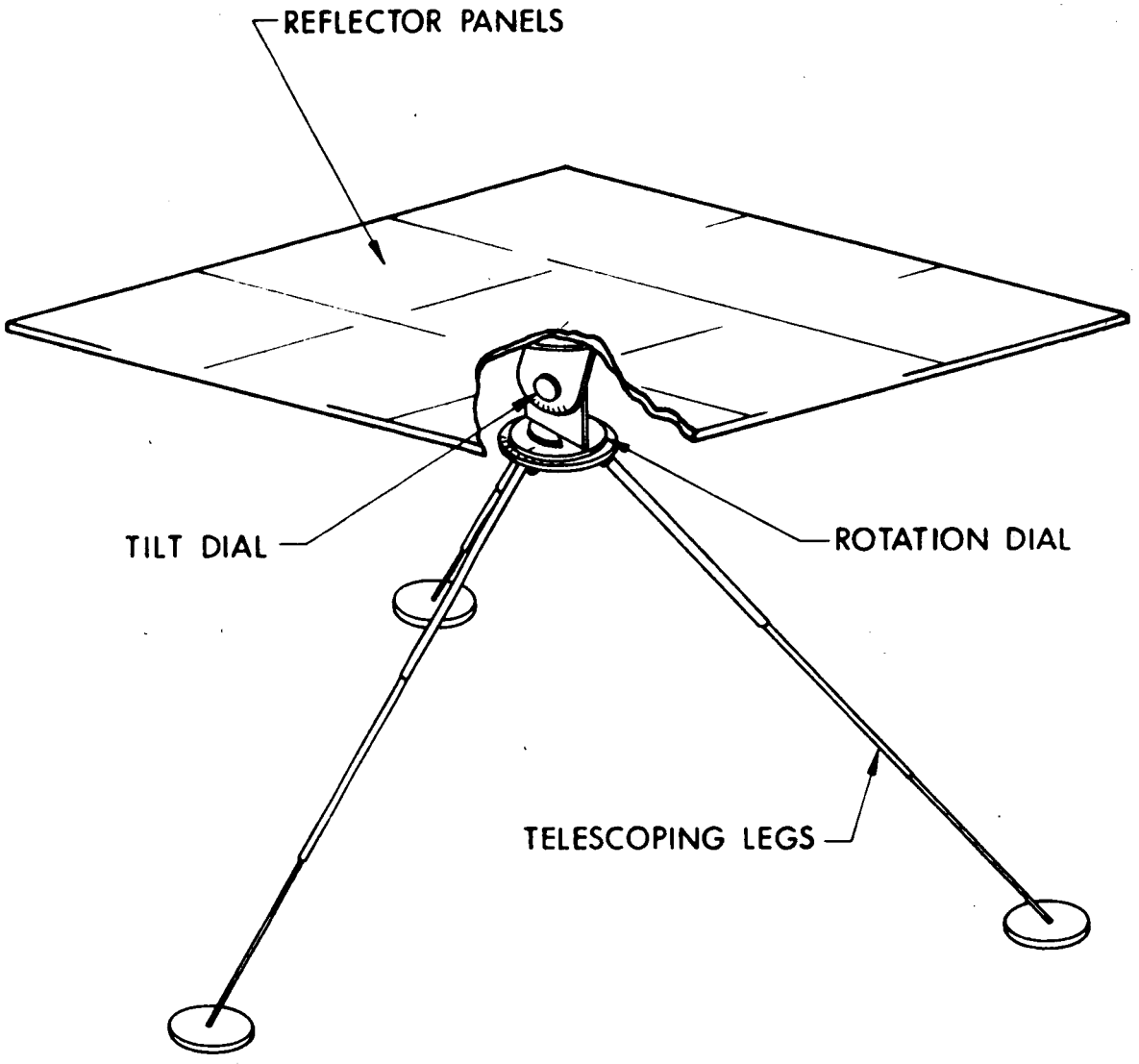

FIG. 3-17 FLAT EARTH BEACON (frame and panel design) (1.2.3)

1.2.3 FLAT (FRAME AND PANEL DESIGN)

MATERIAL AND WEIGHT ANALYSIS

Component	Material	Size	Weight (lbs)	Comments
Reflector Panels - 3 sets	Al honeycomb or	3 x 33 ft^2	7.8	3 separate units
Structural Support	Al		4.0	Includes tripod, base, lugs, pads
Reflector Panel Frame	Al	3" x 69" x 69"	4.0	
Orientation Instrument and divided circles			2.8	Includes setting
Shipping Container	Al honeycomb or fiberglass	1 ft^3	1.4	

Advantages	Disadvantages
Reliability high.	Small field of view.
Three separate units.	Orientation alignment may be extremely critical, particularly if the lunar surface bearing strength is as low as predicted.
Conventional construction materials.	May be difficult to erect and orient within a reasonable time span.
Meets design packing and weight specifications.	Moderately difficult to protect against dust during LEM ascent.

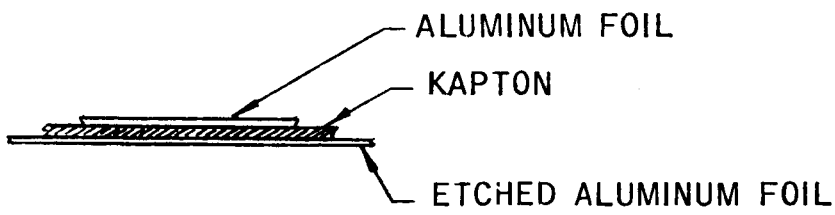

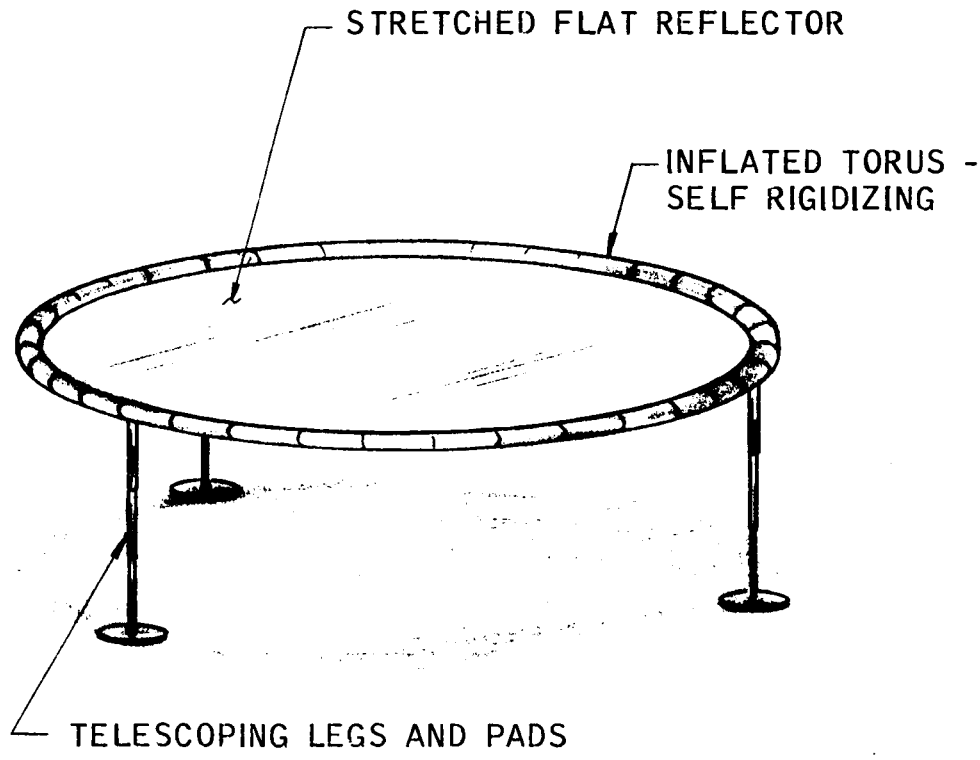

FIG. 3-18 TORUS STRETCHED FLAT BEACON (1.2.3)

1.2.3 STRETCHED FLAT DESIGN

MATERIAL AND WEIGHT ANALYSIS

Component	Material	Size	Weight (lbs)	Comments
Reflective Surface	Al-Kapton-Al etched	~40 ft^2 to allow for sag effects +10% for gores, etc.	12 x 0.34	0.18 mil x 0.5 mil x 0.18 mil etched
Inflated Torus	Al-Kapton-Al etched	7.15 ft diam. x 4" diam. + 10%	12 x 0.29	0.18 mil x 1.0 mil x 0.18 mil
Legs (3) with 2-inch pads	Al		12 x 0.5	1/2 inch diam. x 0.028-inch wall x 36 inches high
Inflation material	Benzoic acid plus anthra-quinine		12 x 0.2	
Alignment Instrument	Al-glass		2.0	
Package	Al honeycomb, reinforced fiberglass	1 ft^3	1.5	
			19.5 lbs	

Advantages

Light weight per flat permits large number of flats.

Twelve separate units give high reliability due to redundancy.

Meets design packaging and weight specifications.

Disadvantages

Flatness highly dependent on torus inflation.

Orientation difficult due to lack of structural rigidity of torus.

Multiple flats increases orientation difficulties.

Difficult to protect against dust during LEM ascent.

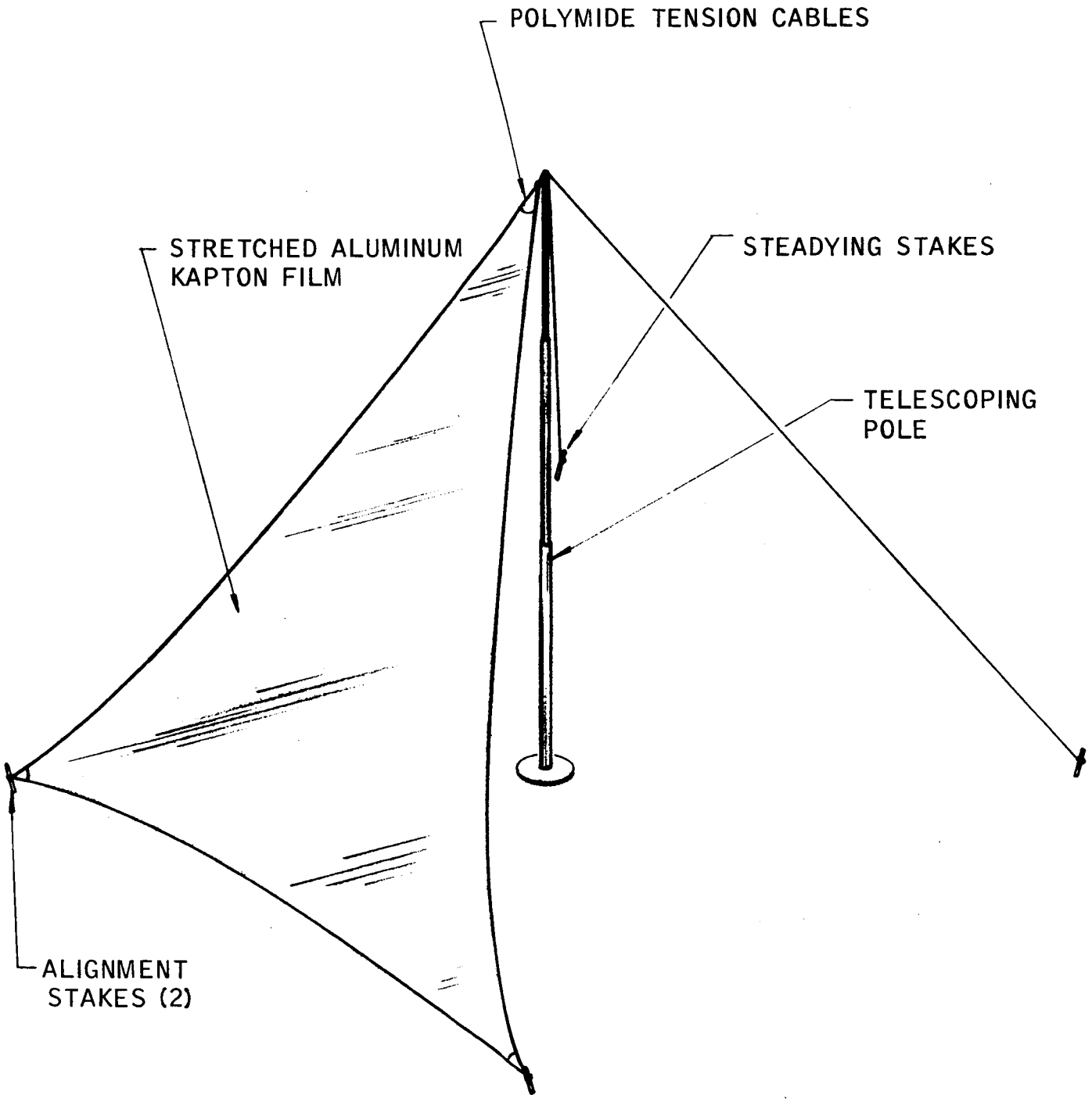

FIG. 3-19 STRETCHED FILM FLAT BEACON (1.2.3)

1.2.3 FLAT-STRETCHED FILM

MATERIAL AND WEIGHT ANALYSIS

Component	Material	Size	Weight (lbs)	Comments
Reflective Surface	Al-Kapton-Al etched	~40 ft^2 to allow for sag effects +10% gores	9 x 0.34	0.18 mil x 0.5 mil x 0.18 mil etched
Tension cables	Polymide Plastic	25 ft x 0.0625 inch diam.	9 x 0.005	
(4) Stakes, Pole, & guy wires			9 x 1.5	
Alignment Instrument			2.0	
Packaging		1 ft^2	1.5	
			20 lbs	

Advantages

High efficiency structural design.

Light weight permits duplicate units.

Meets design packaging and weight specifications.

Disadvantages

Orientation may be difficult.

Attaining and maintaining flat surface may be difficult due to differential thermal expansion.

Proper tensioning may be difficult during erection.

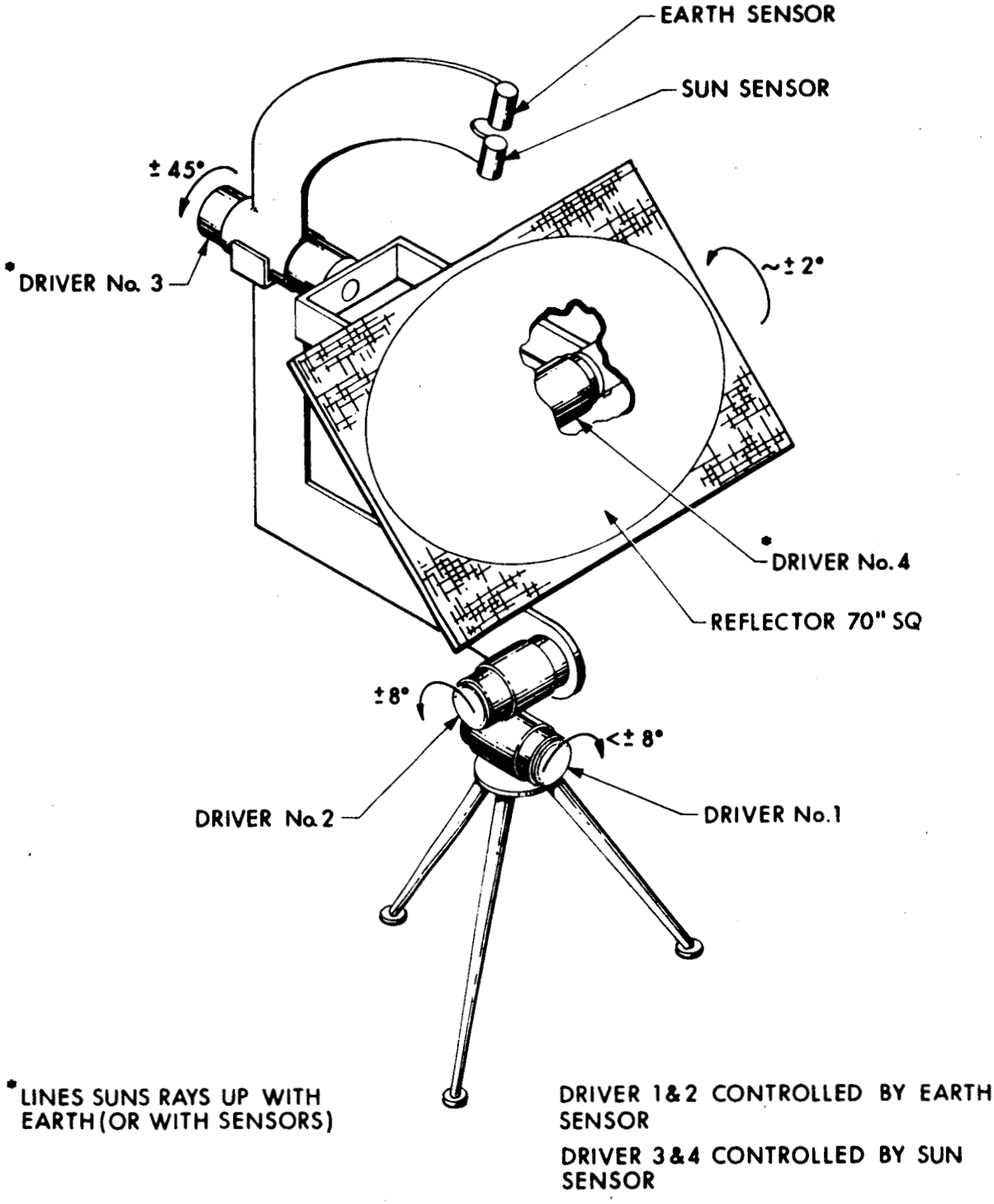

FIG. 3-20 TRACKING FLAT EARTH BEACON (2.2.3)

2.2.3 TRACKING FLAT

MATERIAL AND WEIGHT ANALYSIS

Component	Material	Size	Weight (lbs)	Comments
Reflector Panels			2.6	
Reflector Panel Frame			1.33	
Tripod			0.75	
Yolk			3.1	
Drive units (4)	Ac induction or dc encapsulated motor		3.5	Includes bearings
Earth Sensor			2.9	JPL Design
Sun Sensor			0.6	JPL Design
Solar Cells Panels	Silicon solar cells	6½" x 7¾" x 0.10" (3)	0.4	
Optical storage battery			1.0	
Inverter if necessary	Transistorized		0.2	
Misc. hardware			1.0	
Shipping container	Al honeycomb or fiberglass	1 ft^3	1.5	
			18.8	

Advantages

Can be viewed for a large percentage of time.

Easiest earth beacon concept to protect against dust during LEM ascent.

Uses space proven hardware.

Self-orienting

Disadvantages

Requires electrical power and several bearings.

Large number of components relative to other concepts.

Approximately 60 percent efficiency loss in solar cells due to high ambient lunar temperatures.

Earth tracking difficult near 0^o phase angles.

May require battery storage or a thermal mechanical starting drive to produce high starting torques during the lunar dawn startup period.

2.3.2 Sun Pumped Laser

Advantages

High intensity collimated source.

Beacon signal can be modulated to provide telemetering information.

Disadvantages

Lunar hardware has not been developed

Present designs probably exceed weight constraints

Detection could be difficult due to small field of view

1.1.1 SPHERE

MATERIAL AND WEIGHT ANALYSIS

Component	Material	Size	Weight (lbs)	Comments
Reflective Surface (top hemisphere)	Al-Kapton-Al	4000 ft^2 + 5% gores etc.	32.3	0.18 mil x 0.5 mil x 0.18 mil etched
Lower Hemisphere	Kapton	4000 ft^2 + 5% gores, etc.	15.5	0.5 mil
Subliming material	Benzoic acid plus Anthra-quinine		3.0	
Stand	Al		0.5	
Shipping Container	Al honeycomb or fiberglass reinforced	1.00	1.5	
			52.8	

Advantages	Disadvantages
Omnidirectional	Both weight and design constraints exceeded.
Continuous signal	Difficult to protect against LEM ascent dust.
Space-qualified structure	Micrometeorite resistance low.

1.1.4 CAP

MATERIAL AND WEIGHT ANALYSIS

Component	Material	Size	Weight (lbs)	Comments
Reflective Surface	Al-Kapton-Al	300 ft^2	2.3	$\pm 20^{\circ}$ cone cap 0.18 mil x 0.5 mil x 0.18 mil etched
Lower Cap	Kapton		1.1	0.5 mil
Inflatable Torus	Al-Kapton-Al		0.5	0.18 mil x 1.0 mil x 0.18 mil
Subliming Material	Benzoic Acid and anthraquinine	1.1	0.1	
Legs-telescoping	Al		0.4	
Alignment Instrument			0.2	Level, protractor
Shipping Container	Plastic	0.25 ft^2	0.4	
			5.0 lbs	

Advantages	Disadvantages
Large field of view.	Difficult to protect against dust during LEM ascent.
Easily erected.	Micrometeorite resistance low.
Orientation simple.	
Similar structures space-qualified.	
Meets weight and volume constraints.	

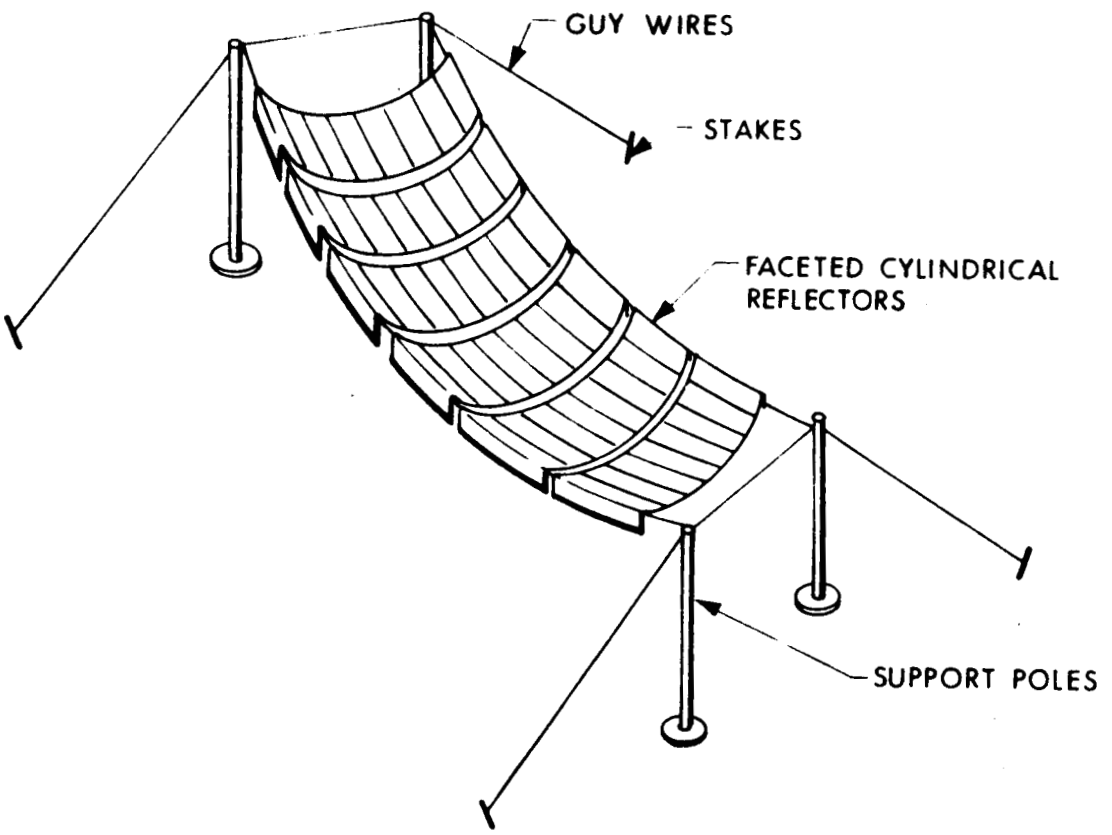

FIG. 3-21 FACETED ARCH (1.2.4)

1.2.4 FACETED ARCH

MATERIAL AND WEIGHT ANALYSIS

Component	Material	Size	Weight (lbs)	Comments
Reflecting Arch Panels	0.002 Al foils	$\pm 47^{\circ}$ arch x 20" diam.	2.23	68 separate arch panels
End Braces	Al brackets	20" long	1.70	Stiffeners for arch foil panels
Wire (guy)	High strength steel	~0.010" diam.	0.034	Wire on which panels are hung
Poles	Aluminum		0.5	
Packaging	Aluminum honeycomb fiberglass	0.25 ft^2	0.5	
			4.964	

Advantages

Orientation simple - beacon axis must be on lunar latitude.

Covers 180° latitudinal field of view.

Meets weight and packaging requirements.

Long signal flash.

Disadvantages

Erection time long.

Flats must be made accurately.

Field of view limited - does not cover 2π steradian field of view.

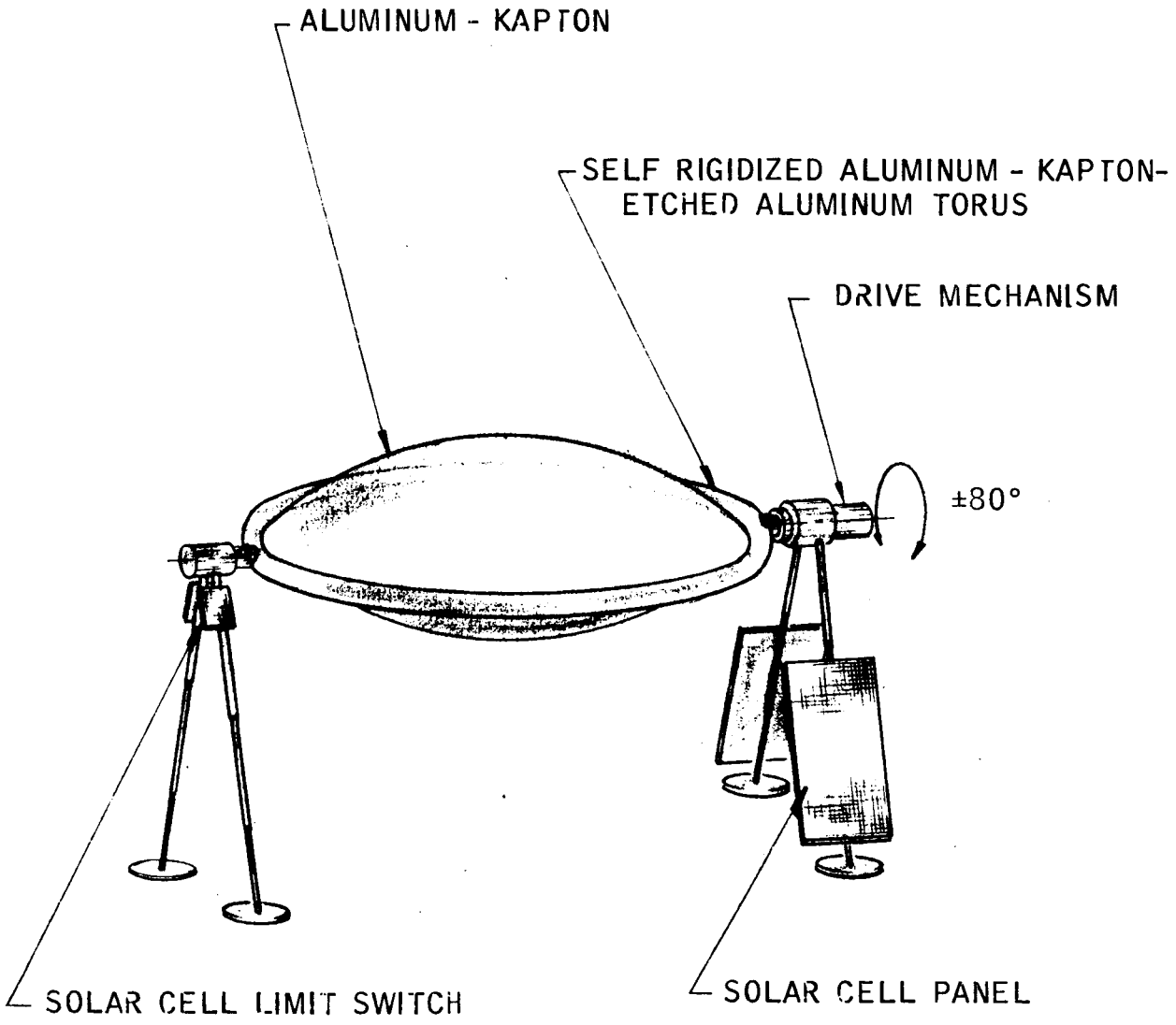

FIG. 3-22 OSCILLATING CAP BEACON (2.1.2)

2.1.2 OSCILLATING CAP

MATERIAL AND WEIGHT ANALYSIS

Component	Material	Size	Weight (lbs)	Comments
Gear Motor	Ac Induction Motor	1.07" diam.	0.25	
Inverter	Transistorized	1 3/4" x 1 5/8" x 1 1/4"	0.20	
Solar Cell Panels	Silicon Solar Cells, etc.	(3) 6 1/2" x 7 1/4" x 0.10"	0.37	
Support Shaft Assembly	Aluminum		0.15	
Spokes	Aluminum	1/4" OD x 0.28	0.15	
Reflector Cap	Al-Kapton-Al	113 ft^2	0.87	$\pm 11.5^{o}$ cap
Lower Cap	Kapton	113 ft^2	0.42	
Torus		12' diam. x 4" diam.	0.43	
Legs, Pads and Support			0.70	
Hardware			0.05	
Packaging			1.40	
			4.99 lbs	

Advantages

Long signal flash as viewed from any one position.

Meets weight and packaging requirements.

Minimum orientation required - i.e. must oscillate with oscillation axis along N-S meridian

Solar cell limit switch reduces oscillation to $\pm 45^{o}$ about solar selenographic longitude reducing cycle time.

Disadvantages

Does not cover complete 2π steradian field of view in one oscillation.

Electrical components, but thermal-mechanical drive can be substituted for photovoltaic-electric motor system.

Battery or thermomechanical starter may be necessary to provide high lunar dawn starting torque.

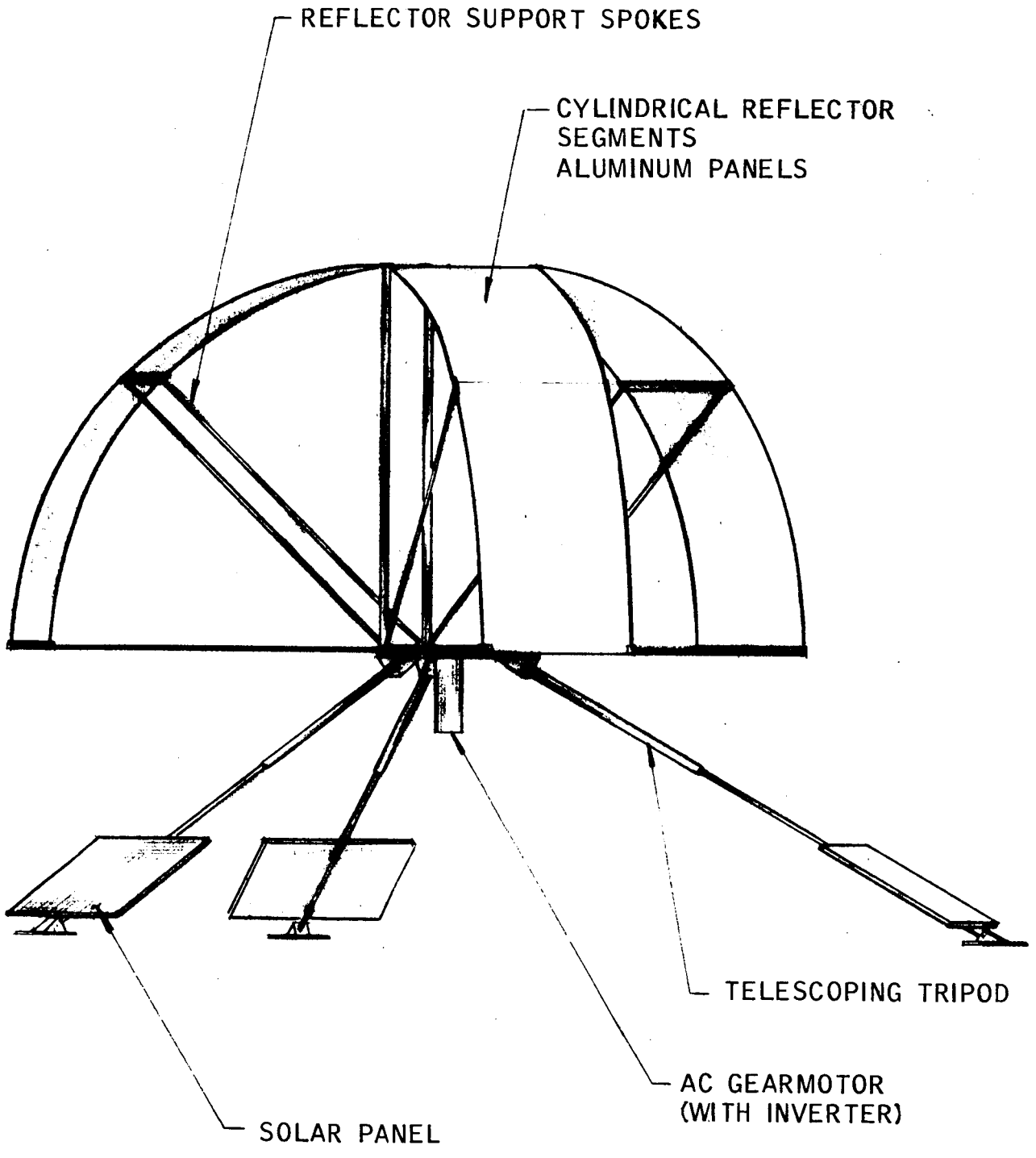

FIG. 3-23 ROTATING OR OSCILLATING CYLINDRICAL SEGMENT (2.1.3)

2.1.3 ROTATING CYLINDRICAL REFLECTOR

MATERIAL AND WEIGHT ANALYSIS

Component	Material	Size	Weight (lbs)	Comments
Gear-Motor	AC Induction Motor	1.07" diam. x 2.8"	0.25	Gaylord Rives
Inverter	Transistorized Construction	1-3/4" x 1-5/8" x 1-1/4"	0.20	Gaylord Rives
Solar Cell Panels	Various Mat'l	6-1/2" x 7-1/4" x 0.10 (3) Req'd	0.37	For (3) Panels
Drive Train-Brgs., Shaft Assy. (w/Hub & Cross-arm), Hsg.	Brgs. - Teflon Shaft Assy - Aluminum		0.05	
Spokes	Aluminum	1/4" diam x 0.028 wall (18) Req'd	0.60	
Reflector	Aluminum Panels	19" chord x 20" x 0.010"	1.20	For 3 Segments and 3 panels
Support Ring & Hsg. Assy.	Aluminum		0.15	
Tripod Legs & Pads	Aluminum	1/2" diam. x 0.028 wall x 30" (3) Req'd	0.50	For (3) Legs
Hardware (Screws, Lugs, Pins, etc.)	Aluminum		0.05	
Shipping Container		1/4 ft^3	1.40	
Total Weight (with shipping container)			4.77 lbs	

Advantages

Covers 2π steradian field of view.

Meets weight and packaging requirements

Single bearing.

Hardware space qualified.

No orientation required.

Disadvantages

Numerous electrical and mechanical components but thermal-mechanical drive can be substituted for photovoltaic electric drive.

Field of view too large for maximum efficiency in utilizing reflector area.

Flash time short for photographic detection and navigational sightings.

Battery or thermomechanical starter may be necessary to provide high lunar dawn starting torque.

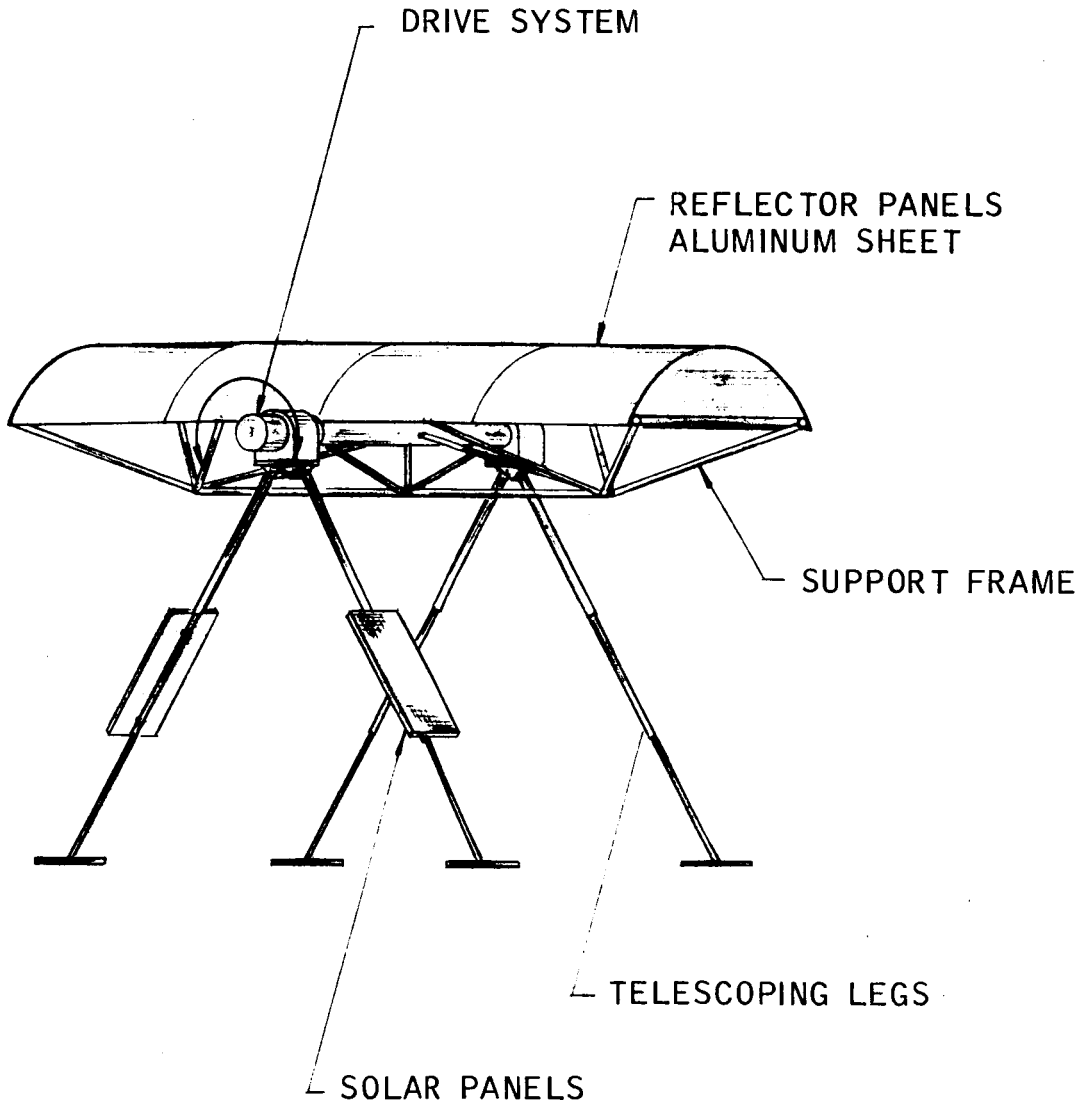

FIG. 3-24 OSCILLATING ARCH BEACON (2.2.5)

2.2.5 OSCILLATING FACETED ARCH

MATERIAL AND WEIGHT ANALYSIS

Component	Material	Size	Weight (lbs)	Comments
Gear-Motor	AC Induction Motor	1.07" diam. x 3"	0.25	
Inverter	Transistorized	1-3/4" x 1-5/8" x 1-1/4"	0.20	
Solar Cell Panels	Various Mat'l	6-1/2" x 7-1/4" x 0.10", (3) Req'd	0.37	Wt. for (3) Panels
Support Shaft Assy.	Aluminum		0.15	Includes Ball Bearings
Spokes	Aluminum	1/4" OD x 0.028 wall	0.25	
Reflector	Aluminum Panels	4 x 4.75	1.50	0.005"
Support Base	Aluminum		0.20	
Tripod Legs & Pads	Aluminum	1/2" diam. x 0.028 wall x 36", 2" diam. x 0.062"	0.50	Wt. for (3) Legs & Pads
Hardware (Screws, etc.)	Various Mat'l		0.05	
Shipping Container	Aluminum	0.016" thick	1.40	Volume = 1/4 ft^3
			4.87 lbs	

Advantages

Wide latitudinal field of view.

Minimum orientation required - axis of oscillation in N-S meridian.

Meets weight & packaging requirements.

Most efficient use of reflector area.

Frequent flashes (1/4.25 sec)

Solar cell limit switch reduces oscillation to $\pm 45^{\circ}$ about solar selenographic longitude, reduces cycle time.

Disadvantages

Flash time short for navigational sightings and photographic detection; probability of photographic detection but can be increased by varying oscillation angular speed continuously throughout cycle, measuring photographic frames per unit time.

Electrical components, but thermomechanical drive can be substituted for photoelectric drive.

Battery or thermomechanical starter may be necessary to provide high lunar dawn starting torque.

APPENDIX A

BEACON PHOTOMETRIC ANALYSIS

APPENDIX A

BEACON PHOTOMETRIC ANALYSIS

1. DETECTION VARIABLES

The reflective area required for the detection of lunar beacons depends upon the following variables:

1. Background brightness, B_f
2. Beacon reflectance, r_b
3. Sun-moon-instrument phase angle, θ
4. Instrument beacon range, R
5. Integrated instrument optical transmittance, T_t
6. Integrated instrument angular resolution as a function of aperture, instrument errors, atmospheric seeing (and for photographic records of the detector errors), β
7. Atmospheric transmittance, T_e
8. Contrasts required for a given detector and probability of detection, C_v - visual, C_p - photographic
9. Lunar beacon location

The following sections describe the analysis required for beacon sizing, the major variables in detail, representative calculations, and beacon area recommendations.

2. CAMERA PHOTOMETRY THEORY

With a camera, the field brightness, B_f, is decreased only by the atmospheric and camera transmittance losses, T_e and T_t, so that the apparent field brightness, B_{af}, at the detector is

$$B_{af} = T_e T_t B_f \qquad (1)$$

But B_f is related to the lunar field albedo or reflectance at 0^o phase angle, a_f, the phase angle reflection ratio for a given lunar location, K_θ, the solar illuminance of the moon, E_s, and π so that

$$B_f = \frac{K_\theta \, a_f \, E_s}{\pi} \tag{2}$$

Therefore, from Eqs. 1 and 2

$$B_{af} = \frac{T_e \, T_t \, K_\theta \, a_f \, E_s}{\pi} \tag{3}$$

and

$$E_{af} = B_{af} \, \omega \tag{4}$$

where

$$\omega = \frac{\pi}{4 \, N^2} \tag{5}$$

where

$$N = \frac{f.l.}{D_o} \tag{6}$$

Therefore, from Eqs. 3, 4, and 5,

$$E_{af} = \frac{T_e \, T_t \, K_\theta \, a_f \, E_s}{4 \, N^2} \tag{7}$$

Since the beacon size will be less than the resolution limit of the detection instruments, it can be considered as a point source having an image which is a diffraction pattern, 84 percent of the energy falling into the Airy or first-diffraction disc. The illuminance of the image from a point source, E_{ab}, is then related to the incident illuminance, E_{ob}, the objective diameter, D_o, focal length, f.l., the transmittance loss, T_t, and the integrated resolution limit, β, by

$$E_{ab} = 0.84\ T_t\ E_{ob} \left[\frac{D_o}{\beta\ f.l.}\right]^2 \tag{8}$$

Note that the angle, β, approaches $[1.22\ \lambda/D_o]$ for perfect seing where λ is the light wavelength. E_{ob} is related to the beacon apparent solid angular subtend, Ω_b, the solar solid angular subtend at the beacon, Ω_s, and the beacon illuminance, E_b, and the atmospheric transmittance, T_e, so that

$$E_{ob} = T_e \frac{\Omega_b}{\Omega_s} E_b \tag{9}$$

but the beacon illuminance is directly related to the incident solar illuminance, E_s, and beacon reflectance, r_b:

$$E_b = E_s\ r_b \tag{10}$$

and the beacon angular subtend is related to the projected beacon area, a $\cos\theta/2$ (i.e., the beacon mirror must be perpendicular to the bisector of the phase angle to be seen) and the range, R, so that:

$$\Omega_b = \frac{a\ \cos\frac{\theta}{2}}{R^2} \tag{11}$$

Combining Eqs. 6, 8, 9, 10, and 11

$$E_{ab} = \frac{0.84\ T_e\ T_t\ a\ \cos\frac{\theta}{2}\ E_s\ r_b}{\Omega_s\ R^2\ \beta^2\ N^2} \tag{12}$$

The apparent field and beacon illuminances are related to the photographic contrast for detection, C_p, by the term

$$C_p = \frac{E_{ab} - E_{af}}{E_{af}} = \frac{E_{ab}}{E_{af}} - 1 \tag{13}$$

By direct substitution of Eqs. 7 and 12 into Eq. 13

$$C_p + 1 = \frac{3.36\ a \cos\frac{\theta}{2}\ r_b}{K_\theta\ a_f\ \Omega_s\ \beta^2\ R^2} \tag{14}$$

Transposing

$$\frac{a r_b}{(C_p + 1)} = \frac{K_\theta\ a_f\ \Omega_s\ R^2\ \beta^2}{3.36 \cos\frac{\theta}{2}} \tag{15}$$

Note that this relationship is independent of the solar illuminance, transmittance values, and f/number (N), except as they affect the contrast and resolution values, of the system. In cases where seeing conditions govern the resolution angle, β, the camera diameter will only affect the film speed used and the time over which seeing conditions are integrated.

A log-log plot of the area factor, $ar_b/(C_p + 1)$, versus β yields a series of straight lines for each phase angle. The visual and photographic beacon areas are both closely related. Figures 1 and 2 are plots for ranges of 400 nautical miles and 207,000 nautical miles, earth-moon mean distance, respectively.

Let us now compare visual telescope theory with the above.

3. VISUAL TELESCOPE PHOTOMETRY THEORY

The apparent field brightness of a telescope can be reduced if the exit pupil, d, is smaller than the eye pupil, d_e, which is the case for astronomical telescopes, by the ratio of their areas, $(d/d_e)^2$ so that

$$B_{af} = T_e\ T_t \left(\frac{d}{d_e}\right)^2 B_f \tag{16}$$

which is the same as Eq. 1 when $d = d_e$

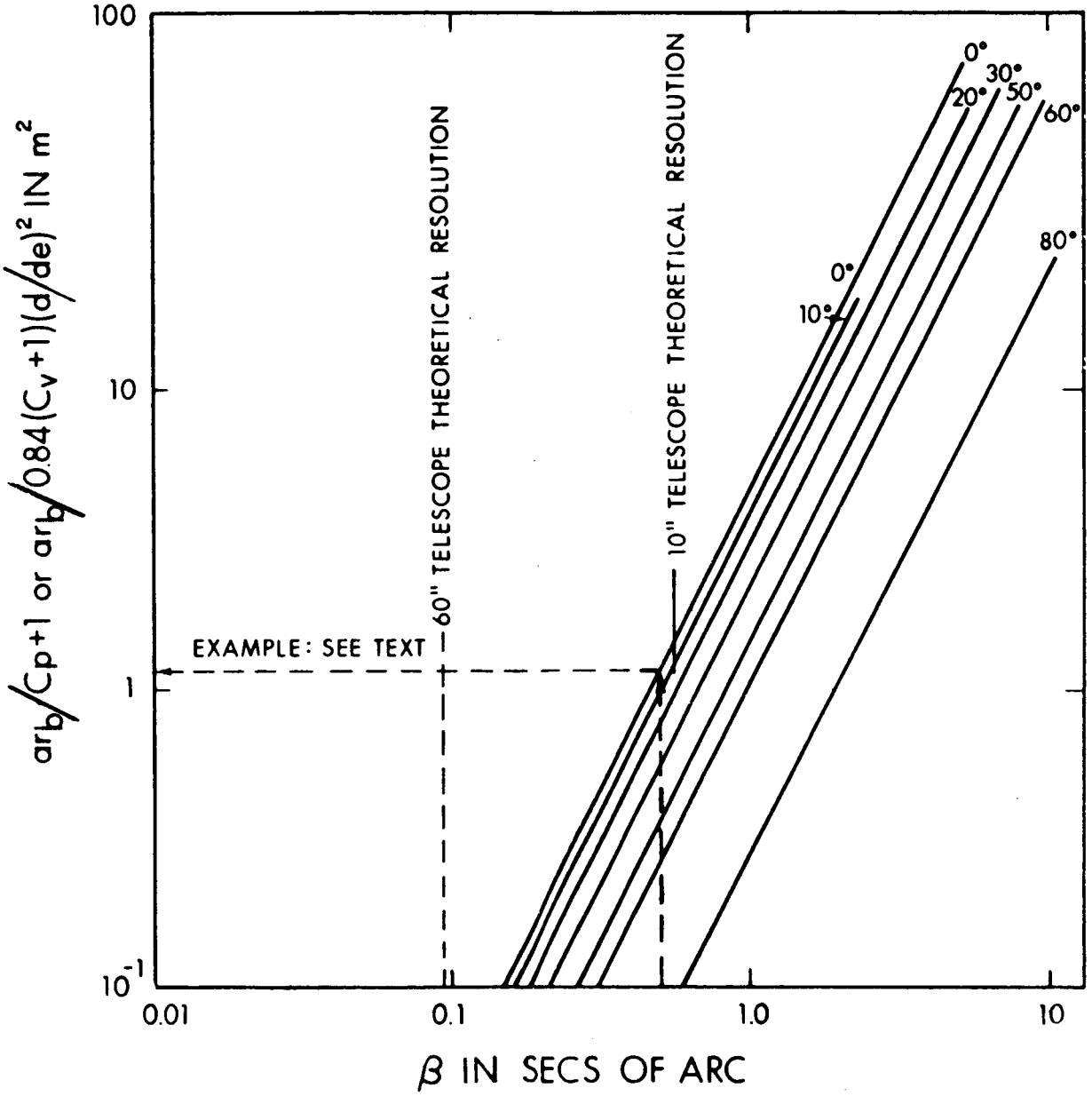

FIG. 1 AREA FACTOR VS RESOLUTION LIMIT FOR VARIOUS PHASE ANGLES FOR 0^{o} LONGITUDE AT A 207,000 NAUTICAL MILE RANGE

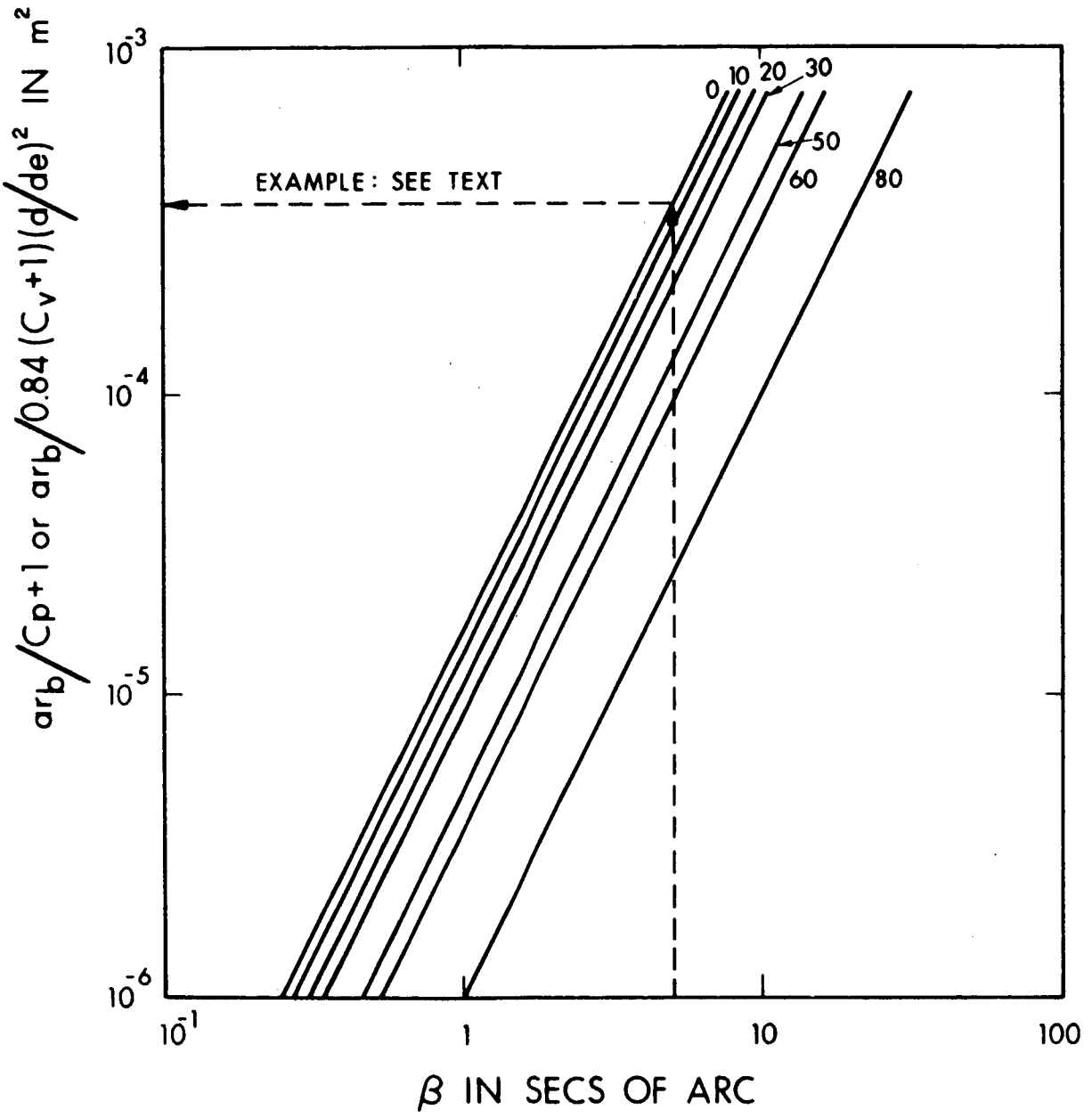

FIG. 2 AREA FACTOR VS RESOLUTION LIMIT FOR VARIOUS PHASE ANGLES FOR 0° LONGITUDE AT 400 NAUTICAL MILES

By combining Eqs. 2 and 16

$$B_{af} = T_e\ T_t \left(\frac{d}{d_e}\right)^2 \frac{K_\theta\ a_f\ E_s}{\pi} \tag{17}$$

The apparent brightness of the beacon, B_{ab}, and the apparent illuminance are related to the solid angle subtended by the eye, ω_e, after magnification, M, of the angle resolved, β, by

$$B_{ab} = \frac{E_{ab}}{\omega_e} \tag{18}$$

$$= \frac{E_{ab}}{\frac{\pi}{4}\ (\beta M)^2} \tag{19}$$

Now E_{ab} is related to the incident illuminance, E_{ob}, and the magnification and transmittance by

$$E_{ab} = T_t\ E_{ob}\ M^2 \tag{20}$$

By substituting Eqs. 9, 10, 11, and 20 into Eq. 19

$$B_{ab} = \frac{T_t\ T_e\ E_s\ r_b\ a\ \cos\frac{\theta}{2}}{\frac{\pi}{4}\ \Omega_s\ \beta^2\ R^2} \tag{21}$$

Now the visual contrast, C_v, required for beacon reflection is related to B_{ab} and B_{af} by

$$C_v = \frac{B_{ab} - B_{af}}{B_{af}} = \frac{B_{ab}}{B_{af}} - 1 \tag{22}$$

Therefore, combining Eqs. 17, 21, and 22 yields

$$C_v + 1 = \frac{4\ a \cos\frac{\theta}{2}\ r_b\ d_e^2}{K_\theta\ a_f\ \Omega_s\ d^2\ \beta^2\ R^2} \tag{23}$$

Recombining and setting 4 = [3.36/0.84]

$$\frac{ar_b}{0.84\ (C_v + 1)}\left[\frac{d_e}{d}\right]^2 = \frac{K_\theta\ a_f\ \Omega_s\ R^2\ \beta^2}{3.36\ \cos\frac{\theta}{2}} \tag{24}$$

Note that the right side of the equation is the same as Eq. 15 and that the left side differs only by the substitution of C_v for C_p and the field brightness reduction ratio of $(d/d_e)^2$ and the fact that eye contrast values already integrate the 0.84 Airy disc energy collection factor. Therefore, with the substitution of the left side of Eq. 24 for the left side of Eq. 15, Figs. 1 and 2 can be used for both photographic and visual beacon calculations. Note that Eq. 24 is independent of the solar illuminance, transmittance, and telescope diameter values except as they affect the contrast and resolution values of the detection system.

The exit pupil, d, is a function of the telescope objective diameter and magnification so that

$$d = \frac{D_o}{M} \tag{25}$$

Equation 24 then becomes

$$\frac{ar_b\ d_e^2}{0.84\ (C_v + 1)}\left[\frac{M}{D_o}\right]^2 = \frac{K_\theta\ a_f\ \Omega_s\ R^2\ \beta^2}{3.36\ \cos\frac{\theta}{2}} \tag{26}$$

where M/D_o is the magnification per unit diameter.

Now let us analyze Eqs. 15 and 16 before discussing C_p and C_v in depth. For any given phase angle and landing site, the terms $K_\theta\ a_f\ \Omega_s/3.36$ are constant. Both K_θ and a_f are discussed in another section. Therefore, the beacon area varies as the square of the range and the square of the resolution angle. For any given viewing case, the range will be constant. Therefore, the resolution angle chosen will be a major factor in determining beacon area. This choice is, therefore, the subject of a complete section. Looking at the left side of Eqs. 15 and 16, the area will be inversely proportional to the beacon reflectance. Of all the variables in each equation, this probably has the greatest possible range in values depending on the degradation analysis and space micrometeoroid data one uses. Therefore beacon reflectance is also the subject of a separate section.

Both equations have similar terms $(C_p + 1)$ and $C_v + 1)$ related to photographic and visual detection contrast respectively. It will be shown that both C_p and C_v are less than 1 so that the beacon areas required are relatively insensitive to contrast changes. The contrast values will be discussed in the next section.

Finally, the visual detection is highly dependent on the magnification per unit telescope diameter where in practice the ratio will be between 0.4 and 2.0 for most conditions. Since the practical magnification per unit telescope diameter seems inversely proportional to seeing conditions which limit β most of the time, using limited data by Bowen, then the area of the beacon appears to vary as β^4 which indicates the great dependence of beacon detection on seeing conditions.

4. CONTRAST

The degree of photographic or visual contrast required for detection is dependent on both the desired probability of detection and the detector efficiency.

4.1 Photographic contrast

Photographic contrast used herein is given by

$$C_p = \frac{E_{ab} - E_{af}}{E_{af}} = \frac{E_{ab}}{E_{af}} - 1$$

Films are classified in terms of development contrast, γ, density differences, ΔD, where D = log 1/transmission, and Δ log I, the differences in the logs of the exposures in meter-candle-seconds, so that

$$\gamma = \frac{\Delta D}{\Delta \log I} \tag{27}$$

but

$$I = Et \tag{28}$$

so that

$$\gamma = \frac{\Delta D}{\Delta \log Et} = \frac{\Delta D}{\log E_{ab}\, t - \log E_{af}\, t} = \frac{\Delta D}{\log \frac{E_{ab}}{E_{af}}} \tag{29}$$

For each photographic film there is an rms graininess density variation of standard deviation, σ, where σ is measured in the same units as D. For a detection probability of 99.7 percent, a density difference ΔD

of 3σ is required. γ is the slope of the D versus log I curve measured at field brightness exposure energy, I_f, level. σ is measured from microdensitometer readings and will vary according to the slit width, d, of the microdensitometer, which ranges from 5 to 25 microns (0.0002 to 0.001 inch) wide according to the relationship

$$\sigma \cdot d = k \tag{30}$$

Therefore, the microdensitometer used to evaluate lunar photographs should have the same width as the slit used in the rms graininess measurement, to achieve the results predicted from theory.

For minimum seeing disturbances, the film exposure time should be short and, therefore, the exposure index high. Exposures, t, 1/25 second or less are desirable. The exposure energy, I, is given by the following term derived by combining Eqs. 7 and 28:

$$I = \frac{T_e\, T_t\, K_\theta\, a_f\, E_s\, t}{4N^2} \tag{31}$$

and

$$\text{A.S.A. film reading} = \frac{1}{I} \tag{32}$$

For $T_e = 0.70$, $T_f = 0.70$, $K_\theta = 1$, $a_f = 0.065$, $E_s = 140{,}000$ lumens/m^2
$N = 16$, and $t = 0.04$

$$\text{A.S.A.} = \frac{1}{0.174} = 5.75$$

For films of equal or higher A.S.A. value, many have γ's equal or greater than 3.0 and σ's less than or equal to 0.1. Therefore

$$C_p + 1 = \log^{-1} \frac{0.1}{3.0} = 1.08 \qquad \text{(by combining Eqs. 13 and 29)}$$

This value has been used in all photographic calculations and appears quite conservative due to the conservative film assumptions.

Assume that 1/2 sec seeing, β = 1/2 sec, is practical for a given site, i.e., at least 10 percent of the time at Pic-du-Mich in France and that the telescope has a resolution better than 1/2 sec of arc. Then from Fig. 1 drawn with this example the area factor $ar_b/(C_p + 1)$ is 1.13 square meters for a 0-degree phase angle sighting at 0 degree longitude. Therefore, for a reflectance of 0.80 and $(C_p + 1)$ = 1.08 above, a = 1.53 square meters (16.5 square feet).

Other photographic detection beacon areas were calculated in a similar fashion.

4.2 Visual Contrast

Visual contrast required for detection has been the subject of numerous investigations, many of which are summarized by Taylor (1964). In general, most calculations refer to the work of Blackwell (1946) who reported the Tiffany Data. These data represented special viewing conditions characterized by the following factors:

1. Uniform circular targets
2. Uniform background
3. Binocular vision
4. Known time of stimulus
5. Known direction of stimulus
6. Trained observers

The Tiffany data are reported for a 50-percent probability of detection, C_{50}. Taylor has summarized various correction factors for modifying the original Blackwell data for application to practical conditions. These are summarized in Table 1. For beacon calculations, the contrast, C_v, used is related to the correction values in the table, K_p, K_b, K_v, K_t, and the original data, Tiffany Data C_{50}, by

$$C_v = K_p K_b K_v K_t C_{50} \qquad (33)$$

TABLE 1

CORRECTION FACTORS FOR BLACKWELL DATA

					Factor
1.	1. Detection Probability, K_p				
	50%				1.0
	90%				1.50
	95%				1.64
	99%				1.91
	2. Target Properties, K_b				
	Known Factors				
	Location	Time	Size	Duration	
	X	X	X	X	1.00
	X		X	X	1.40
	X		X		1.60
	X			X	1.50
	X				1.45
		X	X	X	1.31
	3. Vigilance, K_v				1.19
	4. Training, K_t				
	Trained				1.00
	Untrained				1.90

Values of $K_p = 1.91$, $K_b = 1.40$, $K_v = 1.19$, and $K_t = 1.00$ were chosen representing a 99-percent detection probability, unknown flash time (i.e., not an omnidirectional beacon), a vigilant and trained observer or $C_v = 3.18\ C_{50}$. This is the range of presently accepted conversion factors for the Tiffany data. Even if this factor is in error by a factor of 2, beacon areas will only increase by 20 percent for the worst practical telescopic visual case.

The visual contrast is a function of apparent field brightness, B_{af}, and apparent beacon angular subtend, $M\beta$. B_{af} can be determined from a plot of $B_{af}\ d_e^2$ versus B_{af} (Fig. 3) where by rearranging Eq. 16

$$B_{af}\ d_e^2 = T_e\ T_t\ d^2\ B_f \tag{34}$$

which by substitution of Eq. 25 is

$$B_{af}\ d_e^2 = T_e\ T_t \left[\frac{D_o}{M}\right]^2 \frac{K_\theta\ a_f\ E_s}{\pi} \tag{35}$$

For the 28X, 1.58-inch CM sextant sighting on 0-degree phase angle at $T_e = 1.0$, $T_t = 0.27$, $D_o/M = 1.443$ mm $= d$, $K_\theta = 1$, $a_f = 0.065$, $E_s = 14.0$ candles/cm^2. Therefore, $B_{af}\ d_e^2 = 1.61 \times 10^{-3}$ candles (and log $B_{af}\ d_e^2 = -3.206$).

Reading from Fig. 3, which is drawn showing this example, the apparent field brightness is 1.58×10^{-2} candles/cm^2.

Original smoothed Tiffany data, taken from Blackwell (1946) and converted to brightnesses in candles/cm^2, are shown in Fig. 4. Assuming a sextant resolution of 5 seconds, which is conservative compared with the 3.5 seconds value determined from $(1.22\ \lambda/D_o)$, the apparent beacon angular subtend will be 2.33 minutes of arc. A cross plot of C_v versus θ, not shown here, for constant, $B_{af} = 1.58 \times 10^{-2}$, using Fig. 4 for cross plot data, shows that $C_{50} = 4.95 \times 10^{-2}$ at $\theta = 2.33$ minutes. From above, $C_v = 3.18\ C_{50}$. $\therefore C_v + 1 = 1.157$. Knowing $B_{af}\ d_e^2$ and B_{af}

$$d_e = \sqrt{\frac{B_{af}\ d_e^2}{B_{af}}} \tag{36}$$

$= 3.2$ mm for the above case

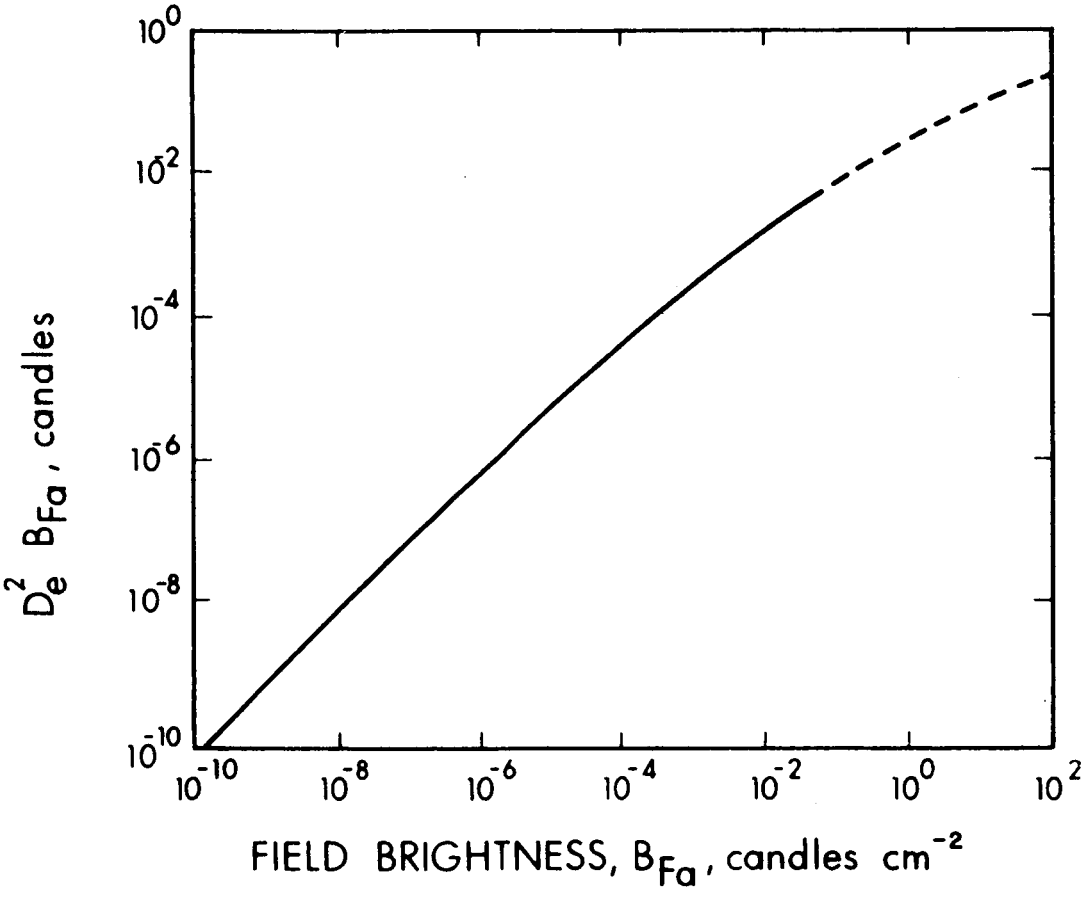

FIG. 3 RESPONSE OF THE PUPIL OF THE EYE TO FIELD BRIGHTNESS LEVEL

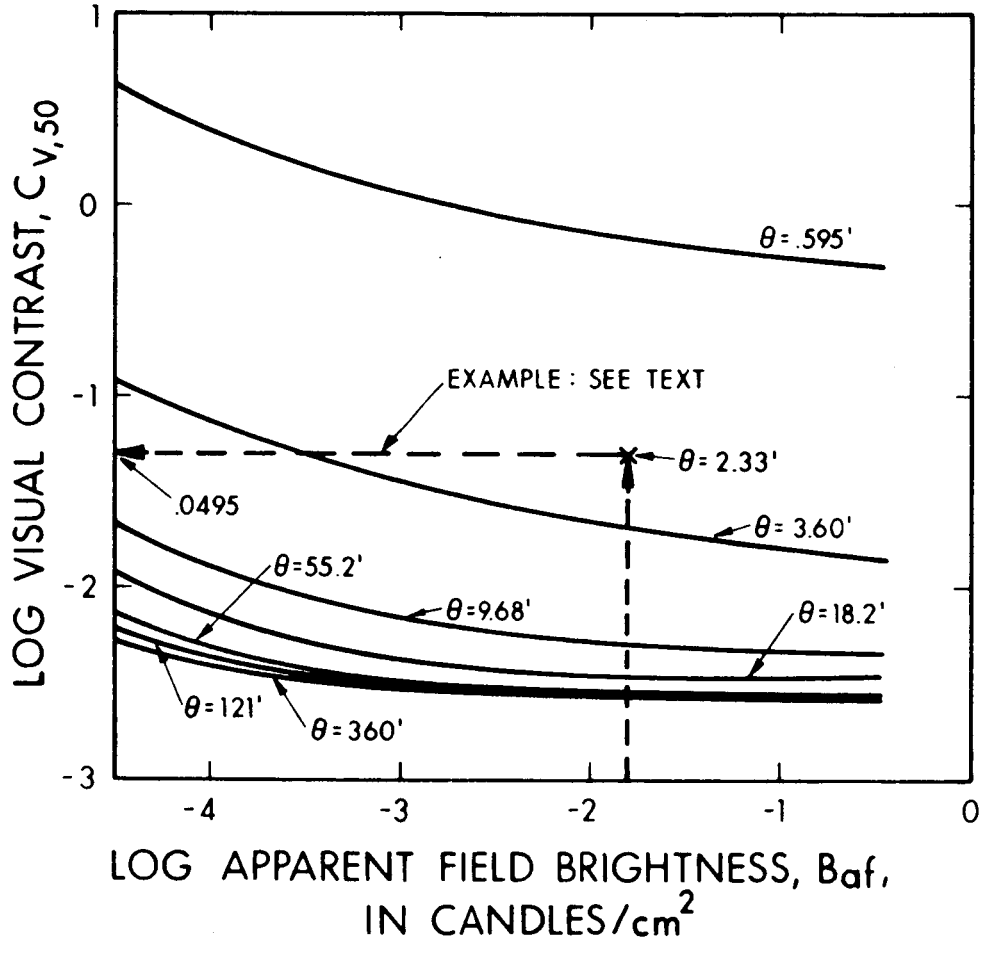

FIG. 4 VISUAL CONTRAST VS FIELD BRIGHTNESS FOR VARIOUS ANGULAR SUBTENDS, θ

Assume $r_b = 0.80$; d was 1.443 mm from above. From Fig. 2 for a $\beta = 5$ seconds of arc resolution

$$\frac{ar_b}{0.84\ (C_v + 1)\left(\frac{d}{d_e}\right)^2} = 4.21 \times 10^{-4}\ m^2$$

Substitution of the values listed above yields a required beacon area of 1.03 cm^2 or 0.16 square inch. Other beacon areas for visual detection were calculated in a similar fashion. This corresponds to a spherical beacon diameter, d_s, of 4.95 meters (or 16.3 feet) disregarding the negative contrast effects of the apparently nonreflective portions of the moon. The spherical diameter is related to the area by the relationship

$$d_s = \frac{8}{\alpha}\sqrt{\frac{a}{\pi}} \qquad (37)$$

where α is the solar angular subtend.

5. BEACON REFLECTANCE

Possible degradation in the beacon reflectance is the major unknown in sizing the lunar beacon. Empirical and experimental analysis of the problem by Button (1964), Marks (1964), and others have predicted or extrapolated losses in spectral reflectance from between 1 and 50 percent due to uv, high energy proton, and micrometeorite impingement. No space experimental data are available to corroborate these analyses, though an experiment is now being planned to study the degradation of reflective samples in space.

Unprotected aluminum has a practical visible reflectance of 91 percent. Therefore, the assumed reflectance value of 0.80 percent would allow an 11-percent reflectance loss due to lunar dust, coating transmittance, micrometeorite damage, etc., and appears valid based on some reflectance predictions.

Silicon-monoxide-overcoated aluminum has a visible reflectance of 87 percent, when deposited under standard development conditions. Though this reflectance system is 4 percent lower than aluminum and although silicon monoxide coatings are more susceptible to failure when folded over sharp corners as in an inflatable beacon, aluminum coatings overcoated with a 1000Å-micron-thick silicon monoxide coating show 1.2 times less degradation over comparable intensities of simulated micrometeorite flux. Silicon monoxide overcoatings have the added advantage that they are much more easily cleaned than aluminum alone. Quartz-overcoated aluminum will yield reflectance values of 88 percent over the visible spectrum and have high abrasion resistance also. However, quartz overcoatings are supplied by only a limited number of installations at this time.

Note that the reflectances cited are lower than textbook or experimental reflectance values. These lower values represent practical minimum limits for a metal mirror for this beacon program. Beacons with plastic substrates will have lower reflectance values.

6. SEEING CONDITIONS

For terrestrial telescopes, used either as photographic or visual instruments, the limiting angular resolution will determine to a large extent the detectability of a given beacon size. Since for most observatories the theoretical resolution of the telescope is achieved 10 percent or less of the night time, seeing is used in this analysis almost interchangeably with the integrated angular resolution of the detector instrument.

Seeing is a function of the changes in the index of refraction of the atmosphere through which the object rays pass to reach the telescope. Seeing is therefore an angular condition rather than a uniform loss of intensity which is a transmittance loss, or a non-uniform loss of intensity over the aperture called scintillation.

Irregularities in the index of refraction are due primarily to thermal nonhomogeneities, water vapor variations and ozone variations. Seeing is adversely affected by the following factors summarized from Stock and Keller, and Meinel (1960).

1. Moist climate
2. Cold fronts
3. Jet streams (high-velocity high-altitude air streams)
4. Observatory dome radiation
5. Observatory heat sources-instruments astronomers
6. Observations located close to the ground
7. Aircraft condensation trails
8. Air pollution
9. Temperature inversion
10. Skyglow
11. Haze

Seeing will be generally improved by using short time exposures in photographic work. Excellent high-altitude sights such as Pic-du-Mich in France and Kitt Peak have 1/2-second seeing between 10 and 20 percent of the time from Kopal (1963) and Meinel (1960) while 1 to 1-1/2 seconds seeing is "normal" for such observatories as Mount Wilson and Mount Palomar.

Earth-photographed beacon areas have been based initially on 1/2 second seeing conditions; visual observations on 1-second seeing.

7. MISCELLANEOUS FACTORS

The diameter magnification factor $\frac{M}{D_o}$ varies practically between 0.4 and 2.0. For "normal" magnification, i.e., $d = d_e$, the factor is between 0.3 and 0.5, depending on B_{af}. Generally the larger the telescope the lower the magnification factor. Bowen (1947) has reported a magnification factor of 0.56 for the Mount Wilson 60-inch telescope under 1 to 2 seconds seeing conditions and 1.31 for a 6-inch telescope.

The effect of diameter magnification factor and magnification upon beacon area is shown in Fig. 5 for 10 inches, 24 inches

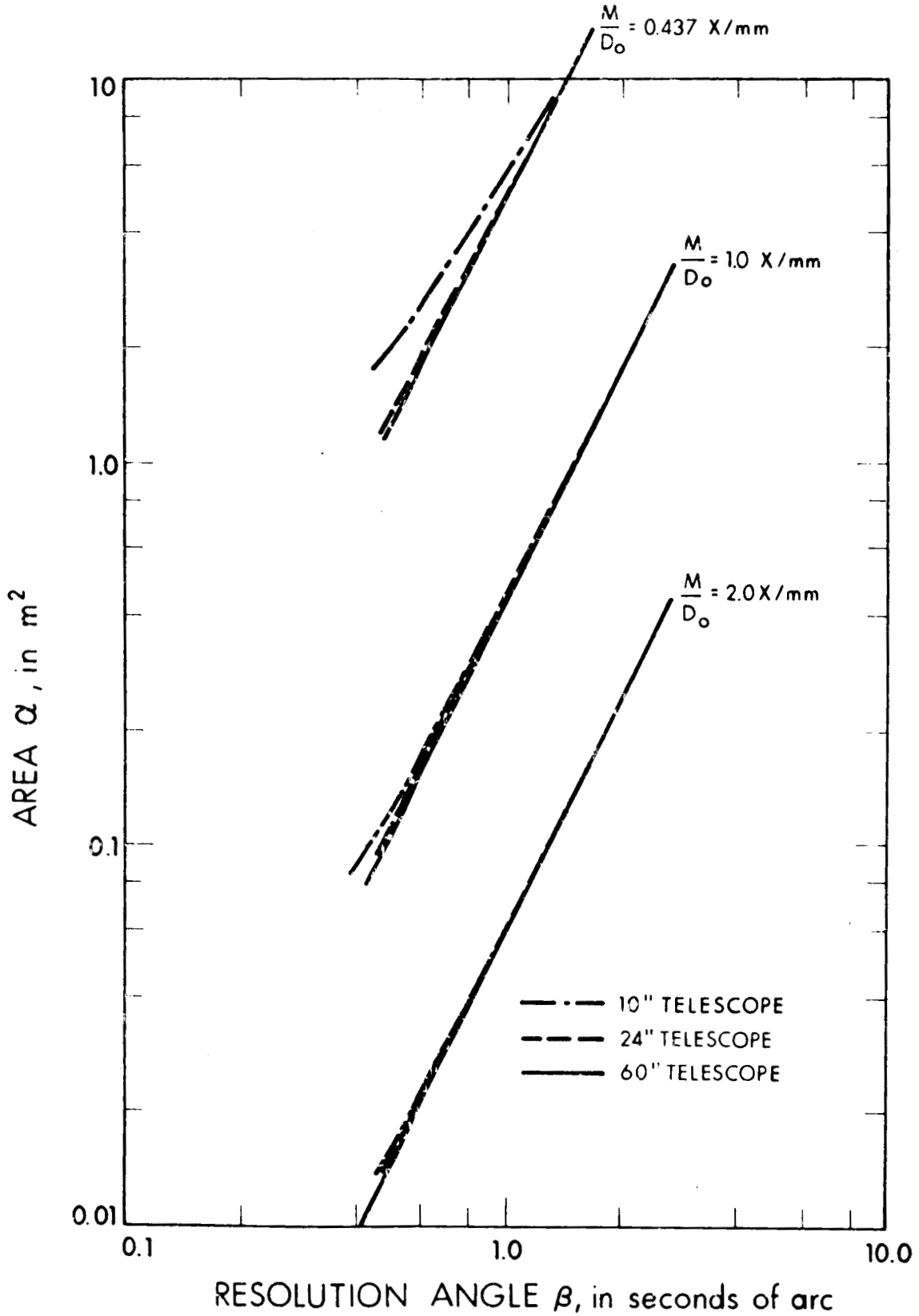

FIG. 5 BEACON AREA VS RESOLUTION ANGLE FOR VARIOUS DIAMETRICAL MAGNIFICATION FACTORS AND TELESCOPE APERTURES

(size of Pic-du-Mich in France) and 60 inches (Mount Wilson) telescopes. The area difference between telescopes are greater with smaller magnification factors so that with large factors there is little value in increasing the telescope aperture above 24 inches. Scintillation effects also practically limit lunar observation to telescopes in the range of 10 to 40 inches since little if anything is gained in going to larger diameters, since seeing and scintillation limit the usefulness of large apertures except for energy-gathering purposes.

The phase angle factor, K_θ, relates to the variation in albedo as a function of both phase angle and longitudinal location. The factors used to calculate Figs. 1 and 2 were taken from Minnaert (1961) for zero degree longitude. The phase angle factors do not vary with latitude, i.e., are constant along north-south meridians. The factors will vary with other longitude angles.

The atmospheric transmission factor, T_e used in calculating the beacon sizes was 0.7. Depending upon the observatory altitude, the telescope elevation angle, and the water vapor in the atmosphere, the actual atmospheric transmission can be greater or less than the 0.7 factor. Figure 6 depicts the air masses for various observatory altitudes for a telescope with a 90 degree elevation angle. Figure 7 depicts the air mass versus elevation angle for various elevation angles. By multiplying the air mass factors in Fig. 6, the total air mass through which the earth-lunar solar reflecting beacon signal must pass can be determined. From this calculated air mass plus the curves shown in Fig. 8 for various amounts of percipitable water vapor in the atmosphere, the fractional atmospheric transmission to either solar radiation or the beacon reflected signal can be determined.

Figure 7 indicates that those observatories that are close to the artic or antarctic circles will have relatively larger transmission losses when viewing the moon than those observatories located closer to the equator.

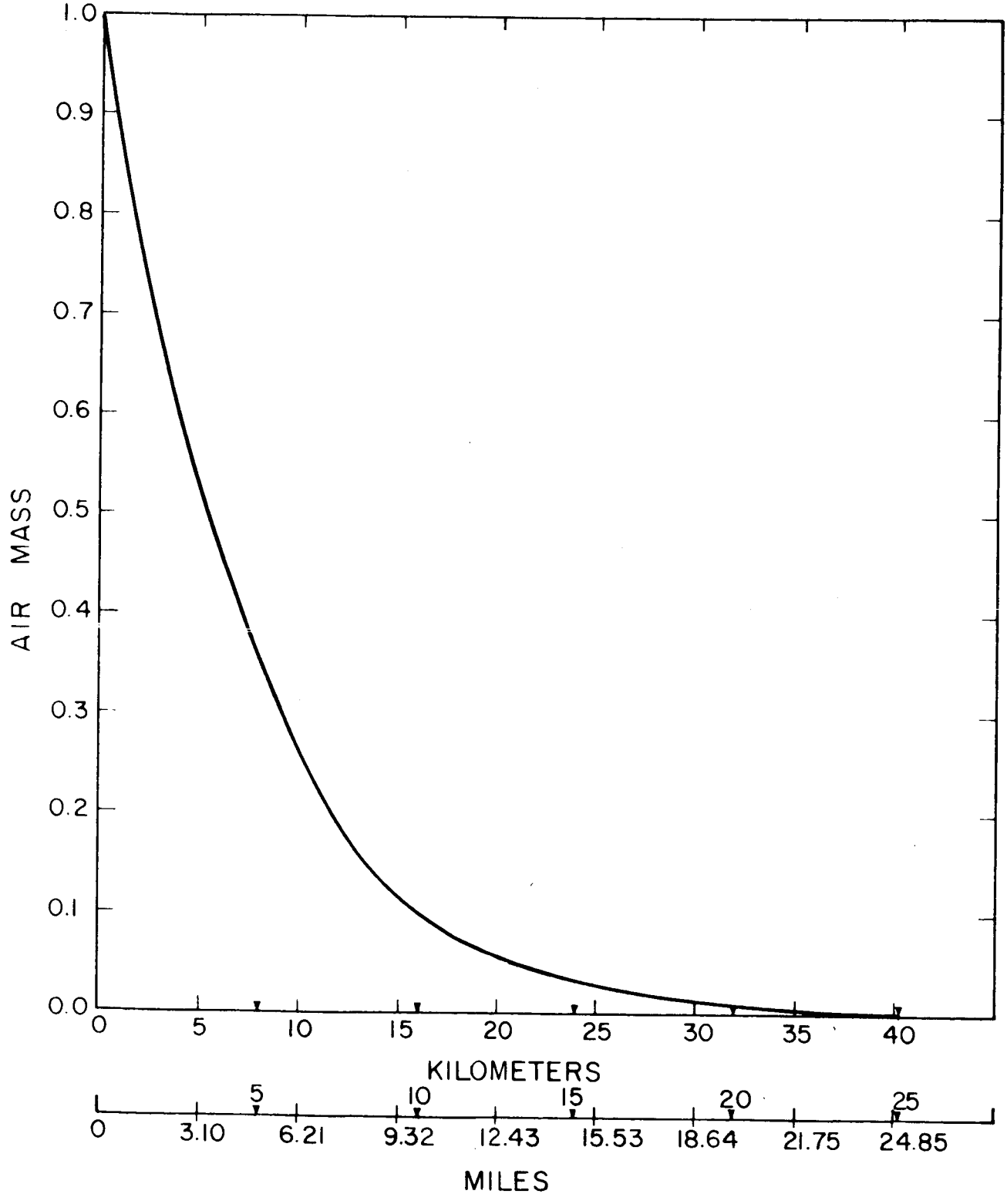

FIG. 6 AIR MASS VERSUS ALTITUDE FOR 90° ELEVATION

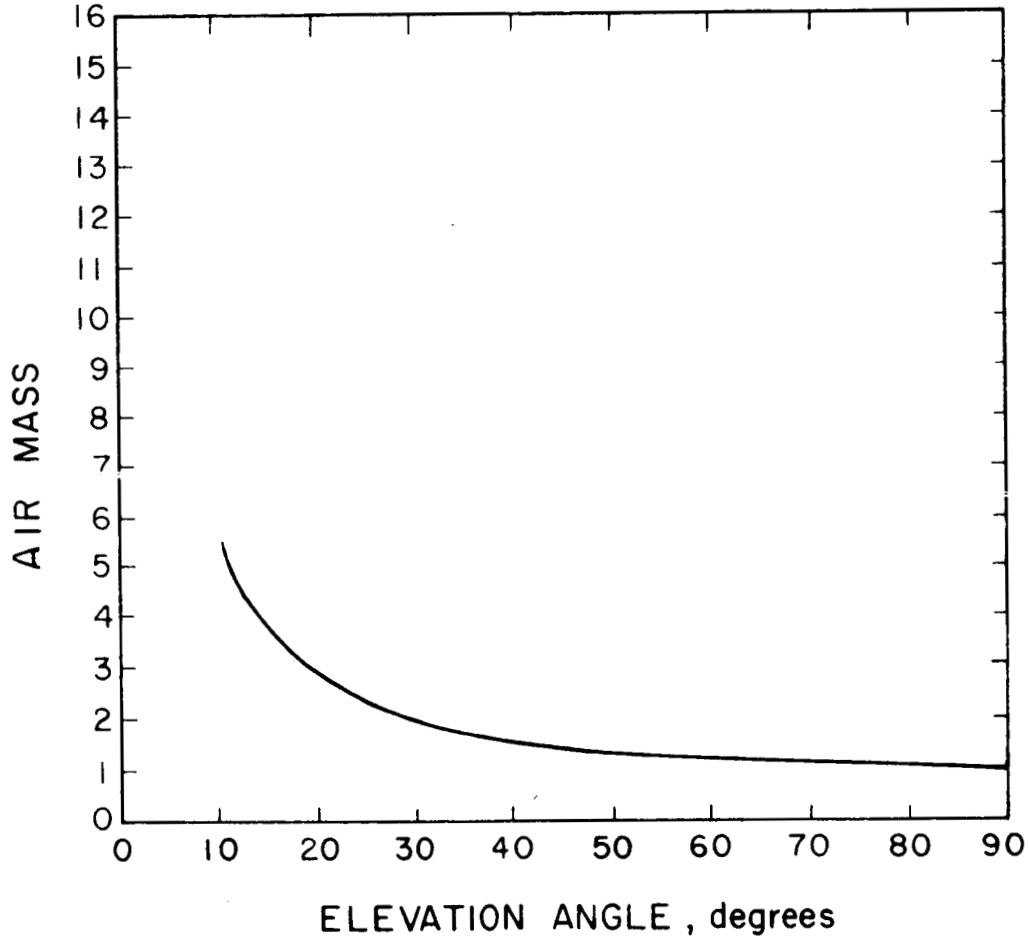

FIG. 7 AIR MASS VERSUS ELEVATION ANGLE

TRANSMISSION OF ATMOSPHERE TO SOLAR RADIATION

THE GRAPH SHOWS:
WATER-VAPOUR IN CM OF PRECIPITABLE WATER
PER UNIT MASS

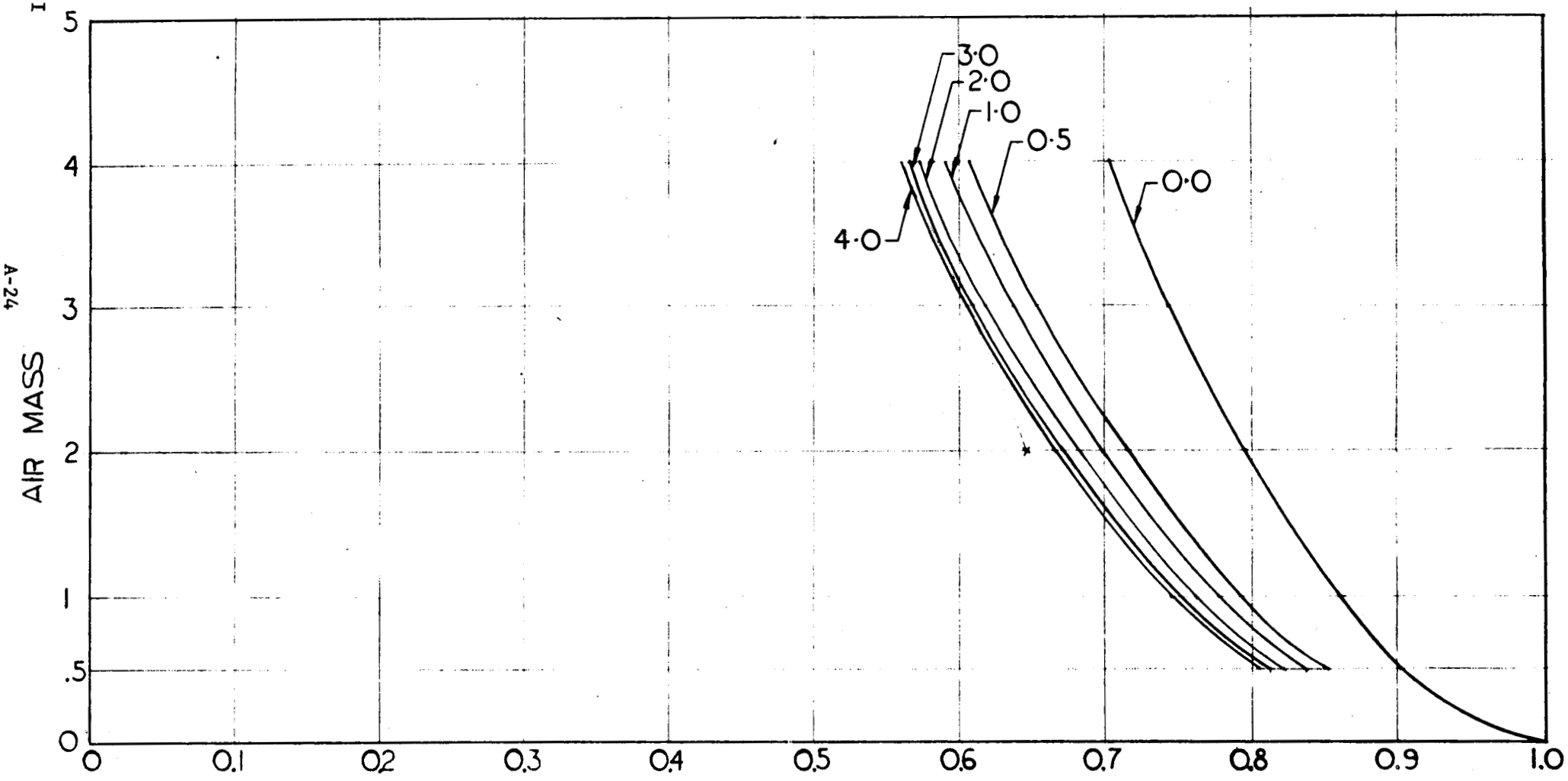

FIG. 8

8. ACKNOWLEDGMENT

The work of many previous authors has been helpful in understanding and presenting the beacon detection problem. These are listed in a bibliography at the end of this report.

APPENDIX B

DIFFUSE BEACON PHOTOMETRIC ANALYSIS

APPENDIX B

DIFFUSE BEACON PHOTOMETRIC ANALYSIS

The nomenclature and formulae of Appendix A will be helpful in understanding this section.

1. Flat Beacon

For a diffuse flat reflector, the illuminance at the instrument objective, E_{ob}, is related to the diffuse beacon area, a_d, range, R, solar illuminance, E_s, beacon albedo, a_b, the angle of solar incidence, ψ, the angle of reflection or observation, ϕ, and the atmospheric transmission, T_e, by the relationship

$$E_{ob} = \frac{T_e E_s a_b \; a \cos\psi \cos\phi}{\pi R^2} \tag{1-B}$$

From 1-B and 6, 7, 8, and 15 of Appendix A

$$\frac{a_d a_b}{(C_p + 1)\pi} = \frac{k_\theta a_f R^2 \beta^2}{3.36 \cos\psi \cos\phi} \tag{2-B}$$

So that the ratio of the ratio of the diffuse and specular flat beacon areas from 2-B and 15 of Appendix A is

$$a_d/a_s = \frac{\pi r_b}{\Omega_s a_b} \; \frac{\cos\frac{\theta}{2}}{\cos\psi \cos\phi} \tag{3-B}$$

Since the solar solid angle in steradians is 6.76×10^{-5}, then the ratio of the beacon areas for diffuse and specular flats which can be detected photographically is

$$\frac{a_d}{a_s} = 4.65 \times 10^4 \frac{\cos\frac{\theta}{2}}{\cos\psi \cos\phi} \frac{r_b}{a_b}$$

Similarly it can be shown that the same ratio holds for visual observations.

At 0° phase, incident, and observation angles, the related areas for flat specular and diffuse beacons having the same diffuse and specular reflectance would be:

Case	Recommended Specular Area	Corresponding Diffuse Area
Earth Beacon 207,000 nm	32.9 ft^2	1.53×10^6 ft^2
Cislunar Beacon 400 nm	1.09×10^{-2}	5.05×10^2 ft^2

2. Spherical Beacons

From equation 37 of Appendix A, the spherical diameter of a specular sphere is

$$d_s = \frac{8}{\alpha}\sqrt{\frac{a_s}{\pi}} = 4.86 \times 10^2 \sqrt{a_s}$$

Therefore relative illuminance of a diffuse spherical beacon, E_{bd}, to a specular spherical beacon, E_{bs}, is a function of the phase angle, θ,

specular and diffuse reflectances, r_b and a_b, and the spherical diameters for the specular and diffuse spheres, d_{ss} and d_{sd}, as given by

$$\frac{E_{bd}}{E_{bs}} = \frac{8}{3\pi}\left(\sin\theta + [\pi-\theta]\cos\theta\right)\frac{a_b}{r_b}\frac{d_{sd}^2}{d_{ss}^2} \qquad (4\text{-B})$$

Therefore a diffuse sphere of the same diameter as a specular sphere would have an intensity of

$$\frac{2.67\ a_b}{r_b}$$

times that of the speculat sphere at 0° phase angle. The intensities of specular and diffuse spheres of equal diameter are equivalent when the phase angle, θ, is $\pm 0.46\pi$ radians or ± 83 degrees.

Therefore the relative diameters of diffuse and specular spheres having the same reflectances would be as follows:

Case	Recommended Specular Sphere Diameter	Recommended Diffuse Sphere Diameter for $\theta = \pm 83^\circ$	Recommended Diffuse Sphere Diameter for 0° phase angle
Earth Beacon 207,000 nm	2790 ft	2790 ft	1740 ft
Cislunar Beacon 400 nm	50.5 ft	50.5 ft	31 ft

APPENDIX C

REFLECTOR ORIENTATION COMPUTER PROGRAMS

APPENDIX C

REFLECTOR ORIENTATION COMPUTER PROGRAMS

1. $\underline{i, \Lambda, \Omega'}$

$$\cos i = \cos(I + \rho) \cos(\bar{\epsilon} + \Delta\epsilon) + \sin(I + \rho) \sin(\bar{\epsilon} + \Delta\epsilon) \cos(\Omega + \sigma + \Delta\psi)$$

$$\underline{21^\circ < i < 25^\circ}$$

$$\Lambda = \Delta + \zeta + \tau - \Omega - \sigma$$

$$\underline{0 < \Lambda < 360^\circ}$$

$$\sin\Omega' = - \sin(\Omega + \sigma + \Delta\Psi) \csc i \sin(I + \rho)$$

$$\underline{-4^\circ < \Omega' < 4^\circ 10'}$$

where

$\bar{\epsilon} = 23^\circ.4457874 - 0^\circ.01301376\ T$ = mean obliquity of date

$\Delta\epsilon = 0^\circ.255833(10^{-2}) \cos\Omega - 0^\circ.25(10^{-4}) \cos 2\Omega + 0^\circ.1530555(10^{-3}) \cos 2L$

= nutation in obliquity

$\Delta\Psi = - [0^\circ.47895611(10^{-2}) + 0^\circ.47222(10^{-5})\ T] \sin\Omega$

$+ 0^\circ.58055(10^{-4}) \sin 2\Omega - 0^\circ.3533(10^{-3}) \sin 2L$

$$I = 1^{\circ}\ 32.1'$$

$$\Omega = 12^{\circ}.1127902 - 0^{\circ}.0529539222\ d + 0^{\circ}.20795(10^{-2})T + 0^{\circ}.2081(10^{-2})T^2$$

$$\Pi = 64^{\circ}.37545167 + 13^{\circ}.1763965268\ d - 0^{\circ}.1131575(10^{-2})T - 0^{\circ}.113015(10^{-2})T^2$$

$$\sin\Delta = -\sin(\Omega + \sigma + \Delta\Psi)\ \csc i\ \sin(\bar{\epsilon} + \Delta\epsilon),$$

$$\cos\Delta = -\cos(\Omega + \sigma + \Delta\Psi)\ \cos\Omega' - \sin(\Omega + \sigma + \Delta\Psi)\ \sin\Omega'\ \cos(\bar{\epsilon} + \Delta\epsilon)$$

$$L = 280^{\circ}.08121009 + 0^{\circ}.9856473354\ d + 0^{\circ}.302(10^{-3})\ T + 0^{\circ}.302(10^{-3})T^2$$

$$\sigma \sin I = -0^{\circ}.0302777 \sin g + 0^{\circ}.0102777 \sin (g + 2\omega) - 0^{\circ}.305555(10^{-2}) \sin (2g + 2\omega)$$

$$\tau = -0^{\circ}.3333(10^{-2}) \sin g + 0^{\circ}.0163888 \sin g' + 0^{\circ}.5(10^{-2}) \sin 2\omega$$

$$\rho = -0^{\circ}.0297222 \cos g + 0^{\circ}.0102777 \cos (g + 2\omega) - 0^{\circ}.305555(10^{-2}) \cos (2g + 2\omega)$$

$$g = 215^{\circ}.54013 + 13^{\circ}.064992\ d$$

$$g' = 358^{\circ}.009067 + 0^{\circ}.9856005\ d$$

$$\omega = 196^{\circ}.745632 + 0^{\circ}.1643586\ d$$

Here, d is measured in Julian days from January 1.0, 1950, and T is measured in Julian centuries (of 36,525 days) from January 1.0, 1950.

2. PROGRAM I

$$\sin\mu_e = \sin i \cos\delta_m \sin(\alpha_m - \Omega') - \cos i \sin\delta_m$$

$$\tan\lambda_e = \frac{B - \tan\Lambda \cos(\alpha_m - \Omega')}{B \tan\Lambda + \cos(\alpha_m - \Omega')}$$

$$B = \cos i \sin(\alpha_m - \Omega') + \sin i \tan\delta_m$$

$$\sin\mu_s = \frac{R_{se}}{R_{sm}} [\sin\delta_s \cos i - \cos\delta_s \sin i \sin(\alpha_s - \Omega')] + \frac{R}{R_{sm}} \sin\mu_e$$

$$\tan\lambda_s = \frac{\cos\delta_s \cos\Lambda [- \tan\Lambda \cos(\alpha_s - \Omega') + F] + \frac{R}{R_{se}} \sin\lambda_e \cos\mu_e}{\cos\delta_s \cos\Lambda [\cos(\alpha_s - \Omega') + F \tan\Lambda] + \frac{R}{R_{se}} \cos\lambda_e \cos\mu_e}$$

$$F = \cos i \sin(\alpha_s - \Omega') + \sin i \tan\delta_s$$

$$\cos\lambda_s = \frac{\cos\delta_s \cos\Lambda [\cos(\alpha_s - \Omega') + F \tan\Lambda] + \frac{R}{R_{se}} \cos\lambda_e \cos\mu_e}{\frac{R_{sm}}{R_{se}} \cos\mu_s}$$

$$|\mu_e| < 8^o, \; |\lambda_e| < 8^o, \; |\mu_s| < 2^o$$

Here,

$$\alpha_m = \sin^{-1} \frac{y_m}{(x_m^2 + y_m^2)^{1/2}} = \cos^{-1} \frac{x_m}{(x_m^2 + y_m^2)^{1/2}}; \qquad \delta_m = \sin^{-1} \frac{z_m}{R}$$

$$\alpha_s = \sin^{-1} \frac{y_s}{(x_s^2 + y_s^2)^{1/2}} = \cos^{-1} \frac{x_s}{(x_s^2 + y_s^2)^{1/2}}; \qquad \delta_s = \sin^{-1} \frac{z_s}{R_{se}}$$

$$x_m = R_e \left[X_{em} \cos\tau - Y_{em} \sin\tau \cos\bar{\epsilon} - Z_{em} \sin\tau \sin\bar{\epsilon}\right]$$

$$y_m = R_e \left[X_{em} \sin\tau \cos\bar{\epsilon} + Y_{em} (\cos^2\bar{\epsilon} \cos\tau + \sin^2\bar{\epsilon}) + Z_{em} \sin\bar{\epsilon} \cos\bar{\epsilon} (\cos\tau - 1)\right]$$

$$z_m = R_e \left[X_{em} \sin\tau \sin\bar{\epsilon} + Y_{em} \sin\bar{\epsilon} \cos\bar{\epsilon} (\cos\tau - 1) + Z_{em} (\cos\tau \sin^2\bar{\epsilon} + \cos^2\bar{\epsilon})\right]$$

$$x_s = Au \left[- X_{se} \cos\tau + Y_{se} \sin\tau \cos\bar{\epsilon} + Z_{se} \sin\tau \sin\bar{\epsilon}\right]$$

$$y_s = Au \left[- X_{se} \sin\tau \cos\bar{\epsilon} - Y_{se} (\cos^2\bar{\epsilon} \cos\tau + \sin^2\bar{\epsilon}) - Z_{se} \sin\bar{\epsilon} \cos\bar{\epsilon} (\cos\tau - 1)\right]$$

$$z_s = Au \left[- X_{se} \sin\tau \sin\bar{\epsilon} - Y_{se} \sin\bar{\epsilon} \cos\bar{\epsilon} (\cos\tau - 1) - Z_{se} (\cos\tau \sin^2\bar{\epsilon} + \cos^2\bar{\epsilon})\right]$$

$R = R_e (X_{em}^2 + Y_{em}^2 + Z_{em}^2)^{1/2}$ = earth-moon distance

$R_{se} = Au (X_{se}^2 + Y_{se}^2 + Z_{se}^2)^{1/2}$ = sun-earth distance

$$R_{sm} = \left[(R_e X_{em} + Au X_{se})^2 + (R_e Y_{em} + Au Y_{se})^2 + (R_e Z_{em} + Au Z_{se})^2\right]^{1/2}$$

= sun-moon distance

R_e = radius of earth = 6378.3255 km; Au = astronomical unit = 149,599,000 km

$\tau = 1^{\circ}.3846\ T$ (This τ is not to be confused with the τ appearing in part 1 above.)

(X_{em}, Y_{em}, Z_{em}) = coordinates of moon in geocentric equatorial reference frame of the mean equator and equinox of 1950.0

(x_m, y_m, z_m) = - - - mean equator and equinox of date.

(X_{se}, Y_{se}, Z_{se}) = coordinates of earth (actually earth-moon center of mass) in heliocentric equatorial (earth's equator) reference frame of the mean equator and equinox of 1950.0

(x_s, y_s, z_s) = - - - mean equator and equinox of date.

3. PROGRAM II

$$\cos\gamma = \cos\varphi\ (n_x \cos\theta + n_y \sin\theta + n_z \tan\varphi); \qquad \underline{0 \le \gamma \le 90^\circ}$$

$$\sin\sigma = \frac{1}{\sin\gamma}\ (n_x \sin\theta - n_y \cos\theta)$$

$$\cos\sigma = \frac{1}{\sin\gamma}\ [-\sin\varphi\ (n_x \cos\theta + n_y \sin\theta) + n_z \cos\varphi]; \quad \underline{0 \le \sigma \le 360^\circ}$$

$$n_x = \frac{\rho_x + \cos\lambda_s \cos\mu_s}{N}, \quad n_y = \frac{\rho_y + \sin\lambda_s \cos\mu_s}{N}, \quad n_z = \frac{\rho_z + \sin\mu_s}{N}$$

$$N = [2\ (1 + \rho_x \cos\lambda_s \cos\mu_s + \rho_y \sin\lambda_s \cos\mu_s + \rho_z \sin\mu_s)]^{1/2}$$

$$\rho_x = \frac{1}{L}\ (A + q_x), \quad \rho_y = \frac{1}{L}\ (B + q_y), \quad \rho_z = \frac{1}{L}\ (C + q_3)$$

$$q_x = R \cos\lambda_e \cos\mu_e - R_m \cos\theta \cos\varphi = p_x D$$

$$q_y = R \sin\lambda_e \cos\mu_e - R_m \sin\theta \cos\varphi = p_y D$$

$$q_z = R \sin\mu_e - R_m \sin\varphi = p_z D$$

$$L = (D^2 + R_e^2 + 2Aq_x + 2Bq_y + 2Cq_z)^{1/2}$$

$$D^2 = R^2 + R_m^2 - 2RR_m\ [\cos\varphi \cos\mu_e \cos(\theta - \lambda_e) + \sin\varphi \sin\mu_e]$$

$$A = R_{ex}\, x_{11} + R_{ey}\, x_{12} + R_{ez}\, x_{13}$$

$$B = R_{ex}\, x_{21} + R_{ey}\, x_{22} + R_{ez}\, x_{23}$$

$$C = R_{ex}\, x_{31} + R_{ey}\, x_{32} + R_{ez}\, x_{33}$$

$$x_{11} = \cos\Omega' \cos\Lambda - \sin\Omega' \sin\Lambda \cos i$$

$$x_{12} = \sin\Omega' \cos\Lambda + \cos\Omega' \sin\Lambda \cos i$$

$$x_{13} = \sin\Lambda \sin i$$

$$x_{21} = -\cos\Omega' \sin\Lambda - \sin\Omega' \cos\Lambda \cos i$$

$$x_{22} = -\sin\Omega' \sin\Lambda + \cos\Omega' \cos\Lambda \cos i$$

$$x_{23} = \cos\Lambda \sin i$$

$$x_{31} = \sin i \sin\Omega'$$

$$x_{32} = -\sin i \cos\Omega'$$

$$x_{33} = \cos i$$

$$R_{ex} = R_e \cos(\Theta + \alpha_s - 180^{\circ} + 15.0\, t_o) \cos\Phi$$

$$R_{ey} = R_e \sin(\Theta + \alpha_s - 180^{\circ} + 15.0\, t_o) \cos\Phi$$

$$R_{ez} = R_e \sin\Phi$$

Here, R = earth-moon distance, R_m = radius of moon = 1738 km

Also, φ, θ are the latitude and longitude, respectively, on the moon's surface of the reflector, and Φ, Θ are the latitude and longitude, respectively, of the "target point" on the earth's surface.

The condition which must be satisfied in order that the reflector on the moon's surface be visible from the point Φ, Θ on the earth's surface, at the time t_o, is

$$Aq_x + Bq_y + Cq_z < 0$$

The condition which must be satisfied in order that the sun be visible from the reflector on the moon's surface (φ, θ), at the time t_o, is

$$\cos(\theta - \lambda_s) + \tan \varphi \tan \mu_s > 0$$

4. PROGRAM III

$$\Phi = \sin^{-1}\left(\frac{Rez}{Re}\right) \qquad \underline{-90^{o} < \Phi < 90^{o}}$$

$$\Theta = \tan^{-1}\left(\frac{Rey}{Rex}\right) - \alpha_s + 180^{o} - 15.0\ t$$

$$\Theta = \sin^{-1}\frac{R_{ey}}{\left(R_{ex}^2 + R_{ey}^2\right)^{1/2}} - \alpha_s + 180^{o} - 15.0\ t \qquad \underline{-180^{o} < \Theta < 180^{o}}$$

Here,

$$R_{ex} = A\ X_{11} + B\ X_{21} + C\ X_{31} \qquad A = L\ \rho_x - D\ p_x$$

$$R_{ey} = A\ X_{12} + B\ X_{22} + C\ X_{32} \qquad B = L\ \rho_y - D\ p_y$$

$$R_{ez} = A\ X_{13} + B\ X_{23} + C\ X_{33} \qquad C = L\ \rho_z - D\ p_z$$

$$L = D\left[\cos\Gamma - \left(\frac{R_e^2}{D^2} - \sin^2\Gamma\right)^{1/2}\right] \qquad \cos\Gamma = p_x\ \rho_x + p_y\ \rho_y + p_z\ \rho_z$$

$$p_x = \frac{R}{D}\left(\cos\lambda_e \cos\mu_e - \frac{R_m}{R}\cos\theta\cos\phi\right)$$

$$p_y = \frac{R}{D}\left(\sin\lambda_e \cos\mu_e - \frac{R_m}{R}\sin\theta\cos\phi\right)$$

$$p_z = \frac{R}{D}\left(\sin\mu_e - \frac{R_m}{R}\sin\phi\right)$$

$$\rho_x = \frac{n_x\left[\left(1-2\ n_z^2\right)\vec{\zeta}\cdot\vec{n} + n_z \sin\mu_s\right] - n_y \cos\mu_s\left(n_y \cos\lambda_s - n_x \sin\lambda_s\right)}{1 - n_z^2}$$

$$\rho_y = \frac{n_y \left[(1-2\,n_z^2)\,\vec{\zeta}\cdot\vec{n} + n_z \sin\mu_s\right] + n_x \cos\mu_s\,(n_y \cos\lambda_s - n_x \sin\lambda_s)}{1 - n_z^2}$$

$$\rho_z = 2\,n_z\,\vec{\zeta}\cdot\vec{n} - \sin\mu_s$$

$$n_x = \cos\gamma\cos\theta\cos\phi + \sin\gamma\sin\sigma\sin\theta - \sin\gamma\cos\sigma\sin\phi\cos\theta$$

$$n_y = \cos\gamma\sin\theta\cos\phi - \sin\gamma\sin\sigma\cos\theta - \sin\gamma\cos\sigma\sin\phi\sin\theta$$

$$n_z = \cos\gamma\sin\phi + \sin\gamma\cos\sigma\cos\phi$$

$$\zeta_x = \cos\lambda_s\cos\mu_s, \quad \zeta_y = \sin\lambda_s\cos\mu_s, \quad \zeta_z = \sin\mu_s$$

The axis of the cone of the reflected light will strike the earth if $\cos\Gamma > S$, and will miss the earth if $\cos\Gamma < S$, where

$$S = \left(1 - \frac{R_e^2}{D^2}\right)^{1/2}$$

5. PROGRAM VII

$$K_1 = \sin\frac{\epsilon}{2} - \sin H_1$$

When, $K_1 < 0$, the reflected light is not visible from Θ_1, Φ_1;

When, $K_1 > 0$, the reflected light is visible from Θ_1, Φ_1;

When, $K_1 = 0$, the reflected light becomes visible, or just ceases to to be visible, from Θ_1, Φ_1 .

Here, Θ_1, Φ_1 are the longitude and latitude, respectively, of an observer on the earth. Also, $\epsilon/2$ = half angle of light cone ($\epsilon/2 \sim 16$ min. of arc), where

$$\frac{\epsilon}{2} = \frac{R_s}{R_{sm}}$$

Here, R_s = radius of sun = 6.965×10^5 km

$$\sin H_1 = \frac{\left(V_1^2 + V_2^2 + V_3^2\right)^{1/2}}{DuZ_1}$$

where

$$V_1 = p_z(B - B_1) + p_y(C_1 - C) + \frac{BC_1 - B_1C}{D}$$

$$V_2 = p_z(A_1 - A) + p_x(C - C_1) + \frac{A_1C - AC_1}{D}$$

$$V_3 = p_y(A - A_1) + p_x(B_1 - B) + \frac{AB_1 - A_1B}{D}$$

$$u = \left[\left(p_x + \frac{A}{D}\right)^2 + \left(p_y + \frac{B}{D}\right)^2 + \left(p_z + \frac{C}{D}\right)^2\right]^{1/2}$$

$$Z_1 = \left[\left(p_x + \frac{A_1}{D}\right)^2 + \left(p_y + \frac{B_1}{D}\right)^2 + \left(p_z + \frac{C_1}{D}\right)^2\right]^{1/2}$$

$$A_1 = R_{elx}\, x_{11} + R_{ely}\, x_{12} + R_{elz}\, x_{13}$$

$$B_1 = R_{elx}\, x_{21} + R_{ely}\, x_{22} + R_{elz}\, x_{23}$$

$$C_1 = R_{elx}\, x_{31} + R_{ely}\, x_{32} + R_{elz}\, x_{33}$$

where

$$R_{elx} = -R_e \cos\Phi_1 \cos(\Theta_1 + \alpha_s + 15.0\, t)$$

$$R_{ely} = -R_e \cos\Phi_1 \sin(\Theta_1 + \alpha_s + 15.0\, t)$$

$$R_{elz} = R_e \sin\Phi_1$$

6. PROGRAM IV

$$\cos\psi = n_x p_x + n_y p_y + n_z p_z$$

$$(0 < \psi < \pi)$$

$$\cos\beta = [(u_2 p_z - u_3 p_y)(n_y p_z - n_z p_y) + (u_3 p_x - u_1 p_z)(n_z p_x - n_x p_z)$$

$$+ (u_1 p_y - u_2 p_x)(n_x p_y - n_y p_x)] \left[(1 - e_n^2)^{1/2} (1 - e_s^2)^{1/2}\right]^{-1}$$

$$\sin\beta = p_x (\chi_y \eta_z - \chi_z \eta_y) + p_y (\chi_z \eta_x - \chi_x \eta_z) + p_z (\chi_x \eta_y - \chi_y \eta_x)$$

$$(0 < \beta < 2\pi)$$

Here,

$$u_1 = \cos\lambda_s \cos\mu_s, \quad u_2 = \sin\lambda_s \cos\mu_s, \quad u_3 = \sin\mu_s$$

$$e_n = \cos\psi$$

$$e_s = u_1 p_x + u_2 p_y + u_3 p_z$$

$$\chi_x = \frac{n_x - e_n p_x}{(1 - e_n^2)^{1/2}}, \quad \chi_y = \frac{n_y - e_n p_y}{(1 - e_n^2)^{1/2}}, \quad \chi_z = \frac{n_z - e_n p_z}{(1 - e_n^2)^{1/2}}$$

$$\eta_x = \frac{u_1 - e_s\, p_x}{(1 - e_s^2)^{1/2}}, \qquad \eta_y = \frac{u_2 - e_s\, p_y}{(1 - e_s^2)^{1/2}}, \qquad \eta_z = \frac{u_3 - e_s\, p_z}{(1 - e_s^2)^{1/2}}$$

7. PROGRAM IV(A)

$$\cos\zeta = \frac{\cos\psi \cos\psi_{es} + \sin\psi \cos\beta \sin\psi_{es}}{Q}, \quad \underline{0 < \zeta < 180^{o}}$$

$$\sin\xi = \frac{-\sin\beta \sin\psi_{es}}{\sin\zeta}$$

$$\cos\xi = \frac{Q}{2 \sin\zeta}, \quad \underline{0 < \xi < 360^{o}}$$

Here,

$$Q = \left[2 \left(1 + \sin\psi_{es} \cos\beta \cos\psi - \cos\psi_{es} \sin\psi\right)\right]^{1/2}$$

$$\cos\psi_{es} = p_x \cos\lambda_s \cos\mu_s + p_y \sin\lambda_s \cos\mu_s + p_z \sin\mu_s, \quad \underline{0 < \psi_{es} < 180^{o}}$$

8. PROGRAM V

$$\cos M = \rho_x \left(\frac{x' - R_m \cos\theta \cos\varphi}{W}\right) + \rho_y \left(\frac{y' - R_m \sin\theta \cos\varphi}{W}\right) + \rho_z \left(\frac{z' - R_m \sin\varphi}{W}\right)$$

Here, ρ_x, ρ_y, ρ_z, are those defined in Program III, and

$$W = \left[(x' - R_m \cos\theta \cos\varphi)^2 + (y' - R_m \sin\theta \cos\varphi)^2 + z' - R_m \sin\varphi)^2\right]^{1/2}$$

9. PROGRAM VI

The expressions for γ, σ are given in Program II. However, the expressions for ρ_x, ρ_y, ρ_z are given by

$$\rho_x = \frac{x' - R_m \cos\theta \cos\varphi}{W}, \quad \rho_y = \frac{y' - R_m \sin\theta \cos\varphi}{W}, \quad \rho_z = \frac{z' - R_m \sin\varphi}{W}$$

APPENDIX D

APPLICATION OF SUN-PUMPED LASER FOR LUNAR BEACON

APPENDIX D

APPLICATION OF SUN-PUMPED LASER FOR LUNAR BEACON

A sun-pumped laser utilizes reflected photons from the sun to excite a Yttrium Aluminum Garnet (YAG) laser rod. Normally, lasers are excited by photons from a flash tube or an electrode discharge.

1. ADVANTAGES AND DISADVANTAGES

The use of a sun-pumped laser as the light source for a lunar beacon is attractive because of the power savings attendant with the direct utilization of solar energy. Additional advantages include the ease with which the output may be collimated and directed, using small optical components, and the ease with which it may be modulated. The principal problem in the use of a sun-pumped laser as a lunar beacon is providing adequate cooling for the laser material itself. The mechanics of tracking the sun with the laser's concentrator mirror and aiming the laser output to the earth are problems common to other lunar-solar tracking beacons using oriented solar cell panels to supply electrical power for other types of light sources.

The following subsections present some discussion of sun-pumped lasers and include data from recent EOS experiments. Suggestions are included for possible work to bring sun-pumped laser beacons closer to a flight hardware status.

2. CHOICE OF MATERIALS AND SOLAR CONCENTRATORS

The laser material chosen must have broad pump bands in the solar spectrum and as low a threshold as possible at temperatures in the vicinity of $300^{\circ}K$. A complete survey of laser materials that have been investigated was recently published by EOS (Ref. 1). Of all the materials, neodymium-doped YAG appears to be the best presently

available for use in sun-pumped laser beacons. The laser output from Nd^{3+}:YAG is at 1.06 microns. Continuous radiation has been obtained from small Nd^{3+}:YAG rods pumped with tungsten lamps with as little as 360 watts input power (Ref. 2).

The optimum concentrator configuration is not universally agreed upon. Paraboloidal concentrators give the highest attainable flux density (Ref. 3). However, with this design it is difficult to obtain efficient pumping of a laser rod since several passes of the rays through the rod are necessary to obtain adequate absorption at the pump bands.

One of the approaches successfully employed at EOS is to mount the laser rod along the axis of a paraboloidal mirror, near the focus, and use a conical lens surrounding the rod to produce a cylindrical image of the sun. Figure 1 is a photograph of such a configuration employed at EOS.

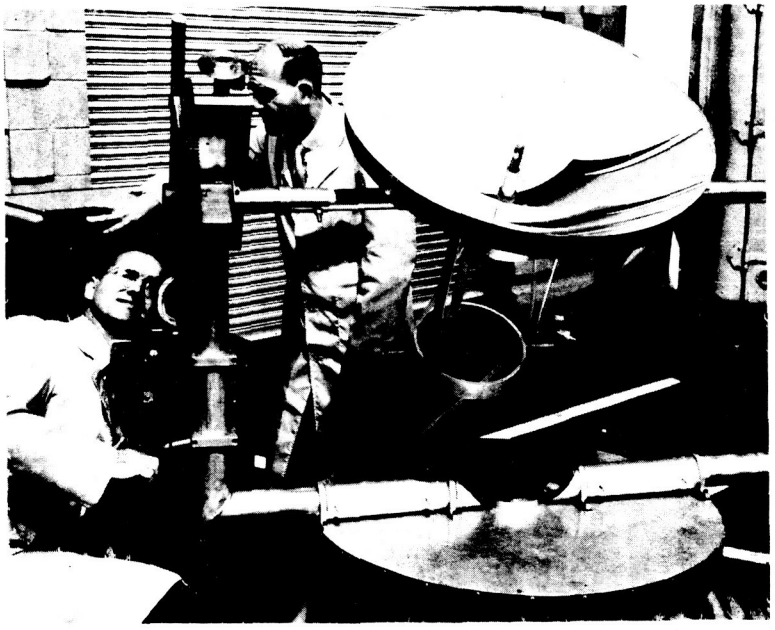

YAG-NEODYMIUM SUN-PUMPED LASER

In practice, the conical lens is filled with a liquid which serves to conduct heat from the laser rod. A special technique for processing a 3M fluorochemical FC-75 has been developed and has made it possible to utilize its excellent cooling characteristics in this application. It is possible that the cooling system could be designed so as to utilize the back side of the solar concentrator for radiative heat rejection, the coolant being circulated in tubes attached to the collector.

3. EOS EXPERIMENTS

The present EOS sun-pumped laser utilizes a 30-inch electroformed mirror to produce 45 milliwatts from a Nd^{3+}:YAG laser rod. The threshold has been observed to correspond to the radiation received on approximately half the mirror area. The 45-milliwatt output was obtained when the measured solar irradiance was 950 watts/cm^2 at the collector, which is about 40 percent less than the solar constant in space (1350 watts/m^2).

The principal areas, unique to sun-pumped laser beacons, where additional effort could be of most benefit are the following:

1. Improved solar concentrating systems
2. Improved laser materials
3. Design and development of cooling systems

EOS is currently engaged in a company-sponsored program to improve the optical system for collecting and concentrating the sun's energy on the laser rod. Hemispherical concentrators are being investigated and additional work should be devoted to other types of systems.

The second area is probably the most fruitful from the standpoint of increasing the laser output per unit beacon weight. The goal is to obtain a better match between the pumping spectrum and the absorption spectrum. The trivalent rare-earth crystal host lasers have very narrow and relatively weak 4f-4f parity-forbidden absorptions and so

exhibit inherently low system efficiencies when pumped with any of the high-energy broadband sources. Work is being done in the direction of energy transfer from a strong broadband absorber coexisting in the lattice structure to the rare-earth laser ion. Indications are that an immediate gain of 2 in efficiency (YAG:Nd^{3+}, cr^{3+}) is available and long-term gains of nearly an order of magnitude may be expected.

From the standpoint of bringing about a practical working beacon, the investigation of appropriate cooling systems is of extreme importance. If these engineering problems can be solved, the success of the sun-pumped laser beacon is assured.

REFERENCES

1. M. L. Bhaumik, L. W. Carrier, N. E. Johnson, "Characteristics of Lasers 1965," Laser Focus, Supplement, Data Publishing Co., P.O. Box 1, Newtonville, Mass.

2. Op. Cit., Table II

3. A. M. Zarem, D. D. Erway, Introduction to the Utilization of Solar Energy, McGraw-Hill Book Co., 1963

APPENDIX E

PROBABILITY OF PHOTOGRAPHIC DETECTION OF THE CISLUNAR BEACON

APPENDIX E

PROBABILITY OF PHOTOGRAPHIC DETECTION OF THE CISLUNAR BEACON

Photographic beacon detection probability, P, will depend on the product of the following factors:

1. Probability that the beacon flash is detected during the entire period that the camera shutter is open, P_s.
2. Probability that the beacon instantaneous field of view, θ, is pointed at the orbiting camera at any point in time, P_θ, while the beacon is in the camera field of view, θ_c.
3. Number of photographic frames, N_c, taken while passing through θ_c.

Therefore,

$$P = p_s \, p_\theta \, N_c$$

Given a $\frac{1}{50}$ sec camera shutter speed p_s is related to the flash duration, t_f, by

$$p_s = 1 - \frac{2 \times 0.02}{t_f}$$

The maximum diagonal camera field of view is $\pm 47^\circ$ based on the 78° square field cartographic camera format. Therefore, $p_\theta = \frac{\theta}{180}$ for a dynamic beacon reflecting, at a constant angular velocity, to 180° or $p_\theta = \frac{\theta}{\theta_c}$ for a static beacon. For a 67 percent format overlap $N_c = 3$.

The probabilities for the cislunar beacons are calculated in Table I. p_s is conservative.

TABLE I

CISLUNAR PHOTOGRAPHIC DETECTION PROBABILITIES

Beacon Classification	t_f	P_s	θ	P_θ maximum	N_c	P
Sphere	Continuous	1.0	180^o	1.0	3	3.0
Cap	420 sec	1.0	80	0.85	3	2.55
Faceted Arch	180	1.0	37	0.39	3	1.17
Oscillating Cap	0.1	0.6	46	0.256	3	0.46
	1.0	0.96		0.256	3	0.74
	5.0	0.992		0.256	3	0.96
Rotating Cylindrical Segment	0.1	0.6	1.6	0.0092	3	0.017
	0.5	0.92		0.0092	3	0.025
Oscillating Faceted Arch	0.1	0.6	2.13	0.0118	3	0.021
	1.0	0.96		0.0118	3	0.034

Since the orbit slant height within the $\pm 47^{o}$ camera field of view is about $\frac{\sqrt{2}}{2}$ x 400 nautical miles, then the signal strength will be two times stronger than the design signal strength. Therefore, the shutter speed actually necessary for detection would be 1/2 of 1/50 second or 1/100 second. This would increase p_s for the 0.1, 0.5, 1.0, and 5 second flash durations to 0.8, 0.96, 0.98, and 0.996, respectively. p_θ for the static cases is given for the most optimum case, when the beacon axis is pointed to the sun. At other orientations p_θ would decrease.

From this analysis, the static beacons would be superior for photographic missions followed in order by the oscillating cap, oscillating faceted arch, and rotating cylindrical segment concepts. Basically, the ratings vary with the beacon areas; see Table 3-X of Section 3.8. The oscillating cap has not been rated high since it only covers about 1/3 of the 2π steradian field of view. However, since this third is the center of the field of view, it will probably be the most useful. If a simple method of oscillating to the entire 2π steradian field of view is developed, without additional weight penalties, this concept should be rated higher.

For the dynamic beacons, the detection probabilities can be improved by increasing both the time which the beacon reflects to the $\pm 47^{o}$ field of view, t_{94}, so that $p_\theta = \frac{t_{94}}{t_{180}}$, and the number of frames taken over the beacon site, which could be easily programmed into the mapping missions at a minor increase in the use of photographic storage capacity.

p_θ can probably be practically increased by a factor of 3, whereas N_c could be increased by from one to two orders of magnitude. These modifications would increase the probability of photographic detection for even the poorest dynamic beacons to over 1.0.

BIBLIOGRAPHY

1. "Aerospace Expandable Structures," Conference Transactions NCR Sugar Camp,Dayton, Ohio, October 1963
2. Allen, C. W., "Astrophysical Quantities," Athlone Press, 1963
3. Altman, J. H., "Picking out the Grains," Perspective, Vol. 4, No. 4, Dublin
4. Baxter, T., "Ranger Block III Report, Sun Sensors," pp. 1-46
5. Blackwell, H. R. "Contrast Thresholds of the Human Eye," J.O.S.A., 36, 11, p. 624, Nov. 1946
6. Blackwell, H. R. J.O.S.A., Vol. 36, p. 480, 1946
7. Dole, S. H., "Visual Detection of Light Sources On Or Near The Moon," The Rand Corporation, Santa Monica, California, 27 May 1957
8. Edgar, R. F., "A Seeing Monitor for Astronomical Photography," Technical Note No. 1, No. 2 15621, April, 1962
9. Eimer, N., "Photography of the Moon from Space Probes," Report No. 32-347, JPL, January 15, 1963
10. DuPont Kapton* polyimide film, Bulletin H-1, "Summary of Properties"
11. "Feasibility Study Passive Lunar Marker Beacon," Hughes Aircraft Company, 26 March 1965
12. Gault, D. E., Shoemaker, E. M., Moore, H. J., "Spray Ejected from the Lunar Surface," NASA TN D-1767 Report, April 1963
13. Ger - 11793, "Evaluation Satellite Materials by Ground-Based Photometry," Goodyear Aerospace Corp., Akron, Ohio, 14 December 1964
14. Gordon, H. J., "Minutes of the NASA Working Group on Surveyor Landing Aids for Apollo," JPL, 1965
15. "Ground-Based Astronomy - A Ten-Year Program," National Academy of Sciences, National Research Council, 1964
16. Hardy, A. C. and Perrin, F. H., "The Principles of Optics," McGraw-Hill, 1932
17. Hastings, C. S., "Amateur Telescope Making, Book One," Scientific American, 1955, p. 172

*Registered Trademark

18. Jaffee, L. D., and Rittenhouse, J. B., "How Materials Behave in Space," JPL Materials in Design Engineering, September 1962

19. Kincer, R. D. and Rahes, R. G., "Principles of Brushless DC Motor Operation," at Wescon, August 1965

20. Kodak Pamphlet No. C-20, "Astrophotography"

21. Kodak Pub. No. P-9, "Kodak Photographic Films and Plates for Scientific and Technical Use"

22. Kodak Pamphlet No. P-49, "Modulation Transfer Data for Kodak Films"

23. Kodak Tech-Bits, "How to Understand and Use Photographic Speed Values," Vol. 4, 1964

24. Kodak Tech-Bits, "How to Understand and Use Photometric Quantities," Vol. 1, 1965

25. Kopal, Z. "The Moon," London Chapman and Hall, 1960

26. Kopal, Z. and Rackham, T. W., "Photographic Resolution on the Lunar Surface from Ground-Based Facilities," Icarus 2, 329-333, 1963

27. Kuiper and Middlehurst, "Telescopes," Stars and Steller Systems, Vol. 1, 1960

28. Landrock, A. H., "Effects of the Space Environment on Plastics: A Summary with Annotated Bibliography," Picatinny Arsenal, Dover, N. J., July 1962

29. "Lunar Atlas," North American Aviation, 1964

30. "Lunar Laser Ranging System Study," Extract from Report No. TP-592, March 1965

31. "Les Observationes Astronomiques and Les Astronomes," F. Rigaux, Bruxelles, 1959

32. "Les Observationes Astronomiques and Les Astronomes," F. Rigaux, Supplement 1961

33. "Materials Symposium," ASD Technical Report 61-322, September 1961

34. "Passive Lunar Marker Feasibility Study," NASA Contract NASA-3980, Hughes, 1965

35. Pogo, A.,"Annotated Bibliography of Physical Observations of the Moon," Cal Tech 1961

36. "Project Surveyor Study Contract," Extract from Final Report, Vol. III, Part 3, Dec. 1960

37. Rule, B. H., "American Ephemeris and Various Listings," March 1964

38. Russell, H. N., "On the Albedo of the Planets and Their Satellites," Jr. Astro Physics, Vol. 43, p. 173, 1916

39. Russell, H. N., Astrophysical Journal, 45, 60, 1917

40. Russell, I. W., Hanssen, N. S. and McKillip, W. J., "Development of an Inflatable Self-Rigidizing Space Shelter and Solar Collector from Honeycomb Sandwich Material," WPAFB Tech. Report APL TDR 64-29, Dec. 1963

41. "Study of a Flight Experiment of Solar-Concentrator Reflective Surfaces," EOS, 1 November 1963, Contract NAS1-2880

42. "Study of Selenodetic Measurements for Early Apollo Mission," Contract NAS9-2803, Geonautics, Inc., 22 Jan. 1965

43. "Survey of the Physical and Environmental Parameters of the Moon," NAS W 410-20-13-6, General Electric

44. "Surveyor Block II Mission Analysis Study," Extract from JPL Contract 950056, November 1964

45. Tousey, R., and Hulburt, E. O., "The Visibility of Stars in the Daytime Sky," Jr. Optical Society of America, Vol. 38, No. 10, p. 886, October 1948

46. Wilkens, H. P. Dr., "The Moon," Faber and Faber 1955 (Appendix I - Lunar Photography)

47. Willingham, D., "The Lunar Reflectivity Model for Ranger Block III Analysis," JPL Tech. Report No. 32-664, 2 November 1964